Università Degli Studi Del Piemonte Orientale

Amedeo Avogadro

Dipartimento di Scienze e Innovazione Tecnologica

PhD course in

Scienze Ambientali – Acque Interne E Agroecosistemi

XXVII Ciclo

Responses Of Model Plants To Metals And Non-Metals: Two Case Studies.

Nadide AKAY

PhD Supervisor: Prof. Graziella BERTA

PhD Co-Supervisor: Dr. Guido LINGUA

January 2015

Amedeo Avogadro University of Eastern Piedmont

Science And Innovation Department

Responses Of Model Plants To Metals And Non-metals: Two Case Studies.

by

Nadide AKAY

A THESIS SUBMITTED IN PARTIAL FULFILLMENT OF THE REQUIREMENTS FOR THE DEGREE

Doctor Of Philosophy

Approved Thesis Committee:

Prof. Stefano BIFFO

(Università degli Studi di Milano)

Prof. Giovanni LEUZZI

Università degli Studio di Roma “La Sapienza”

Prof. Consolata SINISCALCO

Università degli Studi di Torino

2015, Alessandria / Italy

ACKNOWLEDGEMENTS

I would like to extend my sincere thanks and gratitude to:

- my supervisor Prof. Graziella Berta for her patience, guidance, constructive criticism and words of encouragement and to my co-supervisor Dr. Guido. Lingua for his criticizes and his patience throughout the course of this project,
- Dr. Giuseppe Digilio for his assistance, guidance and encouragement throughout the course of this project,
- the Department of Chemistry, Università degli Studi del Piemonte Orientale for their technical assistance, especially to, Prof. Domenico Osella, Dr. Valentina Gianotti, Dr. Lorenzo Tei, Dr. Marco Clericuzio, Dr. Claudio Cassino and Davide Musso.
- my family, for all their support and encouragement,
- my chemistry class students to date from 2010 for filling me with energy,
- all my thesis students for encouragement,
- my “family-friends” in Italy whom they never leave me alone.

Table Of Contents

LIST OF TABLES

LIST OF FIGURES

Fig. 7A: Overview of the $^{1}H,^{1}H$ COSY NMR spectrum of *Populus alba* leaves methanol extract (sample CF7, T=300 K)

Fig. 7B: Expansion (8.5-4.0 ppm) of the $^{1}H,^{1}H$ COSY NMR spectrum of *Populus alba* leaves methanol extract (sample CF7, T=300 K) with assignment.

Fig. 7C: Expansion (5.6-0.6 ppm) of the $^{1}H,^{1}H$ COSY NMR spectrum of *Populus alba* leaves methanol extract (sample CF7, T=300 K) with assignment.

Fig. 7D: Expansion (7.9-6.2 ppm) of the $^{1}H,^{1}H$ COSY NMR spectrum of *Populus alba* leaves methanol extract (sample CF7, T=300 K) with assignment.

Fig. 8A: Overview of the ^{1}H-NMR spectrum of the methanol extract of roots from *Populus alba* (sample CR7, 1D-NOESY pulse sequence, with pre-irradiation of the residual MeOH proton, 300.0 K).

Fig. 8B: Expansion in the range 8.2-6.0 ppm of the 1H-NMR spectrum shown in Fig. 8A (Y-magnification 4x) with resonance assignment (see Tab. 2 for symbols).

Fig. 8C: Expansion in the range 6.2-4.0 ppm of the 1H-NMR spectrum shown in Fig. 8A (Y magnification 4x) with resonance assignment

Fig. 8D: Expansion in the range 4.2-2.0 ppm of the 1H-NMR spectrum shown in Fig. 8A (Y-magnification 4x) with resonance assignment

Fig. 8E: Expansion in the range 2.2-0.0 ppm of the ^{1}H-NMR spectrum shown in Fig. 8A (Y-magnification 4x) with resonance assignment

Fig. 9: 1H,13C HSQC spectrum of *Populus alba* roots methanol extract (sample CR7, T=300 K), (F: Leaf, R: Root).

Fig. 10A: Overview of the $^{1}H,^{1}H$ COSY NMR spectrum of *Populus alba* roots methanol extract (sample CR7, T=300 K), (F: Leaf, R: Root).

Fig. 10B: Expansion (8.5-4.5 ppm) of the $^{1}H,^{1}H$ COSY NMR spectrum of *Populus alba* roots methanol extract (sample CF7, T=300 K), (F: Leaf, R: Root).

NOMENCLATURE AND ABBREVIATIONS

TNT	Trinitrotoluene
TCE	Trichloroethylene.
MeOD	Deuterated Methanol
ICP-AES	Inductively Coupled Plasma Atomic Emission Spectrometer
ICP-MS	Inductively Coupled Plasma Mass Spectrometer
NMR	Nuclear Magnetic Resonance
HSQC	Heteronuclear Single Quantum Coherence
NOESY	Nuclear Overhauser Effect Spectroscopy
COSY	Correlation Spectroscopy
TSP	3-(trimethylsilyl)-2,2,3,3-tetradeuteropropionate
TFA	Trifluoroacetic
amu	Atomic Mass Units
ESI-MS	Electrospray Ionization Mass Spectrum
HYV	High Yielding Variety
DW	Dry Weight
FW	Fresh Weight
nd	Not Detected
FAO	Food And Agriculture Organization Of The United Nations
WHO	World Health Organization
Da	Dalton

Chapter 1: Soil Pollution

1.1 Introduction To Soil Pollution

Soil pollution is the phenomenon of the alteration of the chemical composition of the soil caused by human activity (Erfan-Manesh and Afiuni 2005). This kind of alteration of chemical-physical and biological properties of the soil may results in the introduction of harmful substances in the food chains.

Not all the pollutants have the same persistence and impact on the soil: while some organic substances are biodegradable their effects can be considered less dangerous, since they can eventually be metabolized as carbon dioxide and inorganic substances, some other pollutants can be accumulated in the soil, persisting for an indefinite period (Burgess, L.C., 2013). This is the case, for instance, some metals such Zn, Cu, Ni, Cr and Co, that can be considered, in some cases, essential for plants but that, if accumulated in high concentrations, can become toxic for the soil.

An important cause of toxic metal uptakes in crop plants is the long term use of effluents of breeding: they can be rich of organic and inorganic pollutants that, in high concentrations, can enter the food chain.

Soil pollution has several negative effects on different aspects of the environment and the human activities: if from one side it can be considered an important form of ecological and health threat, also some economic aspects should be taken in account like reduced productivity. Anyway, the health problems that soil pollution may involve are obviously the main ones, consisting in cancers, neurological damages and skeletal and bone diseases (Davis, et al, 2012).

Even if today, air, soil and water pollution are known to be key topics and primary aspects in the determination of the quality of life, until recently, they have not been considered as much as needed. Researchers and scientists have made, in the

recent past, an excellent work in terms of understanding and spreading results regarding the study of the effects of pollutants on the soil and, consequently, on the chain food and the human health.

Soils vary significantly their composition in different geographic areas; this location-related parameters can affect water drainage, living organisms and nutrients presence and, consequently, how a soil can react to potentially harmful substances exposure.

In order to study pollution, it is very important to determine some measures to use to evaluate soil health. A healthy soil should be rich of organic matter, present a good level of biodiversity and present an adequate structure (Morgan, 2013). Pollution can significantly affect these parameters, arriving, in extreme cases, to deteriorate so much the soil properties that it can be considered "functionally dead". In particular, contamination by heavy metals and some organic pollutants can be irreversible.

1.2 Metallic And Non-metallic Elements As Soil Pollutants And Effects Of Them On Human Health And The Environment

The practice of applying effluents of bleeding to agricultural soils is known to be useful as a resource of nitrogen, phosphorous and organic matter, improving soil fertility. Anyway, effluents can contain significant amounts of organic and inorganic toxic materials that can be accumulated in the soil, causing pollution.

In order to study the different contaminations that can affect soil, it could be a useful starting point to evaluate the different chemicals that can be considered an harmful threat for human health.

The first chemicals group to be considered while talking about health threat are heavy metals. With the term "heavy metals", a set of elements with metallic properties (the ones with density higher than 5 $g/cm^{3)}$ are referred: As, Pb, Cd, Cr, Cu, Hg, Ni and Zn are the main heavy metals that are considered in relation with

human health. All these elements are naturally present in soil and several of them are necessary for human health. Some of them, instead, are not essential, like Hg and As. Finally, it should be mentioned that also some essential elements, like Cu, for example, can become toxic at high concentrations. Human activities release into the environment huge quantities of heavy metals that soils naturally store. Actually, the understanding of the impact of heavy metals on soils is very limited with respect to the knowledge of the effects of their accumulation in air and water.

If, on one side, this can be considered a form of protection, avoiding, for instance, that these toxic substances reach water sources, at the same time the soil itself can become a threat for peoples that live or grow crops on it.

As is one of the most important chemicals to be considered in terms of soil pollution; high As concentrations can be detected in combination with different sources, like pesticides, mining activities (Cu, Au, Pb, Ni, etc), coal burning and wood preservatives. Generally, main As exposures are related to its presence in underground water supplies used for food preparation or food crop irrigation. A long period As contamination can lead to Arsenicosis, a chronic As poisoning. It can affect different organs, causing gastrointestinal, skin, heart, liver and neurological damages and bone marrow and blood diseases. It is known to be carcinogenic and to be involved in diabetes (Ferreccio et al, 2013; Smith, 2013).

Case-control study of arsenic in drinking water and kidney cancer in uniquely exposed northern Chile (Epidemiol, 2013).

Also Pb has important effects on plants, affecting seedling length, gaseous exchanges, chlorophyll production and germination. Cd, in toxic concentrations, can affect the soil structure while Cu and Ni have some important effects on the dry matter production (Khan and Scullion, 2002). Of course, all these contamination effects should be considered with respect to the specific soil characteristics that can lead to different damages and health threat.

1.3 Exclusion, Accumulation And Tolerance Of Soil Pollutants By Plants

Evidences of plants accumulation heavy metals in their tissues have been observed (Subashini, 2014). Numerous plants have been used with profit in phytoremediation of soil pollutants (Meeinkuirt et al, 2012) . In general, not all the plants accumulate metal in the same way, but several factors are involved in this process: species and growth stage, for instance can control the uptake, accumulation and translocation of metals. An accurate selection of plant species for phytoremediation can greatly improve the metal removal process (Wong, 2003).

Heavy metals induce several biochemical changes in plants, like the inhibition of the enzymes involved in photosynthetic reactions (Puig and Thiele, 2002). Great accumulation of metals by plants is a form of adaptation to the environment.

The binding properties of the cell wall and its role in the mechanism of metal tolerance has been controversial (Thurman and Collins, 1983; Verkleij and Schat, 1990). The walls of roots cells are directly exposed to the metals in soil solution. The interaction of the metals with the cell wall has been reported in several articles reviewed by Ernst et al, (1992) but since then, only a few more papers appeared covering this topic. Most of the cell wall-associated heavy metals are bound to polygalacturonic acids, to which the affinity of metal ions vary according to the metal (Ernst et al, 1992). The plasma membrane is the first "living" structure that is target for heavy metal toxicity and, consequently, could also be involved in tolerance. Such toxicity could result from various mechanisms including the oxidation and cross-linking of protein thiols, inhibition of key membrane proteins such as H+-ATPase, or changes in the composition and fluidity of membrane lipids (Meharg, 1993). A direct effect of Cd and Cu has been reported on the lipid composition of membranes (Fodor et al, 1995; Hernández and Cooke, 1997; Quartacci et al, 2001). Moreover, Cd treatment has been shown to reduce ATPase activity of the plasma membrane fraction of wheat and sunflower roots (Fodor et al, 1995).

In many cases natural hyperaccumulators are metallophyte plants that can tolerate and incorporate high levels of toxic metals (Whiting et al, 2004). A metallophyte is a plant that can tolerate high levels of heavy metals (Schickler and Caspi, 1999). Such plants range between "obligate metallophytes" (which can only survive in the presence of these metals), and "facultative metallophytes" which can tolerate such conditions but are not confined to them. Metallophytes commonly exist as specialised flora found on spoil heaps of mines. Such plants have potential for use for phytoremediation of contaminated ground.

Plants able to colonize soils with high concentrations of heavy metals and accumulate them are called hyper accumulators. Several studies have been conducted in order to understand the mechanisms of tolerance of hyper accumulator plants. One of these mechanism is the liberation of a complex mixture of organic compounds through the roots. Some other studies suppose the possible role of mucilage in protecting roots from metals like aluminium. Anyway, the mechanism behind hyper accumulation are not yet completely understood and are currently an increasingly explored research area (Samarghandi et al, 2007).

1.4 Plant Responses To Metallic And Non-metallic Pollutants

Plants, like all other organisms, have evolved different mechanisms to maintain physiological concentrations of essential metal ions and to minimize exposure to non-essential heavy metals (Ashrafi et al, 2011). Some mechanisms are ubiquitous because they are also required for general metal homeostasis, and they minimize the damage caused by high concentrations of heavy metals in plants by detoxification, thereby conferring tolerance to heavy metal stress (Cobbett and Goldsbrough, 2002). Other mechanisms target individual metal ions (indeed some plants have more than one mechanism to prevent the accumulation of specific metals) and these processes may involve the exclusion of particular metals from the intracellular environment or the sequestration of toxic ions within

compartments to isolate them from sensitive cellular components (Yang and Poovaiah, 2003). As a first line of defense, many plants exposed to toxic concentrations of metal ions attempt to prevent or reduce uptake into root cells by restricting metal ions to the apoplast, binding them to the cell wall or to cellular exudates, or by inhibiting long distance transport. If this fails, metals already in the cell are addressed using a range of storage and detoxification strategies, including metal transport, chelation, trafficking, and sequestration into the vacuole. When these options are exhausted, plants activate oxidative stress defence mechanisms and the synthesis of stress-related proteins and signalling molecules, such as heat shock proteins, hormones, and reactive oxygen species (Ebbs et al, 2002).

Contaminant uptake by plants has been widely studied by researchers in order to optimize the phytoremediation performances. Plants can act as "accumulators" or "excluders". Accumulators can concentrate high quantities of contaminants in their aerial tissues. These plants biodegrade or biotransform the pollutants into aerial tissues. Excluders, instead, restrict contaminants uptake into their biomass (Robinson et al, 2000).

Plants uptake of contaminants depends from several factors: plant species, medium properties, root zone and vegetative uptake (Colangelo and Guerinot, 2006).

The sensitivity of plants to heavy metals depends on an interrelated network of physiological and molecular mechanisms that includes uptake and accumulation of metals through binding to extracellular exudates and cell wall, complexation of ions inside the cell by various substances, for example, organic acids, amino acids, ferritins, phytochelatins, and metallothioneins; general biochemical stress defence responses such as the induction of antioxidative enzymes and activation or modification of plant metabolism to allow adequate functioning of metabolic pathways and rapid repair of damaged cell structures (Verkleij and Schat, 1990; Prasad, 1999; Hall, 2002; Cho et al, 2003). The mechanisms involved in

conferring tolerance to heavy metal toxicity has been proved difficult to resolve since large differences in plant and fungal species in the response to metals has been observed (Hall, 2002).

Soil properties and some agronomic procedures can affect significantly the remediation: as an example, pH values, organic matter and P concentration in a soil are fundamental parameters that regulate the lead uptake. Another important aspect regards the root apparatus of the plant: enzymes exuded by root can degrade contaminants in the soil. Finally, some environmental conditions can determine the vegetative uptake: as an example, the temperature affects growth substances and consequently root length (Salt et al, 1995).

1.5 Phytoremediation

Phytoremediation is a general term coined in the early 1990s for an emerging green technology using plants to clean up or 'remediate' contaminated soil, sediments, groundwater, surface water and air by removing, degrading and containing toxic chemicals (Isebrands, 2007). Phytoremediation is an efficient clean-up technology for a variety of organic and inorganic pollutants (Pilon-Smits, 2005).

In the last decade, phytoremediation has gained popularity in government agencies for several reasons; one of them is certainly the relatively low cost involved in this technology with respect to other traditional environmental clean-up methods. Such a factor is crucial in a scenario in which environmental remediation costs have become increasingly relevant: for example, currently, $6–8 billion per year is spent for environmental clean-up in the United States, and $25–50 billion per year worldwide Another important aspect in the phytoremediation popularity is its environmental-friendly flavor: being considered as a "green" alternative to chemical plants and bulldozer make it appreciated by the public and allows government agencies to invest on it (Glass, 1999).

Phytoremediation has of course several advantages but it implies also some limitation to take in account: for example, plants used to mediate the clean-up have to be where the contamination is and have to be able to work and live on it. Furthermore root depth of plants is crucial: they have to be able to reach the pollutants in the soil in order to the perform an effective cleaning (Pilon-Smits, 2005).

Phytoremediation technologies primarily use six mechanisms to accomplish clean-up goals:

1. Phytoextraction: The uptake and translocation of contaminants from groundwater into plant tissue.
2. Phytovolatilization: The transfer of contaminants to air via plant transpiration.
3. Rhizosphere degradation: Breakdown of contaminants within the rhizosphere, i.e. soil surrounding roots, by microbes.
4. Phytodegradation: The breakdown of contaminants within plant tissue.
5. Phytostabilization: The stabilization of contaminants in the soil and groundwater through absorption and accumulation on to plant roots.
6. Hydraulic Control: Intercepting and transpiring large quantities of water to contain and control migration of contaminants.

In order to increase the efficiency of the clean-up process also some important biological process should be taken in account like plant-microbe interactions and other rhizosphere processes, plant uptake, translocation mechanisms, tolerance mechanisms (compartmentation, degradation), and plant chelators involved in storage and transport (Pilon-Smiths, 2005).

Currently, research is very active in the environmental clean-up field, spending relevant efforts in improving and refine phytoremediation technologies.

Interesting developments on this methodology regards the integration of phytoremediation and landscape architecture or the use of transgenic plants.

In general, a significant impulse in clean-up and phytoremediation technologies should arrive from a multidisciplinary approach, combining knowledge and researches from molecular biology, plant biochemistry and plant physiology, ecology, or microbiology (Ensley, 2000).

1.6. Bibliography

Ashrafi E., Alemzadeh A., Ebrahimi M., Ebrahimie E., Dadkhodaei N., Ebrahimi M., (2011), Amino Acid Features Of P1B-ATPase Heavy Metal Transporters Enabling Small Numbers Of Organisms To Cope With Heavy Metal Pollution, Bioinf. Biol. Insights, 5: 59–82.

Burgess, L.C., (2013), Organic Pollutants In Soil, Soils And Human Health, 12: 83-102.

Cobbett C.S., Goldsbrough P., (2002), Phytochelatins And Metallothioneins: Roles In Heavy Metal Detoxification And Homeostasis. Annu. Rev. Plant. Biol., 53: 159–182.

Colangelo E.P., Guerinot M.L., (2006), Put The Metal To The Petal: Metal Uptake And Transport, Curr. Opin. Plant Biol., 9: 322–330.

Davis M., Mackenzie T.A., Cottingham K.L., Gilbert-Diamond D., Punshon T., Karagas M.R.,(2012), Rice Consumption And Urinary Arsenic Concentrations In U.S. Children, Environmental Health Perspectives, 120: 1418-1424.

Ebbs S., Lau I., Ahner B., Kochian L., (2002), Phytochelatin Synthesis Is Not Responsible For Cd Tolerance In The Zn/Cd Hyperaccumulator Thlaspi Caerulescens, Planta, 214: 635–640.

Ensley B.D., (2000), Rationale For Use Of Phytoremediation In Phytoremediation Of Toxic Metals, Using Plants To Clean Up The Environment, 11: 3–12.

Erfan-Manesh M. and Afiuni, M., (2005), Environmental Pollution, Organ Publications, Isfahan/Iran.

Ernst W.H.O., Verkleij J.A.C., Schat H., (1992), Metal Tolerance In Plants, Acta Bot. Neerl., 41: 229-248.

Ferreccio C., Smith A.H., Durán V., Barlaro T., Benítez H., Valdés R., Aguirre J.J., Moore L.E., Acevedo J., Vásquez M.I., Pérez L., Yuan Y., Liaw J., Cantor

K.P., Steinmaus C., Smith A.H., (2013), Environ. Health Perspect, Applied Soil Ecology, 20: 145–155.

Fodor A., Szabó-Nagy A., Erdei L., (1995), The Effects Of Cadmium On The Fluidity And H+-ATPase Activity Of Plasma Membrane From Sunflower And Wheat Roots, J. Plant Physiol., 14:787–792.

Isebrands J.G., Best Management Practices Poplar Manual For Agroforestry Applications in Minnesota, (2007), Environmental Forestry Consultants, LLC

Khan M., Scullion J., (2002), Effects Of Metal Enrichment Of Sewage-Sludge On Soil Micro-Organisms And Their Activities, Applied Soil Ecology, 20: 145-155.

Meeinkuirt W., Pokethitiyook P., Kruatrachue M., Tanhan P., Chaiyarat R., (2012), Phytostabilization Of A Pb-Contaminated Mine Tailing By Various Tree Species In Pot And Field Trial Experiments, Int. J. Phytoremediation, 14: 925-38.

Meharg A.A., (1993), The Role Of Plasmalemma In Metal Tolerance In Angiosperms, Plant Physiol., 88:191-198.

Morgan R., (2013), Soil, Heavy Metals, and Human Health. Soils and Human Health. Boca Raton. FL: CRC Press, pp. 59-80.

Pilon-Smits E., 2005, Phytoremediation, Biochem. Biophys. Res. Commun., 56: 15–39.

Puig S., Thiele DJ., (2002), Molecular Mechanisms Of Copper Uptake And Distribution, Curr. Opin. Chem. Biol., 6:171–180.

Robinson B.H., Mills T.N., Petit D., Fung L.E., Green S.R., (2000), Cadmium-Accumulation In Poplar And Willow: Implications For Phytoremediation, Plant And Soil, 227: 301-306.

Salt D.E., Blaylock M., Kumar N.P.B.A., Dushenkov V., Ensley B.D., Chet I., Raskin I., (1995), Phtoremediation: A Novel Strategy For Removal Of Toxic Metals From The Environment Using Plants, Biotechnology, 13: 468–474.

Samarghandi M.R., Nouri J., Mesdaghinia A.R., Mahvi A.H., Nasseri S., Vaezi F., (2007), Efficiency Removal Of Phenol, Lead And Cadmium By Means Of UV/TiO2/H2O2 Processes, Int. J. Environ. Sci. Technol., 4: 19–25.

Thurman D.A., Collins J.C.L., (1983), Metal Tolerance Mechanisms Proc. Int. Conf. Heavy Metals In The Environment. Heidelberg, 10: 298-300.

Wong M.H., (2003), Ecological Restoration Of Mine Degraded Soils, With Emphasis On Metal Contaminated Soils, Chemosphere, 50: 775–780.

Yang T., Poovaiah B.W., (2003), Calcium/Calmodulin-Mediated Signal Network In Plants, Trends Plant Sci., 8: 505–512.

Chapter 2: Poplar

2.1 *Populus alba* Linnaeus; White Poplar

Populus alba L. is typical of Mediterranean forest ecosystems from central and southern Europe to West and Central Asia and northern Europe. Due mainly to human influence activity, it occurs in Europe in linear formation along rivers or as isolated trees. In the Italian peninsula, *P. alba* it is distributed uniformly in all regions from sea level to low mountain sites in a variety of edaphic and climatic conditions (Isebrands and Richardson, 2012).

P. alba grows preferentially in a climate which is not too severe, with full light conditions and deep, silt or sandy-silt well-drained soils. In bottomland habitats with seasonal variation, white poplar attains magnificent timber proportions (Kuzovkina et al, 2010).

P. alba reproduces by means of suckers, which develop copiously and vigorously from its shallow roots and also produces abundant seeds. It is a pioneer species, and it can colonize bare soil (Gathy, 1970).

P. alba is a unique pioneer species of riparian ecosystems, contributing to the natural control of flooding and water quality. In Europe, flood-plain forests are among the most recognized ecosystem for biodiversity. Currently, an increasing interest in the riparian ecosystems restoration is due to its involving in the natural control of flooding (Fussi et al, 2010).

Today, human activities, are seriously alterating riparian ecosystems, making white poplar one of the most threatened tree species in Europe. Although it still regenerate with great success, in some regions it has been observable a measurable populations reduction (Stettler et al, 1996).

2.1.1. Poplar as a Plant Model Tree Plat for Phytoremediation

In phytoremediation, poplars and willows are among the most appreciated tree species. This preferences are due to their rapid growth and to their abundant and deep roots apparatus, able to take up large quantities of water and nutrients (Isebrands et al,2000). Beside the important nutrients take up, they also provide root surface area for beneficial microbes and mycorrhizae, performing phytoremediation functions. Since 2000, An International Phytotechnology Society has emerged to promote phytotechnologies with the scope of cleaning up environmental contamination problems. They have also published the International Journal of Phytoremediation, a journal that since 2002 publishes the latest applications of phytoremediation. In this decade, hundreds of articles on the use of poplars and willows for environmental applications have been published. In addition, there has recently been a comprehensive overview published on phytoremediation that features many case studies involving poplars and willows (Nelson, N.D., 1984).

Selective cross-breeding has been performed for many years to select ideal characteristics in Poplar such as fast growth rates (Milton, 1998). Another goal of poplar cross-breeding is heterosis, which means the result when the genetic traits of the hybrid exceed that of the parents (Chappel, 1998). The same selection techniques have been successfully experimented for the phytoremediation field such that scientists want to create hybrid species that are fast growing, large leaved, disease, drought, and pest resistant, hyperaccumulating, and tolerant to high levels of contaminants because these traits effectively maximize the plants ability to perform phytoremediation functions (Rock, 1997). The poplar hybrids most commonly used in phytoremediation applications are Black cottonwood, with leaves that are four times larger than its parents and increase the potential evapotranspiration rates because of the increased surface area (Chappel, 1998), Eastern cottonwood and black poplar.

Poplars have a deep and strong root system, tending to extends vertically and horizontally reaching up to 15 feet of depth. In order to optimize the efficiency of the clean-up maximizing the amount of contaminated water, precipitation and other uncontaminated water sources have to be limited, planting the roots in such a way that only a few inches of the tree are above the ground.

2.1.2. Copper as a Soil Pollutant

On heavy metals (such as Ni, Pb, Zn and Cu) contaminated soils, various trees can grow. Similarly, it happens on soils exposed to organic contaminants such as TNT and TCE (Schnoor, 1997).

Preliminary studies on metal uptake by clones that grow fast, producing large quantities of biomass have been made on the basis of recent research on short rotation coppice culture, especially on willow and poplar.

Poplars able to extract or degrade a number of contaminants; they are adapted to a broad range of climatic conditions and soils, produce high biomass, have a wide-spreading root system and are easy to propagate (Kuzovkina, 2010). All these reasons, made poplar an optimal candidate for the phytoremediation of heavy metal-polluted soils (Bradshaw et al 2000). High quantities of Cu are typical of mine soils and in many industrial areas. Cu has a high affinity with soil colloids, thus it is scarcely mobile. Cu is also an essential micronutrient involved in pollen formation (Wang, et al 2004) and in various enzymatic activities implicated in respiration and photosynthesis (Woolhouse and Walker, 1981; Faust and Christians, 2000). Even though it can be crucial as nutrient, high levels of Cu can induce leaf chlorosis, reduced root and Leaf growth, and leaf senescence (Toler et al 2005; Vangronsveld, 1994; Kamenova-Jouhimenko et al, 2003).

2.1.3. Copper And Poplar: Uptake In The Responses To Metal In General And To Copper In Particular

Facing metals contamination is challenging, since the pollutants cannot be metabolized, but they must be transferred to the leaves, where they can be easily harvested or volatilized. A large part of the research in this area focused on natural hyper accumulating plants but poplar and willow, with their higher biomass, have been used with success, compensating their lack of accumulation ability (Ye et al, 1997).

Copper similarly to transition metals, is a heavy metal that is an essential micronutrient for plants, being involved in several cellular functions as a component of many enzymes and proteins (Cakmak and Engels, 1999). At high concentrations, it is one of the most widespread toxic elements in agro-ecosystems (Roy and Couillard, 1998; Nan et al ., 2002). Plants absorb and distribute toxic heavy metals through the transpiration stream inside the plant, with the same mechanisms used in mineral nutrition (Marschner, 1995). These mechanisms include uptake by the roots, translocation by long-distance transport in the xylem, and accumulation in below- and above-ground organs Plants have developed defence strategies against heavy metals, such as avoidance, chelation and sequestration inside the cells, or efflux from the cytosol to the apoplast. Chelation of heavy metals is achieved in plants by cysteine (Cys)-containing metal-binding ligands, including metallothioneins (MTs) and phytochelatins (PCs) (Rauser, 1999; Cobbett & Goldsbrough, 2002). Phytochelatins are enzymatically synthesized from the tripeptide glutathione [γ -glutamic acid–cysteine–glycine (γ-Glu–Cys–Gly)] (GSH). Heavy metals cause oxidative stress, and transition metals and oxygen metabolism are intimately linked to the redox control of cells (Foyer et al, 1994; Schützendübel & Polle, 2002). As an antioxidant and PC precursor, GSH and its metabolism play an important role in plant response and adaptation to natural stresses (Rennenberg & Brunold, 1994; Xiang & Oliver, 1999). Regulation of enzymes involved in biosynthesis, and the control of the redox

status of GSH, are part of a plant's resistance and /or adaptation to environmental stresses (Arisi et al, 2000; Foyer & Rennenberg, 2000; Di Baccio et al, 2004).

The mechanisms mediating micronutrient accumulation and/or detoxification in *Populus* will help us to clarify the potentiality of these plants in heavy metal tolerance and, eventually, phytoremediation.(Di Baccio et al,2005). Successful phytoremediation of inorganics is based on the ability of the plant to regrow fastly after the foliage is harvested. In this this way, the extracted metals can be removed. Willow is especially well suited for this type of remediation.

In successful phytoremediation applications, poplar and willow are being used successfully, facing some important classes of pollutants. With their high transpiration rates, deep roots, inherent biochemical abilities and amenability to coppicing (Mirck and Volk, 2010).

2.1.4 Nuclear Magnetic Resonance As A Technique For The Study Of Plant Metabolome

Nuclear magnetic resonance (NMR) has its origin in the net magnetic moment or spin of an atomic nucleus that has an odd atomic mass and/or an odd atomic number.

NMR spectroscopy is used to analyse the tissues composition both in *vivo* and in various extracts. Common nuclei exhibiting such magnetic properties are the highly abundant isotopes ^{1}H (99.98% in nature) and ^{31}P (100% in nature) or the low abundance isotopes ^{13}C (1.1% in nature) and ^{15}N (0.37% in nature). The widespread use of NMR in plant metabolism analysis has been reviewed recently (Le Gall et al, 2003).

NMR permits to investigate the metabolism of plants allowing the identification of molecules and ions in tissues or cells as well as in various extracts. It also allows the determination of the absolute concentrations of the more abundant

mobile metabolites, the measurement of the change in concentration of key molecules during biochemical transformations, and the measurement of unidirectional fluxes in intact cells or tissues at steady state. In addition, NMR can be used to reveal unexpected information, that usually would escape detection by other analytical methods.

2.1.4.1. NMR Spectroscopy In Metabolomics

^{1}H-NMR spectroscopy is an analytical platform that is very well suited for metabolomics studies as it can provide a metabolic profile of biofluids or tissue extracts in a short time (typically 5 to 20 minutes), with minimal sample treatment. Each metabolite contributes to the NMR spectrum with its own very characteristic resonances. In general, within a single molecule, each chemically non-equivalent ^{1}H nucleus give rise to a resolved NMR signal having a peculiar resonance frequency (chemical shift) and shape (multiplicity). Compounds having many non-equivalent nuclei yield several resonances in the NMR spectrum, whose ensemble constitute a molecular signature. Therefore, a specific metabolite can be identified within the mixture spectrum by identifying its sub-spectrum, provided that there is no severe resonance overlap with other metabolites. Metabolites that cannot be recognized unambiguously within one-dimensional spectral overlap can be further identified by means of two-dimensional NMR techniques, that offer a greater resolution.

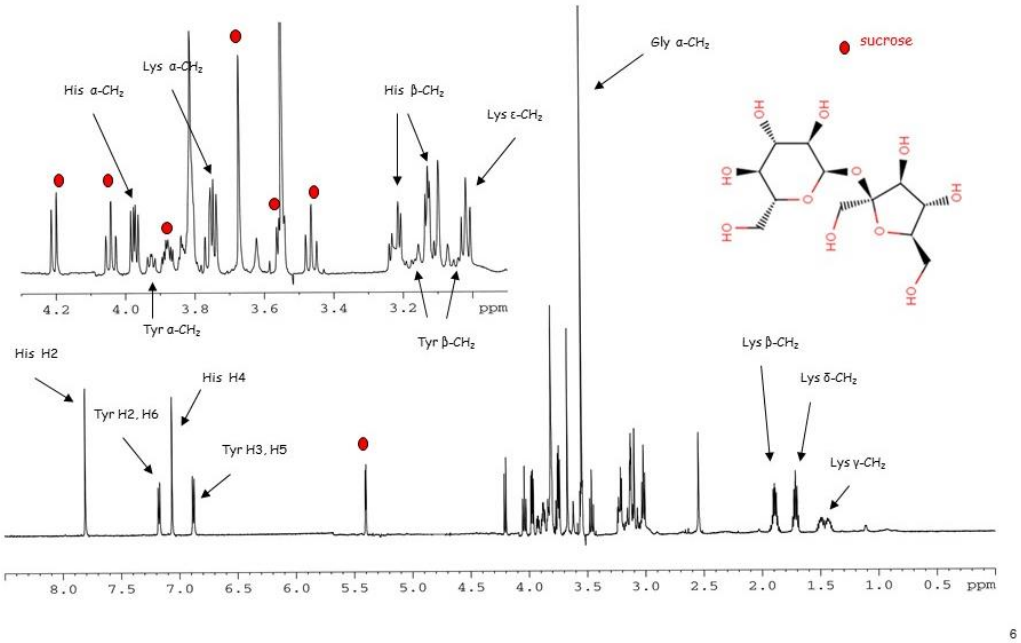

Fig. 1- ^{1}H NMR spectrum of a mixture with assignment of the resonance of several metabolites. Red dots indicate the characteristic sucrose resonances .

Besides metabolite identification, ^{1}H-NMR allows the relative quantification of metabolites, as the intensity (integral) of a signal is linearly proportional to the concentration of the molecule it originates from. The most important point of weakness of ^{1}H NMR spectroscopy is the inherent low sensitivity, allowing the detection of metabolites down to the mid micro molar range with typical NMR instrumentation.

2.1.4.1.1. One Dimensional ^{1}H NMR Spectroscopy.

Most applications of NMR for metabolomics research rely on 1D NMR experiments. This is dictated by long acquisition times of most multi-dimensional NMR experiments making their application a time-consuming task for studies with large sample arrays. The basic pulse sequence for the acquisition of 1D ^{1}H-NMR spectra is the 90deg-acquisition. This sequence yields a profile of all the components that are present in the sample, including either low molecular weight components (true metabolites having sharp NMR signals because of long T_2

relaxation times) and high molecular weight components (such as proteins, having broad signals because of short T_2). In addition to protein, another source of broad signals are protons from LMW compounds that are subjected to chemical exchange dynamic processes. Fig. 2 shows a typical ^{1}H-NMR spectrum of blood plasma, containing hundreds of sharp signals due to LMW compounds together with broader signals (in the region centred at 1-2 ppm) due to lipoproteins (LDL, VLDL, etc).

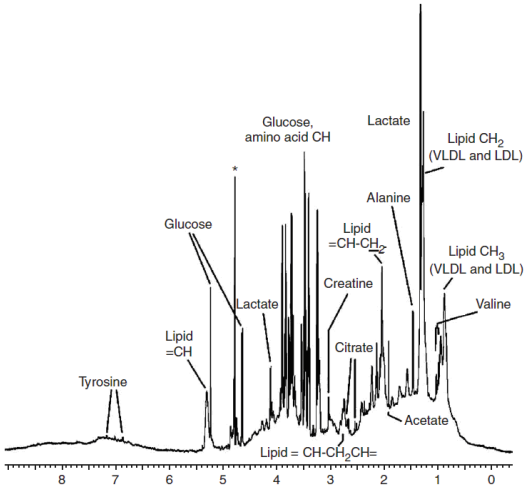

Fig. 2: ^{1}H NMR spectrum (600 MHz) of blood serum with assignment of the resonance of several metabolites, including lipoproteins. Taken from Beckonert, 2007)

There are several pulse 1D NMR pulse sequence that can be used to obtain spectral edited metabolic profiles. Plain 90 degrees-acquisition techniques allow to register ^{1}H-NMR spectra were both the resonance of LMW metabolites and HMW compounds are detected. T_2-filtered sequences (*e.g.* the CPMG sequence) allow to eliminate the broad components, such that only LMW compounds are detected. Gradient selected diffusion techniques, conversely, allow one to filter out the sharp components and to obtain the profile of macromolecular compounds only.

A critical issue to obtain 1D NMR spectra of biofluids and tissue extracts is the suppression of the residual solvent resonance. If samples are dissolved in natural isotopic abundance solvents, the ^{1}H-NMR signal of the solvent will be order of magnitudes higher than that of metabolites, hampering their detection. The solvent can be replaced by one isotopically enriched with the isotope ^{2}H (deuterium, D) to suppress the otherwise intense solvent resonance (for instance, deuterated water D_2O instead of water, H_2O; or fully deuterated methanol CD_3OD instead of CH_3OH). As an alternative or in combination to a deuterated solvent, pulse sequences must be designed to achieve the suppression of the solvent. The most popular sequence used in metabolomics to achieve efficient solvent suppression is the so-called noesy-presat sequence (often abbreviated as noesy1d). The water (or methanol hydroxyl) resonance is saturated by frequency selective irradiation during the inter-scan delay and the mixing time of the sequence thus leading to a reduction of the equilibrium population difference of the spin species resonating at the frequency of the weak (<50 Hz) presaturation radio frequency field applied. The big advantage of this method is given by a chemical shift selectivity superior to any other technique. If a reliable quantification of signals resonating close to water (*e.g.* anomeric proton of glucose) is needed, this technique will be the choice. The mixing time, together with the intense phase cycling used in noesy-presat, has a positive effect on a flat baseline, a feature that is highly desirable to reduce the analytical bias if several NMR profiles have to be compared. This can be explained by a small degree of spatial selectivity encoded in the noesy-presat pulse sequence reducing the influence of protons entering or leaving the sensitive volume of the detection coil during the detection of the FID. In summary, the noesy-presat technique provides a simple, highly reproducible and robust method for the acquisition of high-quality NMR spectra in aqueous solutions. It has to be kept in mind, however, that absolute value quantification is possible only with limited accuracy.

2.1.4.1.2. Two Dimensional NMR Spectroscopy

2D-NMR techniques are very useful and powerful to identify metabolites that escaped assignment in 1D spectra because of spectral overlap or to identify new chemical compounds that are not included into spectral databases nor they were previously characterized. The 2D-techniques used in this thesis are 2D-^{1}H,^{1}H COSY (Correlation SpectroscopY) and 2D-^{1}H,^{13}C HSQC (Heteronuclear Single Quantum Coherence). In these 2D experiments, a NMR cross-peak identifies two nuclei that belongs to the same molecule and that are interacting via a magnetic interaction called scalar coupling. As the scalar coupling is a short range interaction, 2D cross peaks permit to draw short range connectivities between the nuclei belonging to the same molecule.

2.1.4.1.3. 2D^{1}H, ^{1}H COrrelation SpectroscopY (COSY)

2D-^{1}H,^{1}H COSY is a homonuclear scalar coupling correlation technique, meaning that scalar correlations are detected between one ^{1}H spin and another ^{1}H spin. In COSY a cross peak is obtained if two ^{1}H spins are connected by a homonuclear J-coupling (typically over 2–5 bonds). Cross peak intensity depends on the concentration of the compound and on the size of the J coupling, being generally larger (up to 16 Hz) for ^{3}J (*i.e.* vicinal coupling, ^{1}H-C-C-^{1}H) or ^{2}J (*i.e.* germinal coupling, ^{1}H-C-^{1}H) and smaller for long range couplings (J<2-3 Hz). Thus information on spin-system topologies can be extracted. The cross peaks contain fine-structure allowing for the determination of the values of active and passive J-couplings. COSY spectroscopy is very useful to draw the connectivity within a given structure. It allows to group ^{1}H resonances, that can be spread all over all the 1D-^{1}H NMR spectrum, and to assign them to a single molecule. An example of the use of COSY spectroscopy to identify the resonance of benzoic acid is given in the Figure below.

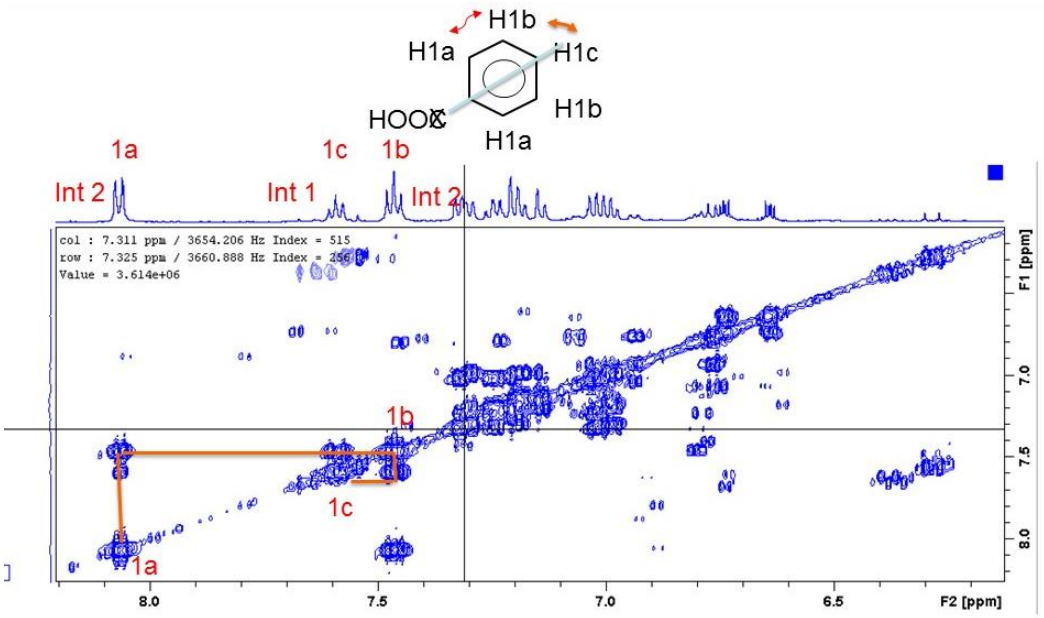

Fig. 3: Identification of benzoic acid within a leaf extract by means of COSY spectroscopy.

Here, in Fig. 3, red lines connect spins (H1a, H1b and H1c) that are no more than 3 chemical bonds far apart in the benzoic acid. Beside achieving the grouping and assignment of three resonances in the 1D spectrum to a single compound, the structural connectivity yielded the identification of the compound, that turns to be benzoic acid.

2.1.4.1.4. Two dimensional $^{1}H,^{13}C$ Heteronuclear Single Quantum Coherence (HSQC) spectroscopy.

Within heteronuclear scalar correlated HSQC spectroscopy, each cross peak appear whenever one ^{1}H spin is coupled to a ^{13}C spin through $^{1}J_{C\text{-}H}$ scalar coupling, i.e. whenever the ^{1}H and ^{13}C nuclei are directly bond. In contrast to the direct 1D-based observation of ^{13}C information, the indirect measurement via J-coupled ^{1}H spins offers several advantages: *i)* the sensitivity of these class of experiments depends on the higher gyromagnetic ratio of the protons. As a consequence, ^{13}C spins are observed with "only" 100 times reduced sensitivity compared to ^{1}H spectroscopy; *ii)* the chemical shift of the carbons is correlated with the chemical shift of J-coupled protons. HSQC experiments, as well as the

many variants of this heteronuclear technique found in metabolomics, make use of these advantages. In HSQC spectra, the chemical shift of ^{13}C is correlated via the large one-bond coupling constant ^{1}JCH to the ^{1}H chemical shift of the directly bound proton. Thus, HSQC cross-peaks can be used to read the ^{1}H resonance frequency of a proton (on the F_2 axis, usually the horizontal axis) and the ^{13}C resonance frequency of the carbon atom to which the proton is directly attached (on the F_1 axis, usually the vertical axis.) If a given ^{1}H signal is assigned within a molecule, it is then straightforward to find the ^{13}C chemical shift of the attached carbon, and *viceversa*. With typical experimental settings the acquisition time for a HSQC experiment will be in the range 6 to 24 hrs, making the application attractive only for selected samples. Usually HSQC spectra are used to assign metabolite signals, provided that a HSQC spectra database of single metabolites is available. This is shown in the Figure below. The HSQC spectrum of poplar leaf methanol extract (blue has been superposed with the HSQC spectrum of standard oleic acid (red) acquired under the same conditions (solvent, temperature). It can be seen that all HSQC signals of the standard oleic acid sample can find a respective signal in the mixture, confirming without any ambiguity that oleic acid is in the sample.

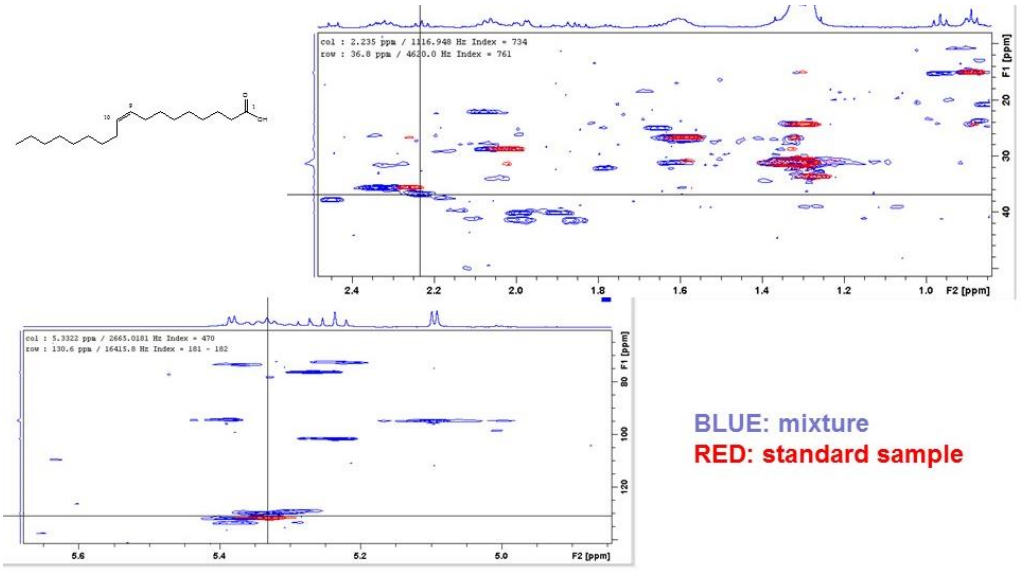

Fig. 4: HSQC spectrum of poplar leaf methanol extract compared to standard sample

2.2. Experimental Details

2.2.1 Plant material

Plantlets of poplar about 7-8 cm tall, with a well-developed root apparatus were taken from the sterile colture. Agar was removed from roots by immersing them in distilled water and plantlets were placed into 5 cm diameter honeycombed pots, letting the roots protruding out. Expanded perlite, previously washed, was added to the pots as a support.

Pots were then inserted in the dedicated space in the X-Stream Aeroponic Propagator (Nutriculture ltd, Skelmersdale, UK) tank, containing Canna Hydro Vega nutrient solution, whose composition is reported in table X.

A water flow of 15 minutes duration was pumped to spray the roots and maintain wet the clay. Pumping was activated every 45 minutes. Tanks were closed with their plastic cap for at least one week, to keep moisture within the plant environment, allowing plantlets to adapt to the new culture conditions. A photoperiod of 16 hours of light (Phylips TLD 36W/33; 400 fc)/8 hours of darkness, with diurne and nocturne temperature of 22 and 19 °C respectively, was applied. A refilling of the nutrient solution was performed weekly. After one month, when plants reached 20-22cm in height and showed a well-developed root apparatus (about 20-25 cm in length), treatments with copper were performed.

N total	6,20%	Mg (MgO 1,3%)	0,80%
(NH_4 0,4%)		S (SO_3 2,0%)	0,8%
(NO_3 5,7%)		B	0,007%
P_2O_5 (P 0,9%)	2,1%	Cu	0,001%
K (K_2O 7,7%)	6,4%	Fe (DTPA)	0,021%
Ca (CaO 4,5%)	3,2%	Mn	0,014%
		Mo	0,002%
		Zn	0,007%

Tab. 1: Percentage Composition of the nutrient solution CANNA Hydro Vega

2.2.1.1. Treatment

Plantlets were taken from the tanks maintaining each of them in its own pot. Roots were washed with bi-distilled water and pots were moved in glass pots with 55 ml of nutrient solution, as it is or with addition of CuCl2 to a final concentration of 0.1 mM. Only roots were submerged. After 72 hours from the beginning of the treatment, plants were harvested them from the pots, roots were washed with bi-distilled water and dried on filter paper. Plantlets were finally split up in roots and Leafs. Each sample was weighed, frozen in liquid nitrogen, lyophilized and stored at room temperature in airtight containers.

2.2.1.2. Extraction in methanol

Lyophilized material (either roots or leaves) has been powdered in liquid nitrogen with mortar and pestle. An aliquot of 150-500 mg of powdered material has been transferred into a flask and added with MeOH (typically 150 ml of solvent per 200 mg of leaves). Flasks are maintained under stirring for 3 days at RT in the dark. The supernatant has been recovered by filtration (Buchner filter under vacuum) and slowly dried in vacuum with a rotary evaporator. The dried material has been weighed.

The dry residue is solubilized again with MeOH/water mixture, with the aid of a spatula. The sample is solubilized again by adding methanol (2 mL) and then water (3 mL) under vigorous stirring and extracted with n-hexane (5 mL) to eliminate the more hydrophobic compounds. The n-hexane phase (usually dark coloured) is removed and the extraction repeated two more times. The methanol/water phase is finally dried by SpeedVac and stored at -20°C until NMR analysis.

2.2.2. NMR spectroscopy

Each lyophilised sample (stored at -80°C) was thawed, weighted and dissolved with 600 µL of CD_3OD and 20µL of 5.6 mM (3-trimethylsilyl)-2,2,3,3-tetradeuteropropionate (TSP) in CD_3OD, to yield a final TSP concentration of 0.18 mM. The sample was transferred into 5mm NMR tubes, inserted into the magnet and allowed to equilibrate to 300 K for 5 min.

^1H NMR spectra of root or leave extracts were acquired on a Bruker Avance III spectrometer operating at 11.7 T (corresponding to a Larmor frequency of 500 MHz for ^1H), equipped with an inverse Z-gradient 5mm TXI probe. Before running each spectrum, field homogeneity was adjusted by means the topshim (either 1D or 3D) routine to achieve a linewidth of the TSP standard < 0.7 Hz. Ninety-degree pulses were calibrated by means of the stroboscopic nutation experiment. Temperature was set to 300.0 K, and controlled within ±0.1 K by means of the BTO2000 VTU system. ^1H-NMR spectra for multivariate analysis were acquired with the 1D-noesy pulse sequence with water suppression by on resonance pre-irradiation of the residual solvent signal. The carrier frequency SFO1 was adjusted sample-by-sample as well within 0.05 Hz precision for optimal solvent suppression and minimal baseline offset. Typical acquisition parameters included 5 s relaxation delay, 128 scans, 4 dummy scans, 20.5 ppm (10274 Hz) spectral width, 64 K complex points, 3.19 s acquisition time, 10 ms mixing time, 25 Hz bandwidth of the water suppression pulse. With these settings, the total acquisition time was about 20 min. Data were multiplied by an exponential decay function with a line-broadening factor of 0.3 Hz, prior to Fourier transform and phase correction. Acquisition parameters were carefully adjusted such that only zero-order phase correction was required to obtain fully phased spectra without baseline distortion.

Homonuclear 2D-COSY as well as heteronuclear 2D-^1H,^{13}C HSQC experiments were carried out on a number of samples to assign the metabolite resonances. Parameter settings for 2D-HSQC experiments (with sensitivity improvement,

echo/antiecho-TPPI gradient selection, decoupling during acquisition and presaturation during the relaxation delay; Bruker pulse sequence hsqcetgpprsisp2.2) were: 3.2 s relaxation delay, 64 scans, 16 dummy scans, 0.170 s acquisition time, 145 Hz for direct XH coupling constant, 25 Hz bandwidth for the water suppression presaturation pulse, 2048 x 200 complex data point, 12 ppm (6009 Hz) and 166 ppm (20820 Hz) spectral width in F2 and F1 respectively, carrier frequency on F2 centred on the water resonance and 75 ppm on F1. Data were zero-filled to a 1024 x 1024 data matrix and treated with squared cosine window functions (both along F2 and F1) prior to FT in the phase-sensitive mode.

2D-COSY spectra were acquired with a gradient selected, phase insensitive mode with presaturation during the relaxation delay (Bruker pulse program cosygpprqf). Acquisition parameters were: 2 s relaxation delay, 32 scans, 16 dummy scans, 0.341 s acquisition time, 25 Hz bandwidth for the water suppression presaturation pulse, 4096 x 256 data points, 12 ppm (6009 Hz) spectral width (both in F2 and F1), carrier frequency centred on the water resonance. Data were treated with sine window functions (both along F2 and F1) prior to FT in the phase-insensitive mode.

2.2.3. Assignment Of Metabolites And Database Search.

Spectra were processed with Bruker TOPSPIN 3.0 and analysed by means of Bruker AMIX 3.9.2 software package, allowing for mixture analysis and assignment of metabolite resonances through database search and match functions between experimental 2D/1D NMR spectra and spectra of single metabolites (the Bruker BBIOREFCODE 2.0 metabolite spectra database has been used for automated analysis, while peaklist search were done with the BMRB metabolomics database [http://www.bmrb.wisc.edu/]). In addition, database searches were done also with the human metabolome database [www.hmdb.ca]. Metabolites were matched to 2D-^{1}H,^{13}C HSQC, 2D-COSY and 1D spectra. 1D and 2D. Those databases mostly contains NMR data of samples dissolved in D_2O,

while we analysed CD_3OD samples. This implies that the database spectra are not fully comparable with our spectra. Therefore, for a number of compounds we acquired NMR spectra (1D, COSY and HSQC) of a number of true standards to confirm assignment.

2.2.4. Multivariate Analysis

For multivariate analysis, 7 extracts (either roots or leaves) from plants treated with copper and 7 extracts of controls were considered. Spectra were referenced to the residual methyl resonance of MeOD (3.34 ppm and 49.86 ppm for 1H and 13C, respectively). The alignment of the spectra was better if methanol is used to reference spectra rather than TSP. Raw NMR data were prepared for MVA analysis with Bruker AMIX 3.9.2. Bucketing of 1H-NMR spectra was done within the 10.00/-0.20 ppm range, with rectangular buckets of 0.02 ppm widths. Bucketed spectra were normalised against the weight of extract. The region corresponding to the residual solvent resonance was excluded from bucketing. The total number of buckets, under these conditions, was 490. These data were subjected to Principal Components Analysis (PCA).

2.2.4.1. Mass Spectrometry

Mass spectrometry is an analytical tool used for measuring the molecular mass of a sample. or large samples such as biomolecules, molecular masses can be measured to within an accuracy of 0.01% of the total molecular mass of the sample i.e. within a 4 Daltons (Da) or atomic mass units (amu) error for a sample of 40,000 Da. This is sufficient to allow minor mass changes to be detected. The sample has to be introduced into the ionisation source of the instrument.

Once inside the ionisation source, the sample molecules are ionised, because ions are easier to manipulate than neutral molecules. These ions are extracted into the analyser region of the mass spectrometer where they are separated according to their mass (m) -to-charge (z) ratios (m/z). The separated ions are detected and this

signal sent to a data system where the m/z ratios are stored together with their relative abundance for presentation in the format of a m/z spectrum (Morse et al, 2007).

2.3. Results and Discussions

2.3.1. Leaves

A typical ^{1}H-NMR spectrum of the methanol extract from *P. alba* leaves is shown in Figure 1A. The spectrum can be coarsely divided into the following spectral regions. **i)** Aliphatic region (0-5.4 ppm), where the resonances of C$\underline{H}_3$, C$\underline{H}_2$ and CH groups fall. This region shows a very intense resonance (at 1.3 ppm) due to the bulk CH_2 groups of fatty acids (including those of mono, di and triglycerides and lipids). In addition, the sub-region within 3-4.5 ppm contains very intense (and highly overlapped) signal, typically from sugars (including sugars phosphates), glycerine, alcohols and polyalcohols (C$\underline{H}_2$-OH and C$\underline{H}$-OH groups). The low field side of the aliphatic region contains the resonances of sugar anomeric protons (either mono or oligosaccharides).

ii) Olefin region (5.0-7.8 ppm). This region is typical of $\underline{H}$-C=C protons, that mostly fall at around 6 ppm. In the poplar extract, the most intense olefin resonances are those due to unsaturated fatty acids (mainly oleic acid and linolenic, either free or esterified, see Table 1). In the region around 6.3 ppm several low intensity doublets characterized by a coupling constant of about 16 Hz are detectable, that can be assigned to olefins with trans conformation of the double C=C bond.

The compounds giving raise to these signals have a much lower concentration than unsaturated fatty acids. It is worth noting that the signal intensity in ^{1}H NMR spectra are linearly proportional to the concentration of the spins, independently from the chemico-physical properties of the molecule. Therefore, the comparison of signal intensities can be interpreted int terms of true relative concentrations.

iii) Aromatic region (6.5-10.0 ppm). Most of the aromatic resonances fall in the 6.6-8.1 sub-region, and mostly belong to benzoic acid, saligenin and related compounds, and catechols (see Table 1)

Overall, 1H-NMR spectra showed a good chemical shift reproducibility, as shown in Fig. 2. except for limited spectral regions: in the aliphatic, some chemical shift variability was found in the 2.18-2.26 ppm range (this region contains a triplet that shift significantly), 2.50-2.53 ppm (shifting singlet). The reasons for such a variability are likely attributable to inter-subject variability of matrix chemico-physical properties, such as pH. Such differences in matrix properties prevented to use the signal of TSP (an organic acid) as a reference for chemical shift. Using the signal of methanol as a reference standard allowed for a better spectral alignment.

Another source of variability can be attributed to ongoing biochemical processes that might alter the concentration of metabolites and also modify pH in a time dependent manner.

The metabolic stability was assessed in preliminary experiments where noesy1d NMR spectra of freshly prepared leaf extracts were analysed immediately and after 8, 24 and 48 hours (sample kept at T=300 K). It was found that these spectra were perfectly superposable, indicating that samples are perfectly stable.

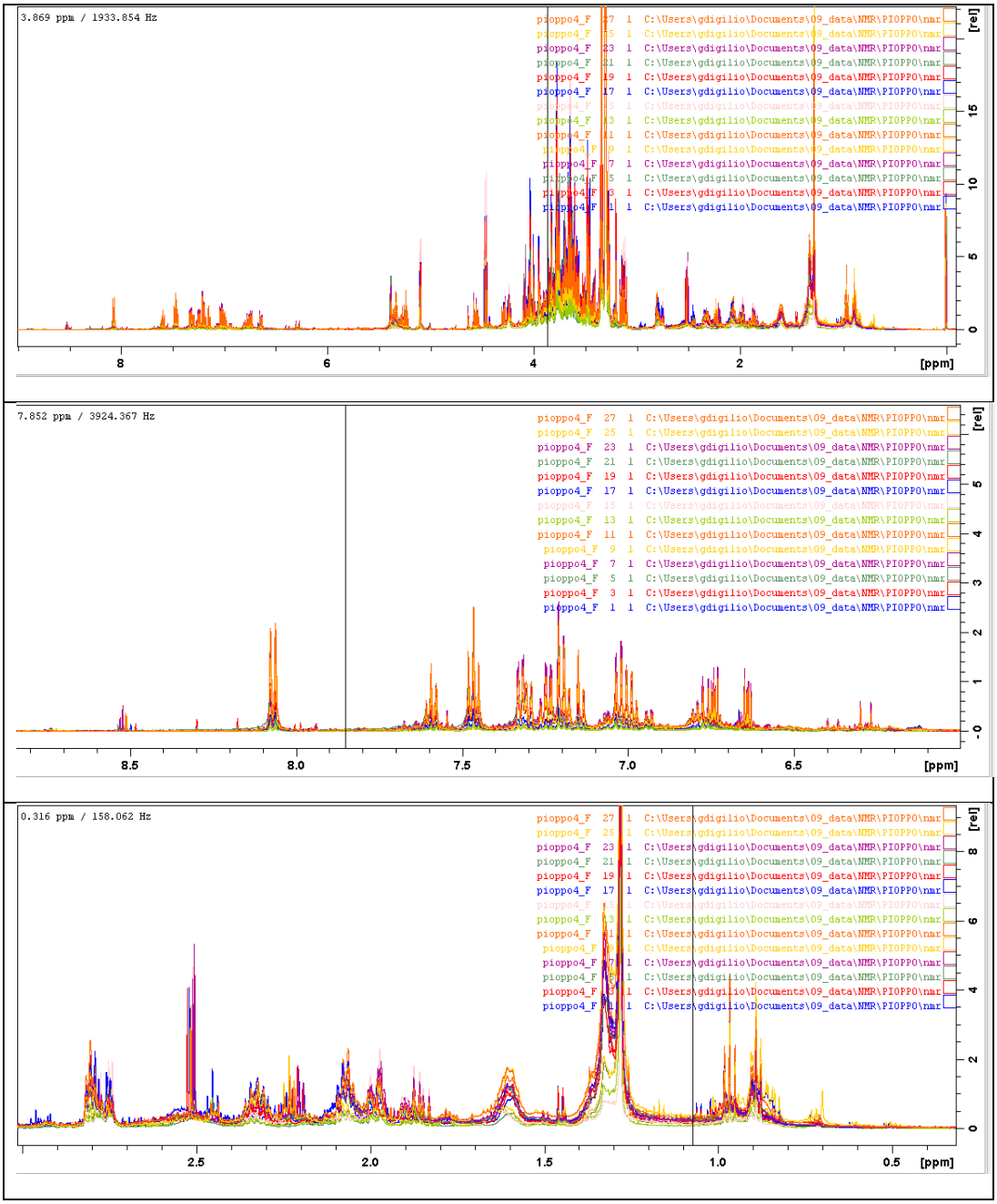

Fig 5: Superpostion of 14 spectra of *P.alba* leaf extract, with expansion of selected spectral regions.

The assignment of metabolite resonances was achieved by: ***i)*** analysis of 2D-^{1}H,^{13}C-HSQC and 2D-COSY spectra (Fig. 5 respectively) ***ii)*** Automated or manual database search with the Bruker BBIOREFCODE 2.0.0 metabolite spectra database, and/or spectral search with the BioMagResBank (BMRB) database or Human Metabolomics database (both 1D and 2D NMR spectra). It is worth noting

that available databases contain mostly data acquired in D_2O, therefore being not fully comparable with our data in methanol; **iii)** spectral match with 1D or 2D spectra in methanol of true standards; iv) ESI-MS spectra were used to confirm NMR assignments.

We have unambiguously assigned as many as 9 metabolites (benzoic acid and esters, salicin, salicortin and phenolic glycosides (Boeckler et al, 2011) catechol, D-glucose, choline and derivatives, oleic acid, linolenic acid). While saligenin and its many derivatives were detected at moderate to high concentration, salicylate and derivatives could not be detected. In addition to these compounds we detected several (at least four) cinnamic acid derivatives, di-polysaccharides, but the resonances could not be assigned to a specific member of this class of compounds. Finally, resonances from precursors of cell wall/lignin components could be found. Assigned spectra and a full listing of assigned signals are given in Figure 1 and in Table 1. To the best of our knowledge this is the first report about the detection by NMR-based metabonomics of saligenin based secondary metabolite at high levels.

The ensemble of compounds that are extracted by our procedure is very different from those available in the literature (but from leaves of plant other than *P. alba*) (Sobolev et al, 2005). A number of compounds that are typically found in water or water/methanol extract from leaves of a variety of plants are not extracted with our procedure (for instance, amino-acids, kaempferol, quercetin, ascorbic acid, chlorogenic acid, phytols). As a matter of facts, we have prepared a number of methanol solutions of true standards of compounds that are usually found in plant extracts. These standard spectra were used to check whether those compounds were present in our methanol extracts and we found that L-Serine, alanine, β-alanine, tyrosine, leucine, tryptophan, myo-inositol, ferulic acid, lactic acid, ascorbic acid, folic acid, lysine, glutamine, histidine, glutamic acid, fumaric acid, citric acid, fosforic acid, salicylic acid, shikimic acidsorbic acid, nicotinic acid, quercetin, and catechin could not be detected.

The poor comparability between our methanol extract and literature data of leaves is strongly dependent on the extraction protocol, as literature data are mostly relative to water/methanol extracts (Verpoorte et al, 2007).

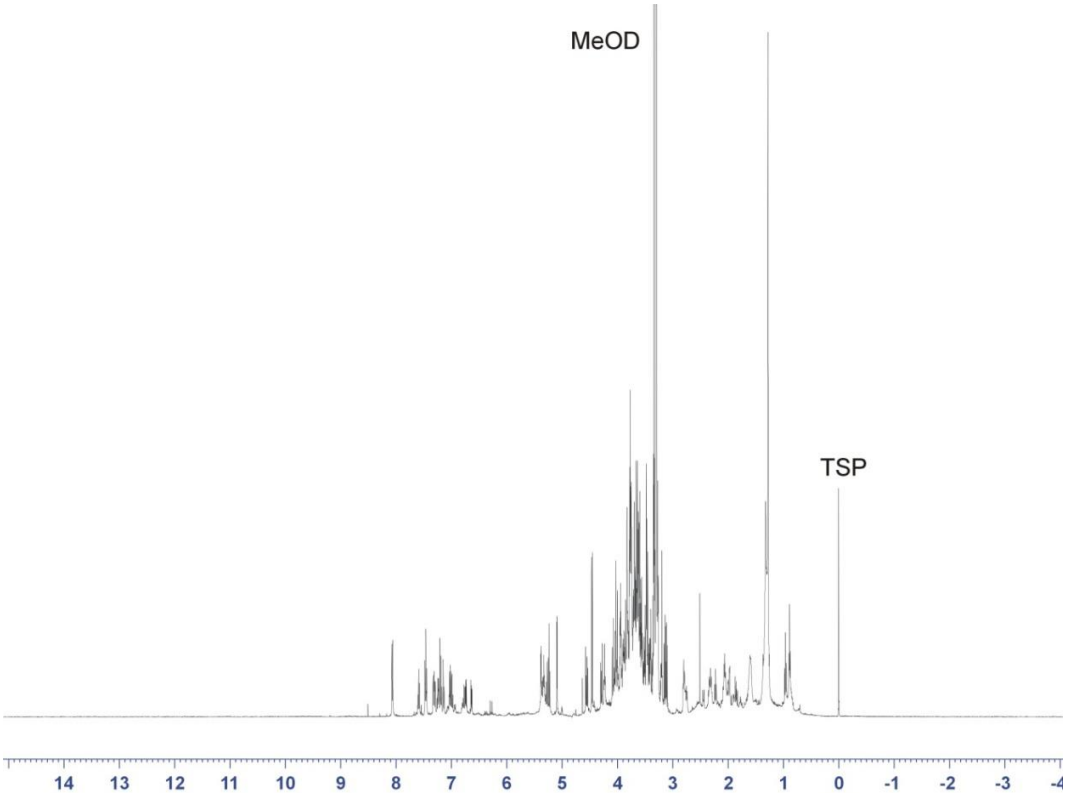

Fig. 6A Overview of the ^{1}H-NMR spectrum of the methanol extract of leaves from *Populus alba* (sample CF7, 1D-noesy pulse sequence, with pre-irradiation of the residual MeOH proton, 300 K).

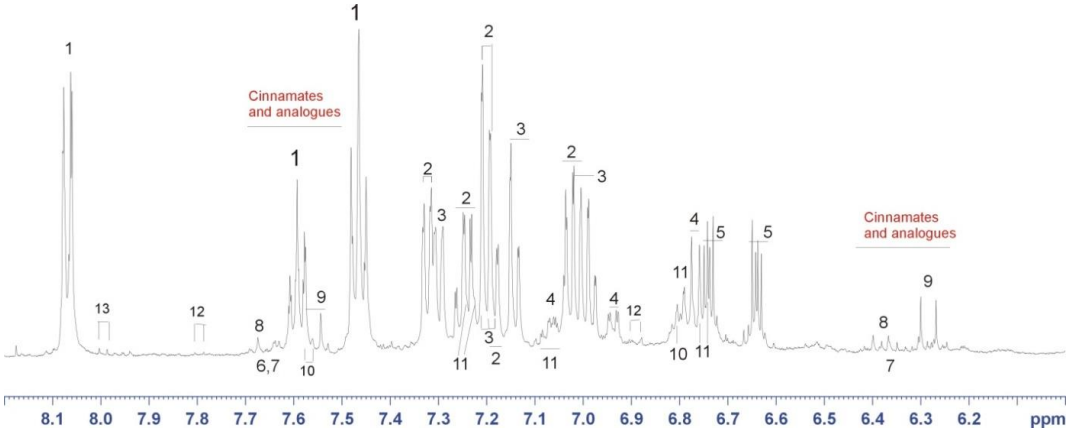

Fig. 6B Expansion in the range 8.2-6.0 ppm of the ^{1}H-NMR spectrum shown in Fig. 6A (Y-magnification 4x) with resonance assignment (see Tab. 2 for symbols).

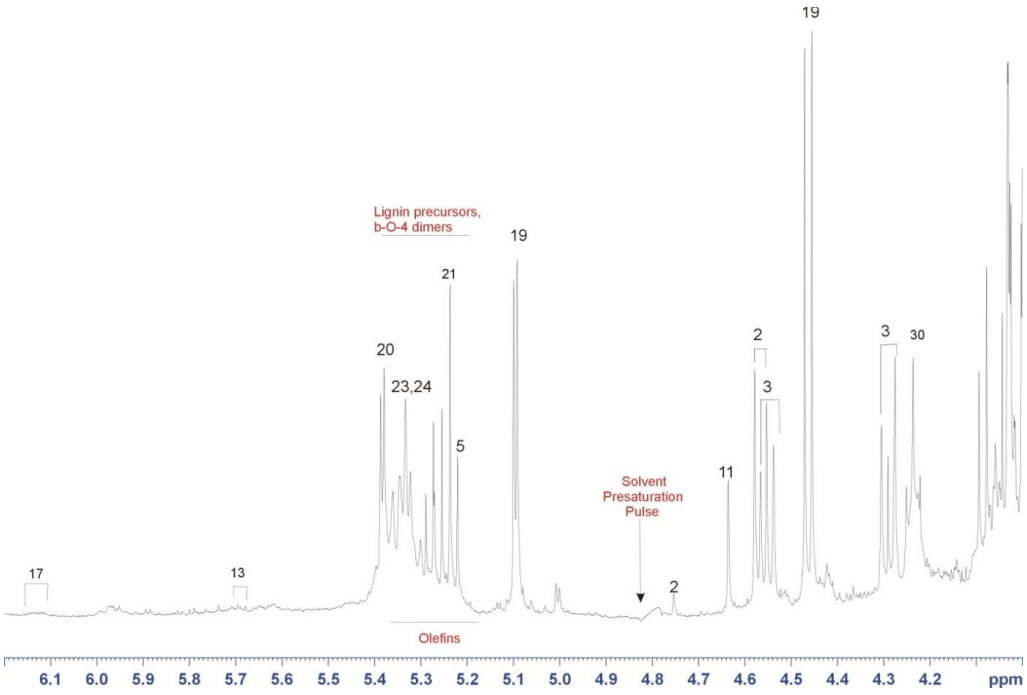

Fig. 6C Expansion in the range 6.2-4.0 ppm of the ^{1}H-NMR spectrum shown in Fig. 6A (Y-magnification 4x) with resonance assignment (see Tab. 2 for symbols).

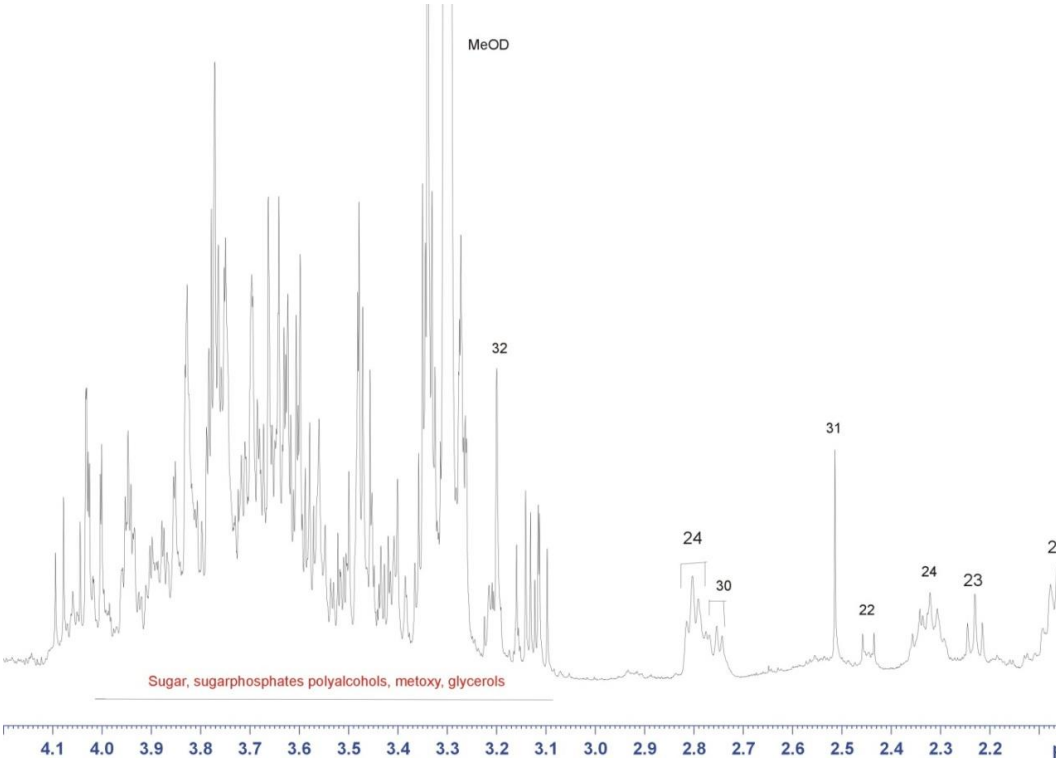

Fig. 6D Expansion in the range 4.2-2.0 ppm of the ^{1}H-NMR spectrum shown in Fig. 6A (Y-magnification 4x) with resonance assignment (see Tab. 2 for symbols).

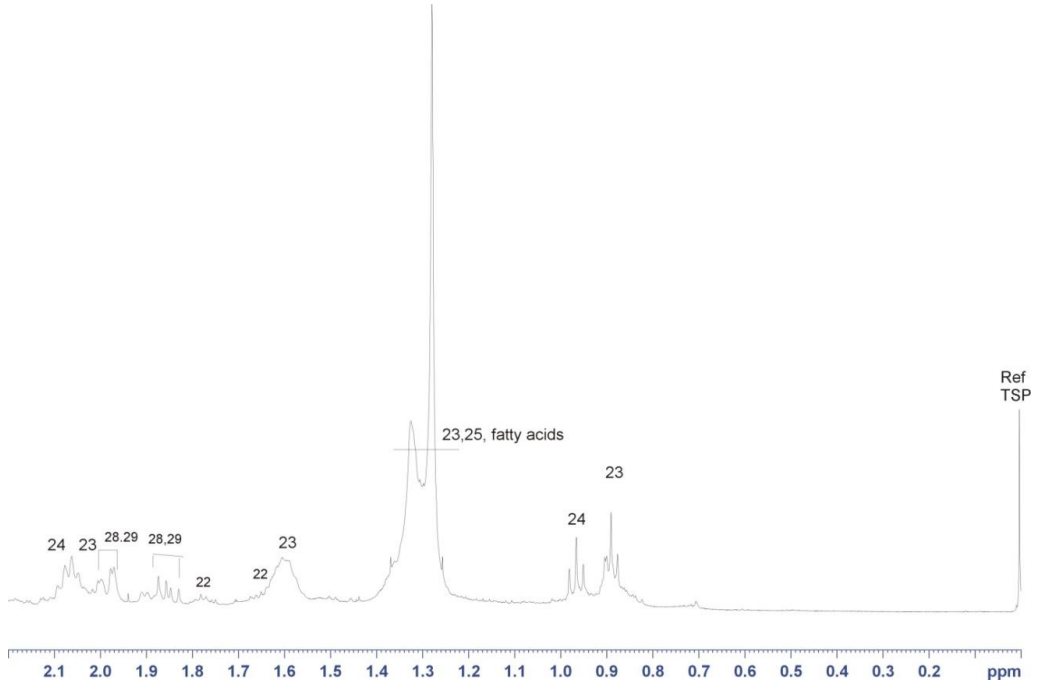

Fig. 6E Expansion in the range 2.2-0.0 ppm of the ^{1}H-NMR spectrum shown in Fig. 6A (Y-magnification 4x) with resonance assignment (see Tab. 2 for symbols).

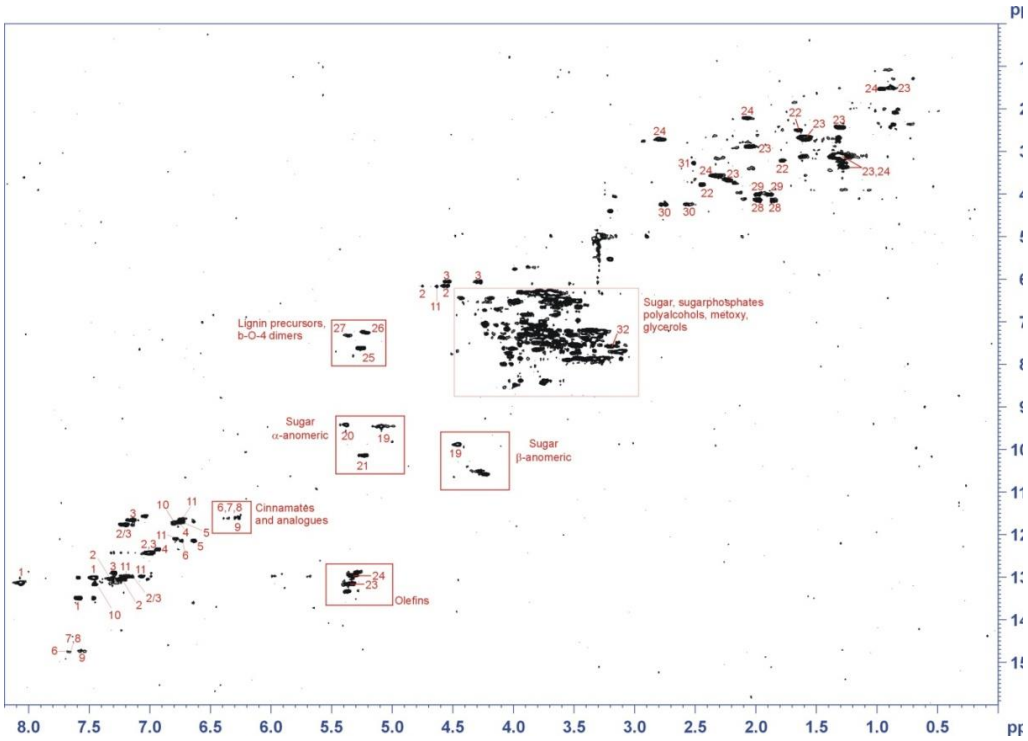

Fig. 7 ^{1}H, ^{13}C HSQC spectrum of *Populus alba* leaves methanol extract (sample CF7, T=300 K) with assignment (see Tab. 2 for abbreviations).

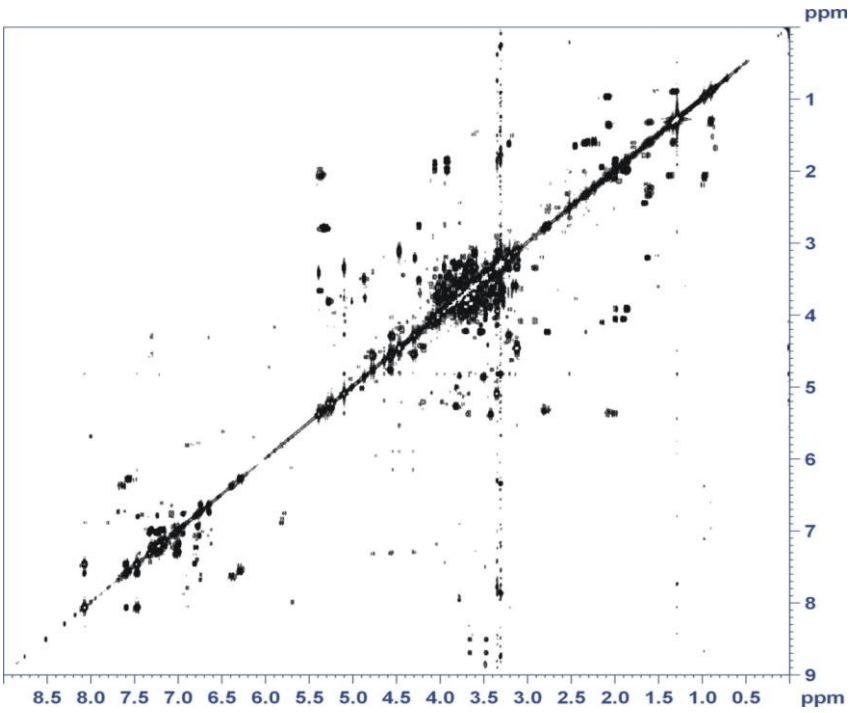

Fig. 7A Overview of the $^{1}H,^{1}H$ COSY NMR spectrum of *Populus alba* leaves methanol extract (sample CF7, T=300 K)

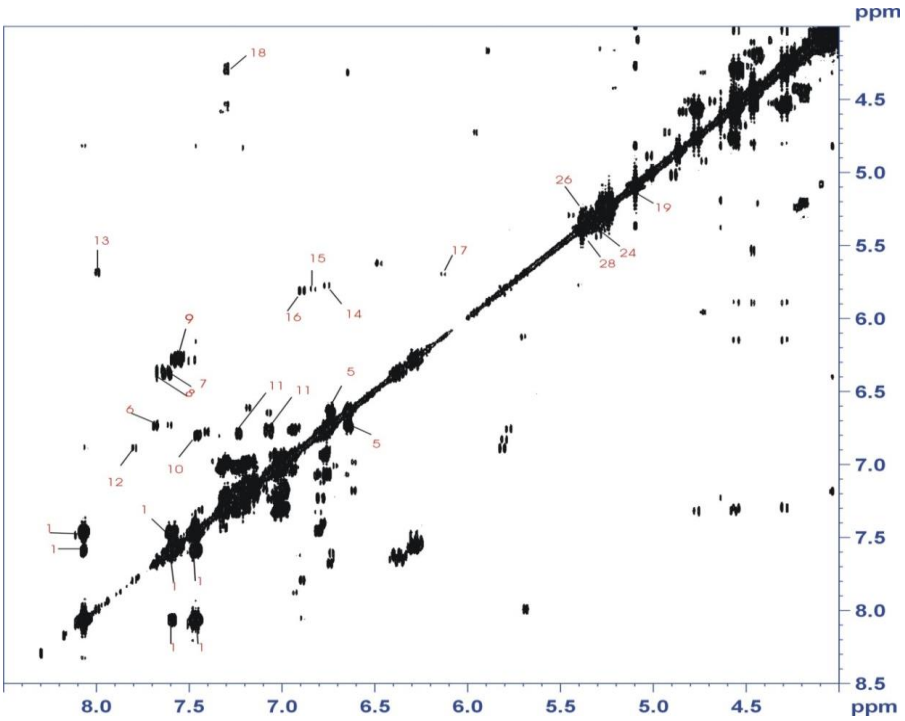

Fig. 7B Expansion (8.5-4.0 ppm) of the $^{1}H,^{1}H$ COSY NMR spectrum of *Populus alba* leaves methanol extract (sample CF7, T=300 K) with assignment (see Tab. 2 for abbreviations).

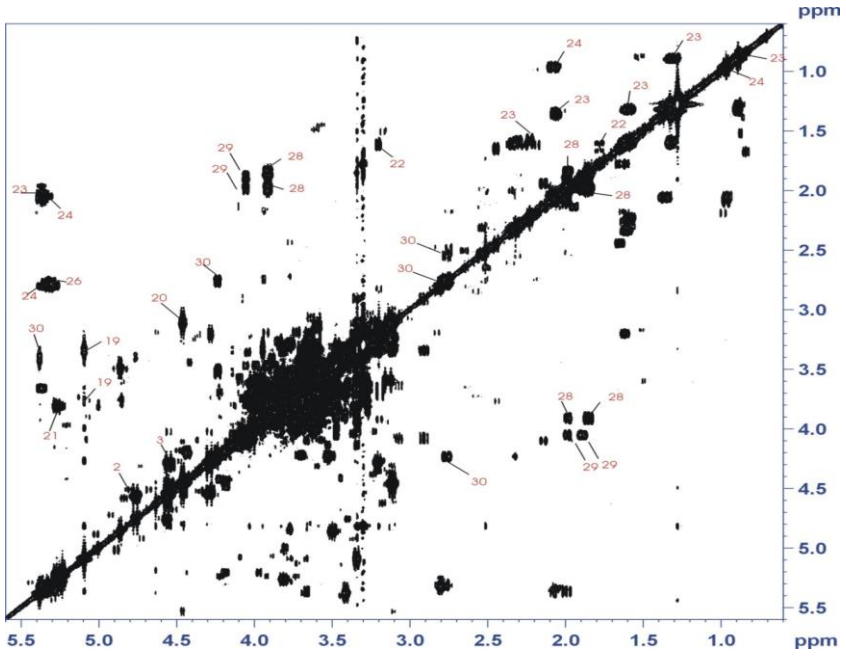

Fig. 7C Expansion (5.6-0.6 ppm) of the $^{1}H,^{1}H$ COSY NMR spectrum of *Populus alba* leaves methanol extract (sample CF7, T=300 K) with assignment (see Tab. 2 for abbreviations).

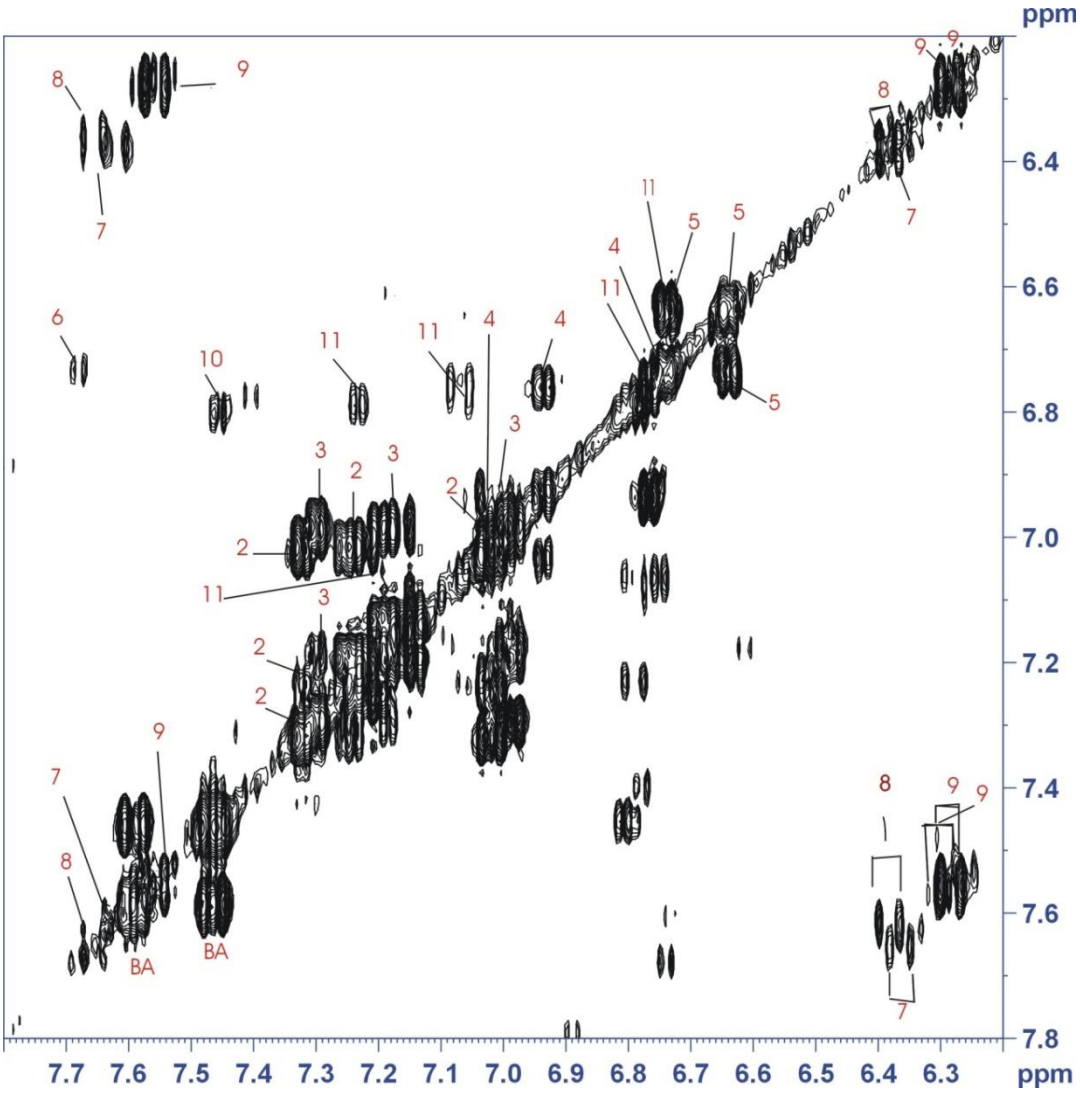

Fig. 7D: Expansion (7.9-6.2 ppm) of the $^{1}H,^{1}H$ COSY NMR spectrum of *Populus alba* leaves methanol extract (sample CF7, T=300 K) with assignment (see Tab. 2 for abbreviations).

Tab. 2 List of the metabolites identified by NMR and ESI-MS in the methanol extract of *Populus alba*. ^{1}H and ^{13}C chemical shifts (ppm) are referenced to 0.5 mM TSP. Metabolites were found in both leaves and roots if not specified otherwise in column "Notes".

Metabolite	^{13}C-chemical shifts from HSQC (ppm)	^{1}H-Chemical shifts (ppm) and multiplicity	ESI-MS	Notes
1 – Benzoic acid (and esters) 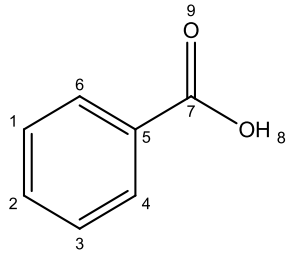	132.7 (C3) 131.5 (C4) 136.3 (C5)	8.06 (H3, d) 7.47(H4, t) 7.58 (H5, t)	Theor. 122.12 Found: nd	Consistent with bmse000300 [a]
2 – Salicin 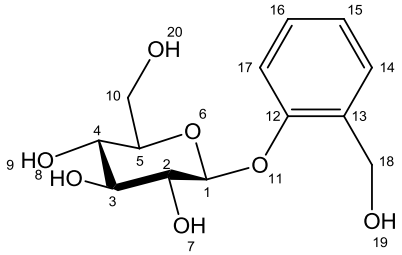	130.4 (C14) 124.2 (C15) 130.4 (C16) 117.6 (C17) 61.6 (C18)	7.32 (H14, dd) 7.02 (H15, td) 7.25 (H16, m) 7.21 (H17, dd) 4.56 (H18a, d) 4.76 (H18b, d)	Theor. 286.27 Found: M+H:287 M+Na :325 weak	Fully super passable with HMDB03546 [b]

3 – Saligenin Containing Phenolic Glycosides 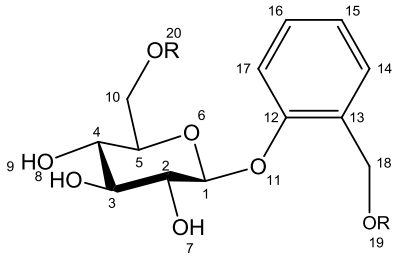 	129.0 (C14) 124.2 (C15) 129.8 (C16) 116.5 (C17) 60.3 (C18)	7.30 (H14, dd) 6.98 (H15, td) 7.19 (H16, m) 7.13 (H17, dd) 4.55 (H18a, d) 4.28 (H18b, d)	Salireposide (**3a**), [c] Theor. 406,38 Found: 429,25 ($M+Na^+$), 445,25 ($M+K^+$) Tremuloidin (**3b**) [d] Theor. 390,38 Found: 413,24 ($M+Na^+$), 429,25 ($M+K^+$) 2'-O-acetylsalicortin (**3c**) Theor. 326,34 Found: 349,16 ($M+Na^+$), 365,23 ($M+K^+$) HCH Salicortin (**3d**) Theor. 562,52 Found: 585 ($M+Na^+$), 601 ($M+K^+$) weak Populoside and Populoside A (**3e**) ($M+H^+$):449,27 ($M+Na^+$): 458,62 weak Populoside B (**3f**) [e]	

			Theor. 562,52 Found:413,24 ($M+Na^+$), 429,25 ($M+K^+$) Populoside C (**3g**) (M+H):463,12 M+Na: 485,16 weak	
4 - Unknown	117.0 123.5 ?	6.76 6.93 7.03		
5 – Catechol 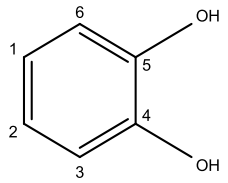 	117.0 (C3, C6) 121.46 (C1, C2)	6.76 (H3, H6 m) 6.64(H1, H2 m)	Theor. 110.11 Found: nd	Consistent with bmse000385 [a]
6 – Cinnamic Acid derivatives	147.5 (C2) 121.4 (C1)	7.68 (H2, d) 6.73 (H1, d)		

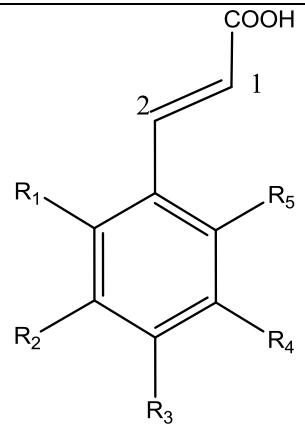				
7 - Cinnamic Acid derivatives	147.5 (C2) 116.1 (C1)	7.65 (H2, d) 6.37 (H1, d)		
8 - Cinnamic Acid derivatives	? 116.1 (C1)	7.61 (H2, d) 6.38 (H1, d)		
9 - Cinnamic Acid derivatives	147.3 (C2) 116.1 (C1)	7.56 (H2, d) 6.28 (H1, d)		
10 – Unknown		7.45 6.80		

11 – Saligenin 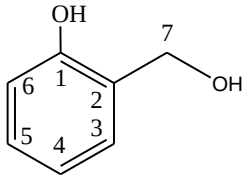 	129.8 (C3) 120.8 (C4) 129.8 (C5) 116.4 (C6) 61.6 (C7)	7.231 (H3) 6.79(H4) 7.07 (H5) 6.75 (H6) 4.63 (H7)	Theor. 124.14 Found: nd	Exact match with 2D-COSY and 2D-HSQC spectra of true standard.
12 – Unknown		7.79 6.89		
13 – Unknown		7.99 d 5.68 d		
14 – Unknown		6.75 5.77		
15 – Unknown		6.83 5.79		
16 – Unknown		6.89 5.80		

17 – Unknown		6.13 5.70		
18 – Unknown	105.1	7.30 d 4.28 d		
19 – D-Glucose	95.9 (C1, α) 100.1(C1,β,)	5.09 (H1, d) 3.33 (H2, d) 4.46 (H1, d) 3.11 (H2, d)		
20 – Disaccharides	95.6 (anomeric C)	5.37 (anomeric H)		
21 – Other Sugar Anomeric	101.3 (anomeric C)	5.23 (anomeric H) 3.80 (H2)		
22 – Unknown	37.6 (C)	2.44 (H) 1.78 (H) 1.64 (H)		
23 – Oleic Acid				

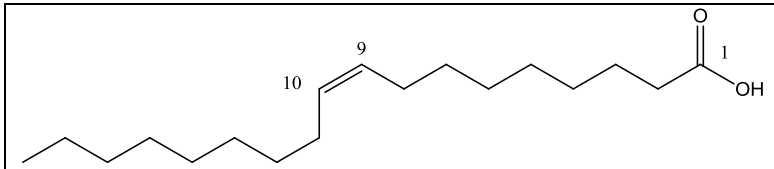				
	16.3 (C18) 16.4(bulk CH_2 132.7(C9-C10) 30.1 (C11-C18) 27.9 (C3) 28.0 (C2)	0.88 (H18, t) 1.31 (bulk $–CH_2$) 5.35 (H9-H10, overlap) 2.03 (H11-H8, overlap) 1.59 (H3, m) 2.26 (H2, t)		Exact match with 2D-COSY and 2D-HSQC spectra of true standard.
24 – Linolenic Acid 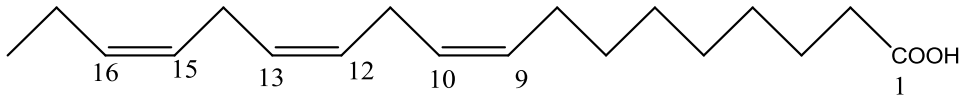				
	15.1 (C18) 22.0 (C17) 129.6 (C=C) 27.0 (C14, C11) 16.4(bulk CH_2	0.96 (H18, t) 2.07 (H17, m) 5.35 (HC=C, m) 2.80 (H14, H11, m) 1.31 (bulk $–CH_2$) 2.33 (H2, m)		Leaf only

	35,6 (C2)			
25 – Lignin Precursors b-O-4 Dimers, 2 Carbon Sidechain (Ambiguous) 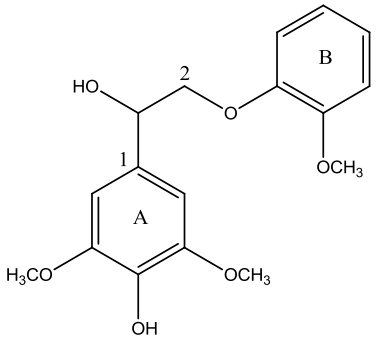	76.2 (C1)	5.27 (H1)		Consistent with bmse010213 or 010013 [a]
26 – See 25	72.5 (C1)	5.22 (H1)		As 25
27 – See 25	73.2 (C1)	5.37 (H1)		As 25
28 – Unknown AMX	ca 65-78 41.3 (CM, CX)	3.91 (HA) 1.98 (HM) 1.85 (HX)		

29 – Unknown AMX	ca 65-78 40.1 (CM, CX)	4.05 (HA) 1.99 (HM) 1.89 (HX)		
30 – Unknown AMX	ca 65-78 42.3 (CM, CX)	4.23 (HA) 2.54 (HM) 2.76 (HX)		
31 – Succinic Acid (Ambiguous) 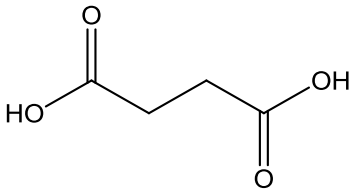	32.6 (C)	2.52 (H, s)		
32 – Choline 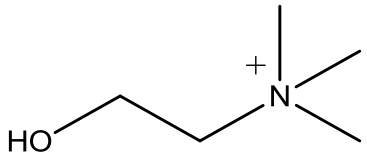	75.7 (CH_3)	3.20 (CH_3)	Theor.: 104.17 Found: 104.03 (M^+)	

33 – Unknown	131.3 125.7	8.06 7.44 7.21		Roots only
34 – (+)-Catechin 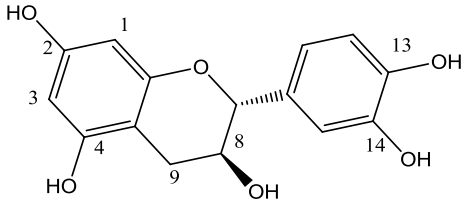 	115.9 (C15) 116.6 (C12) 120.6 (C11) 96.8 (C3) 96.0 (C1) 83.4 (C7) 69.3 (C8) 29.0 (C9) 29.0 (C9)	6.83 (H15) 6.75 (H12) 6.71 (H11) 5.93 (H3) 5.85 (H1) 4.56 (H7) 3.97 (H8) 2.84 (H9a) 2.50 (H9b)		Roots only

[a] The reference spectra used to identify metabolites were taken from the Biological Magnetic Resonance (BMRB) Data Bank – Metabolomics (http://www.bmrb.wisc.edu/metabolomics/). The number provided is the BMRB database accession number.

[b] The reference spectra used to identify metabolites were taken from the Human Metabolome Database (HMDB) (http://www.hmdb.ca/). The number provided is the HMDB database accession number.

[c] Other phenolic glucosides having the same mass of salireposide are deltoidin and Nigracin Salicyloylcalicin (Boeckler, 2011)

[d] Other phenolic glucosides having the same mass of tremuloidin are populin and chaenomeloidin (Boeckler, 2011)

[e] Other phenolic glucosides having the same mass of Populoside B is trichocarposide (Boeckler, 2011).

2.3.2 Roots

Most part of assignment of composts in leaf samples (salicin, saligenin, saligenin derives, oleic acid, monosaccharides, polysaccharides, benzoic acid, cinnamic acid derives, catechol, lignin precursors) there are also exist in root samples with different concentrations. But in root samples there is not linolenic acid. Additionally, there is catechin in root samples which it had been supported with standard analysis.

It has shown in the Figure 5, Figure 6A, 6B, 6C, 6D colour red indicates leaf samples and black colour indicates root samples.

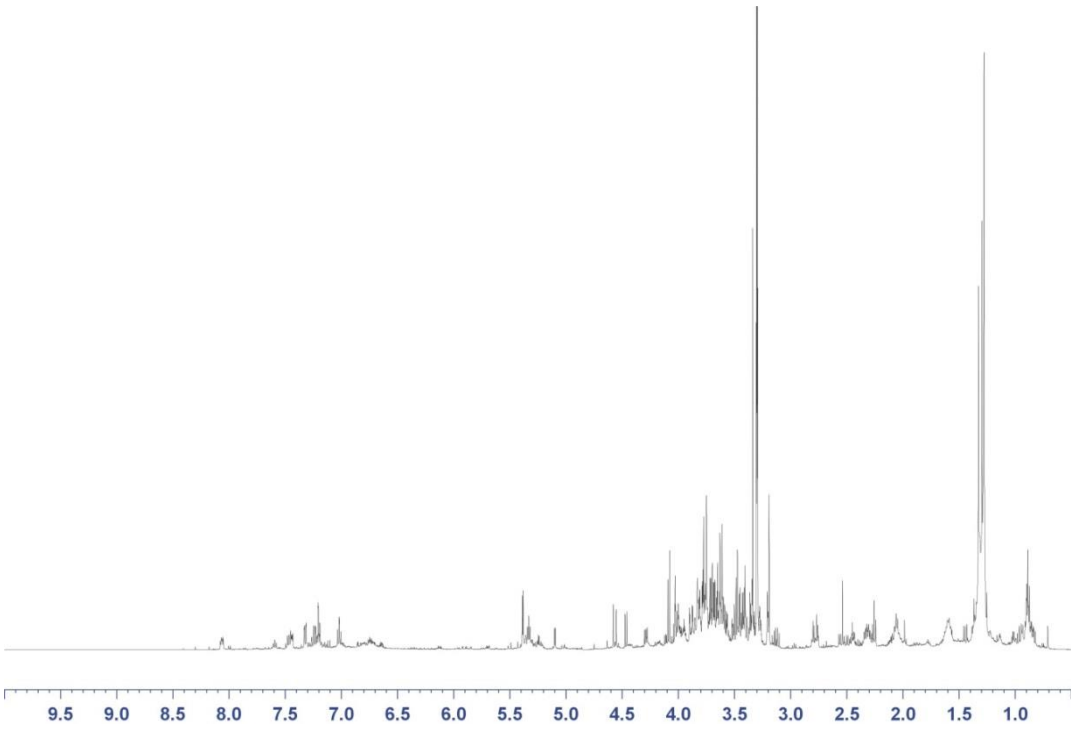

Fig. 8A : Overview of the ^{1}H-NMR spectrum of the methanol extract of roots from *Populus alba* (sample CR7, 1D-NOESY pulse sequence, with pre-irradiation of the residual MeOH proton, 300.0 K).

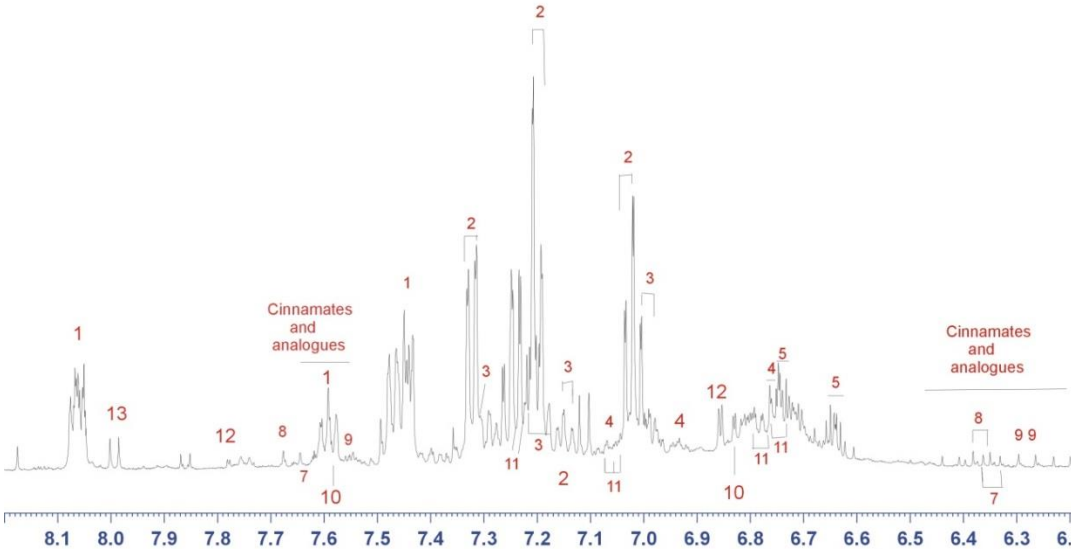

Fig. 8B : Expansion in the range 8.2-6.0 ppm of the ^{1}H-NMR spectrum shown in Fig. 8A (Y-magnification 4x) with resonance assignment (see Tab. 2 for symbols).

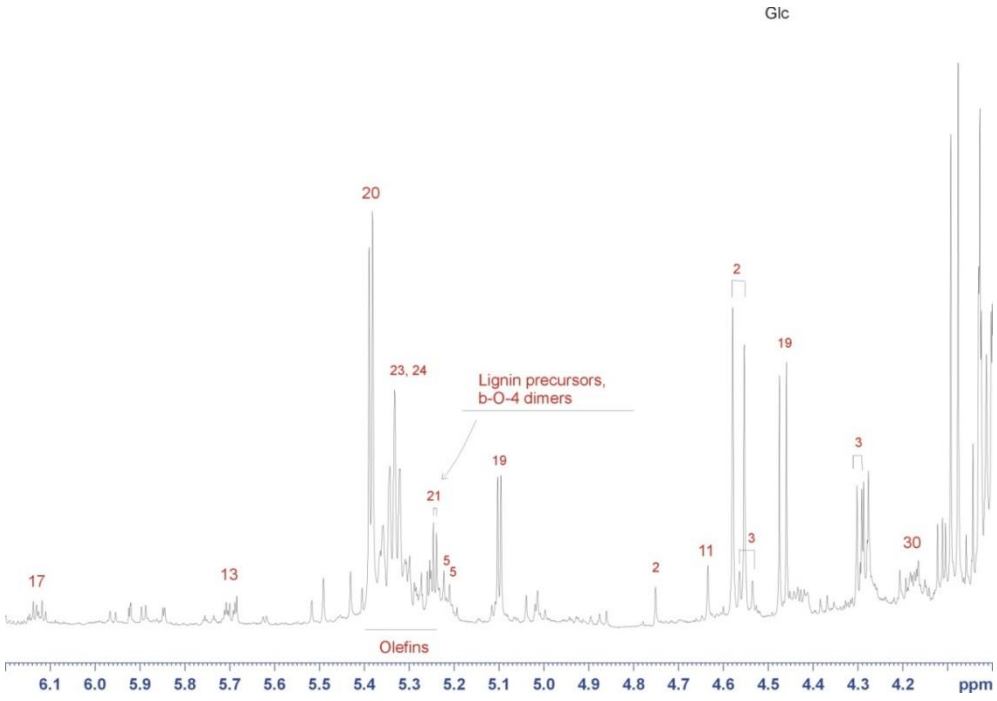

Fig. 8C : Expansion in the range 6.2-4.0 ppm of the ^{1}H-NMR spectrum shown in Fig. 8A (Y-magnification 4x) with resonance assignment (see Tab. 2 for symbols).

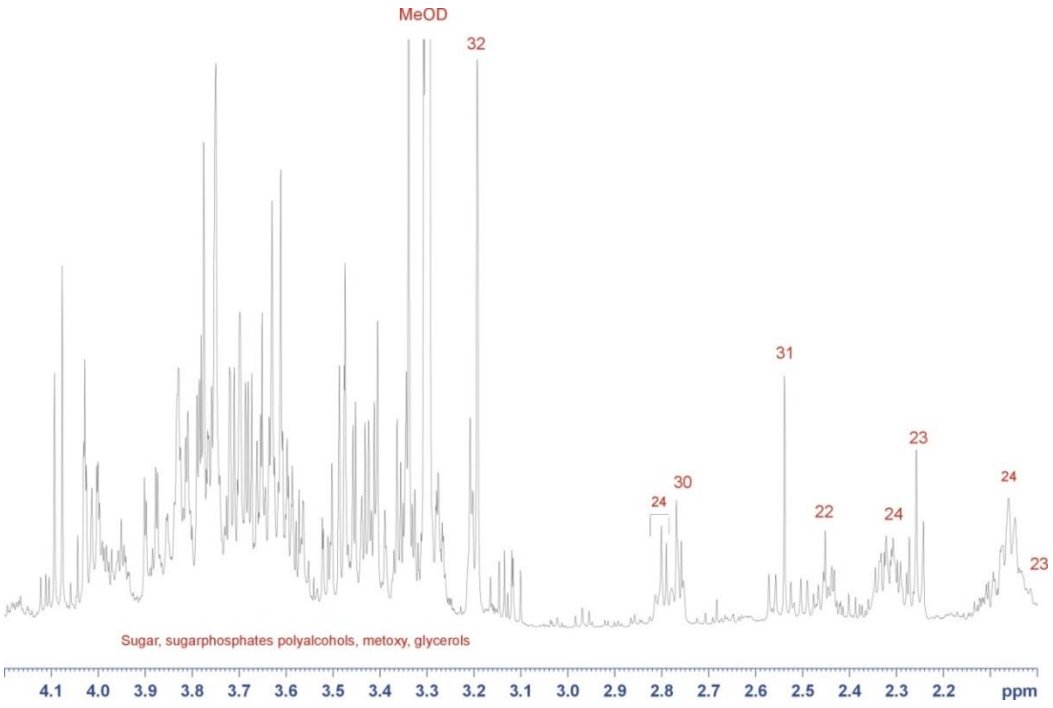

Figure 8D :Expansion in the range 4.2-2.0 ppm of the ^{1}H-NMR spectrum shown in Fig. 8A (Y-magnification 4x) with resonance assignment (see Tab. 2 for symbols).

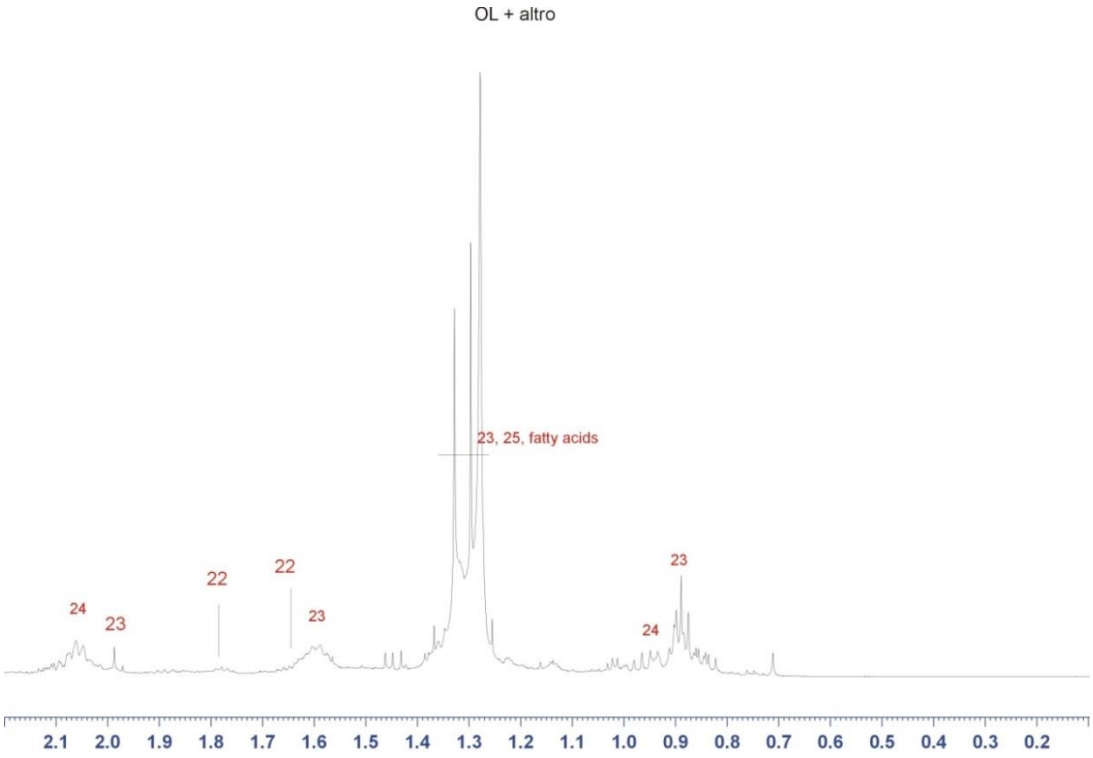

Fig. 8E : Expansion in the range 2.2-0.0 ppm of the ^{1}H-NMR spectrum shown in Fig. 8A (Y-magnification 4x) with resonance assignment (see Tab. 2 for symbols).

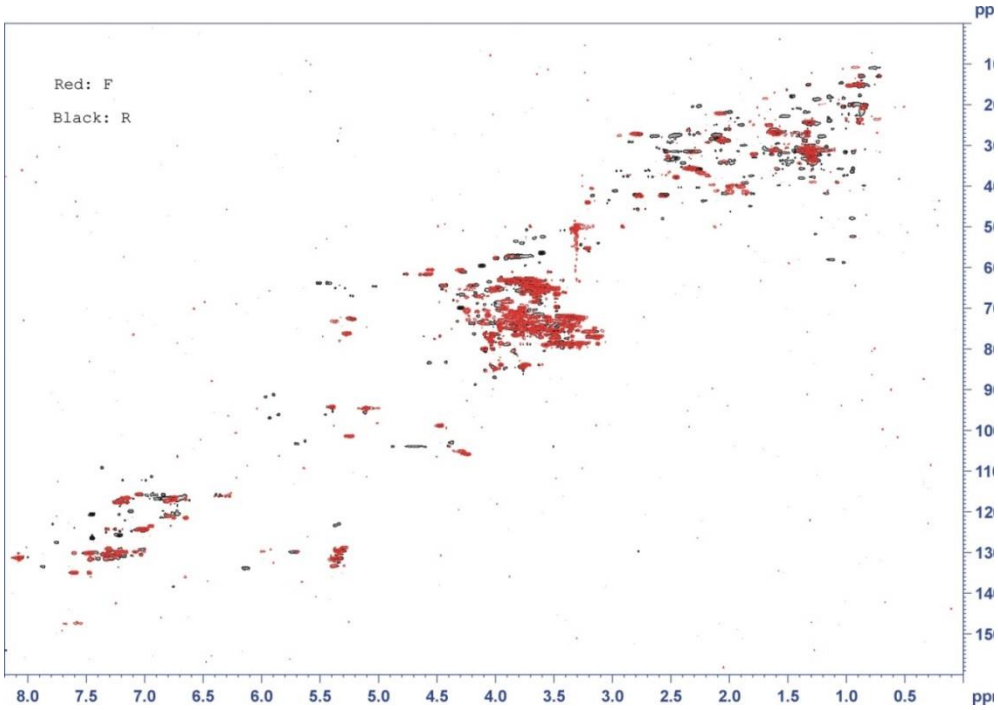

Fig. 9 : $^{1}H,^{13}C$ HSQC spectrum of *Populus alba* roots methanol extract (sample CR7, T=300 K), (F: Leaf, R: Root).

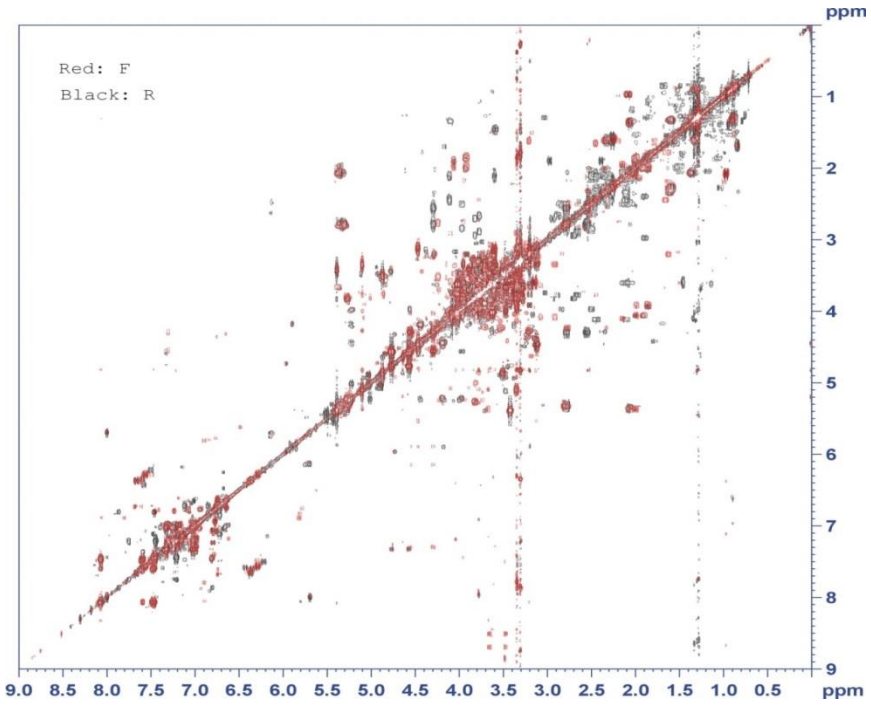

Fig. 10A : Overview of the $^{1}H,^{1}H$ COSY NMR spectrum of *Populus alba* roots methanol extract (sample CR7, T=300 K), (F: Leaf, R: Root).

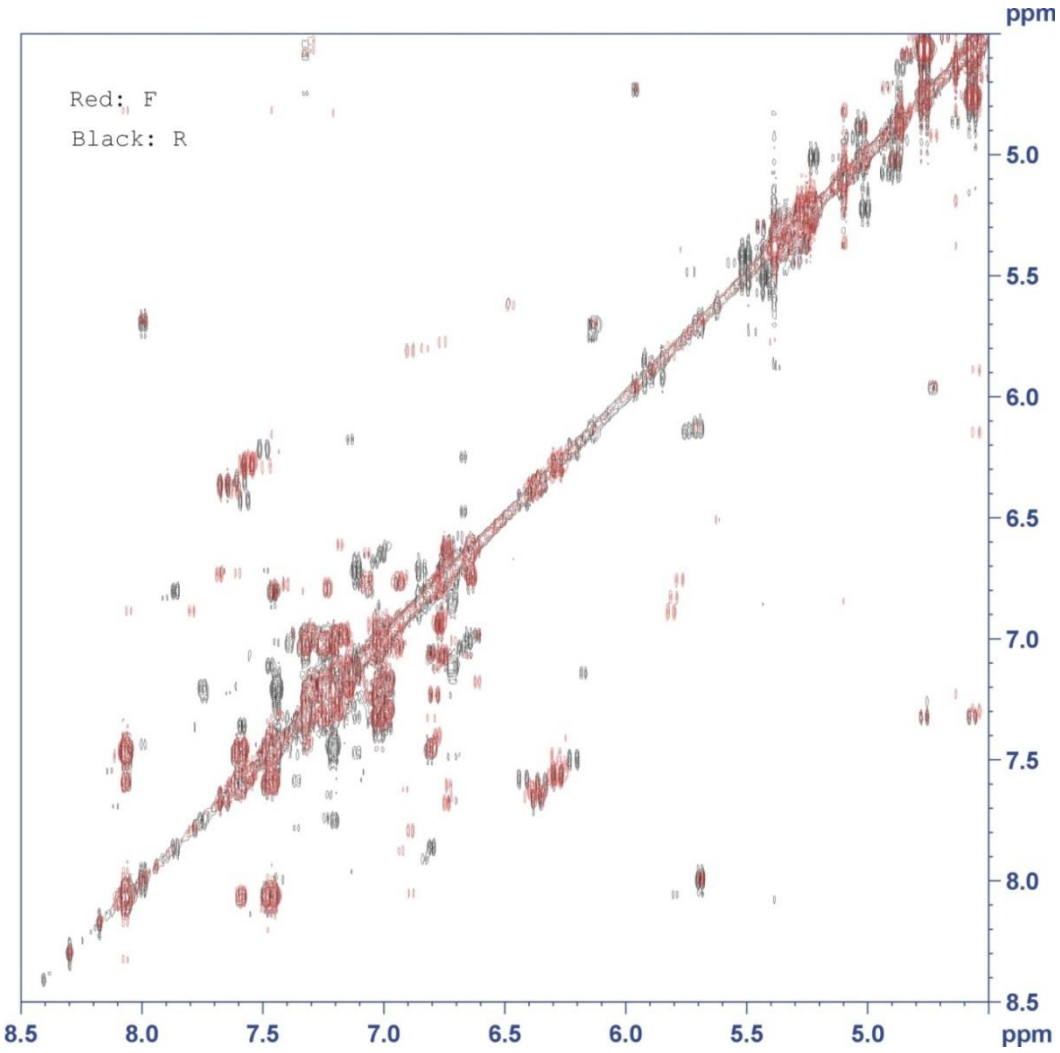

Fig. 10B : Expansion (8.5-4.5 ppm) of the $^{1}H,^{1}H$ COSY NMR spectrum of *Populus alba* roots methanol extract (sample CF7, T=300 K, (F: Leaf, R: Root).

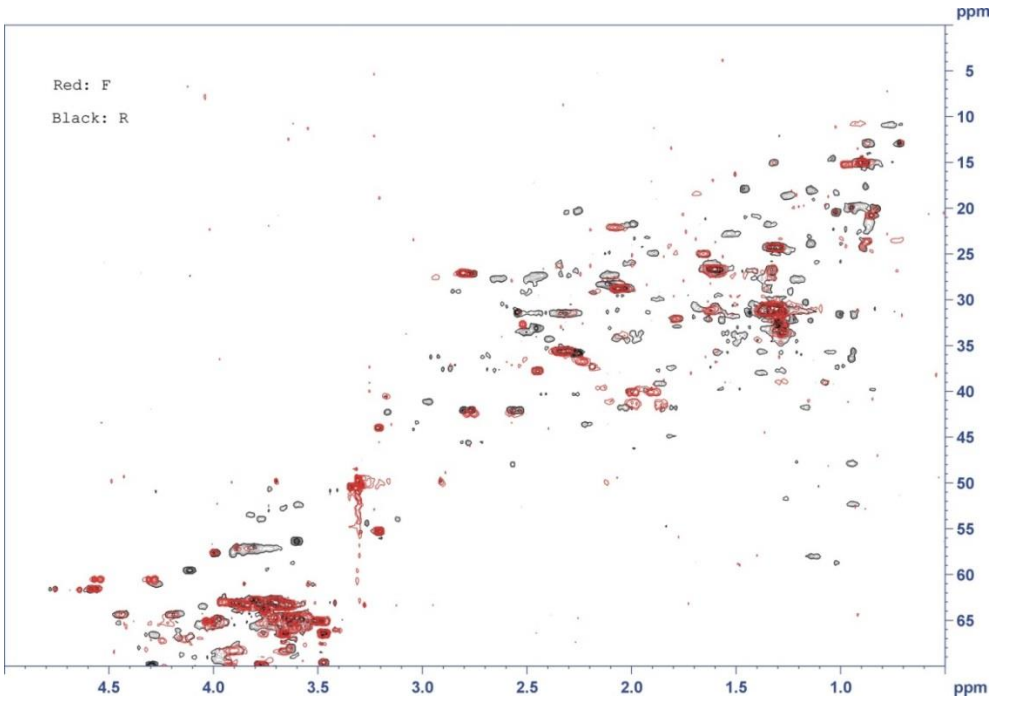

Fig. 10C : Expansion (5.0-0.6 ppm) of the $^{1}H,^{1}H$ COSY NMR spectrum of *Populus alba* roots methanol extract (sample CF7, T=300 K), (F: Leaf, R: Root).

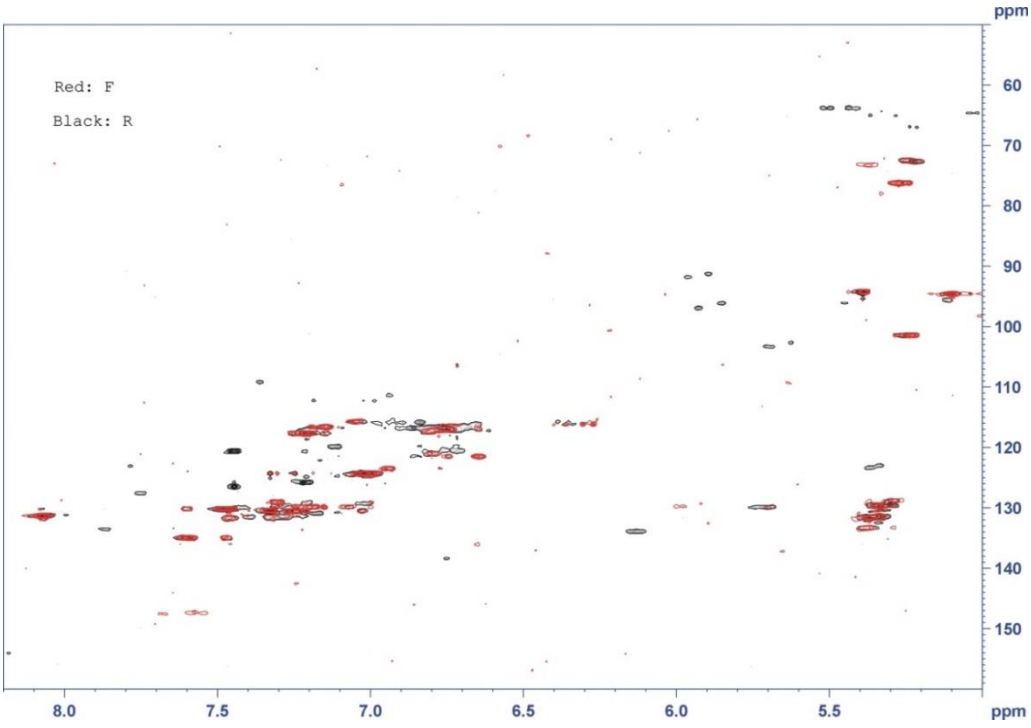

Fig. 10D : Expansion (8.2-5.0) ppm) of the $^{1}H,^{1}H$ COSY NMR spectrum of *Populus alba* roots methanol extract (sample CF7, T=300 K), (F: Leaf, R: Root).

2.4. Mass Spectroscopy

2.4.1. Experimental Details of MS(ESI)

Mass spectra were recorded on electrospray ionization (ESI) mass spectrometer (MS, Waters 515 HPLC pump-3100 mass detector) by direct infusion (200 µL/min) of suitably diluted samples in methanol/water/TFA 90:10:0.1% (v/v). Mass spectra were recorded in the ESI+ mode with capillary voltage 4.00 kV, cone voltage 40 V, source temperature 110 °C, desolvation temperature 250 °C.

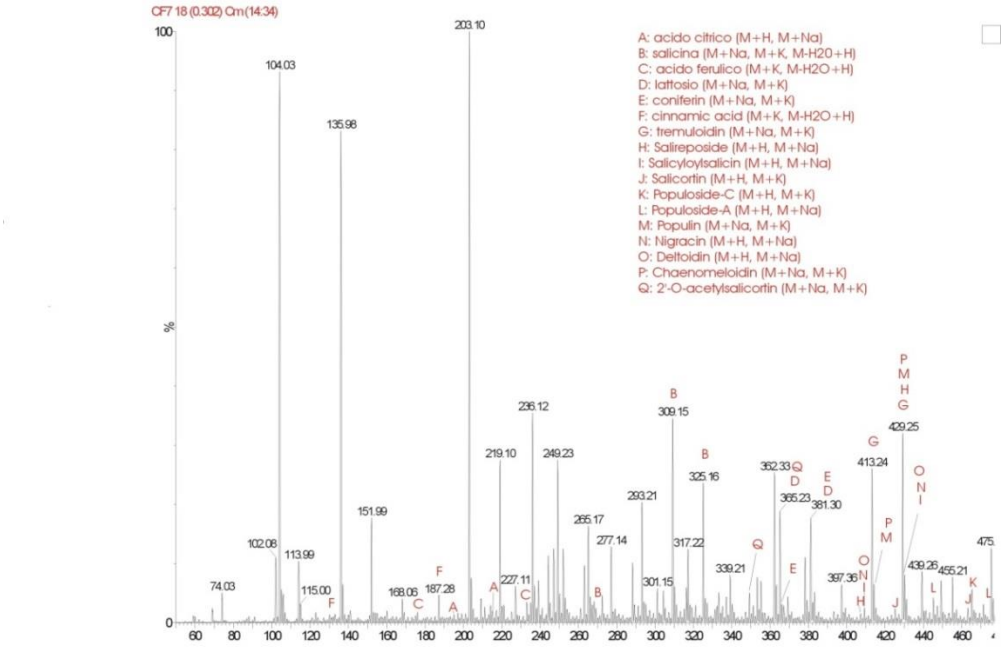

Fig. 11: LC-ESI$^+$ mass spectrum (direct infusion) of leaf methanol extract from *P. alba* with partial assignment of m/z peaks.

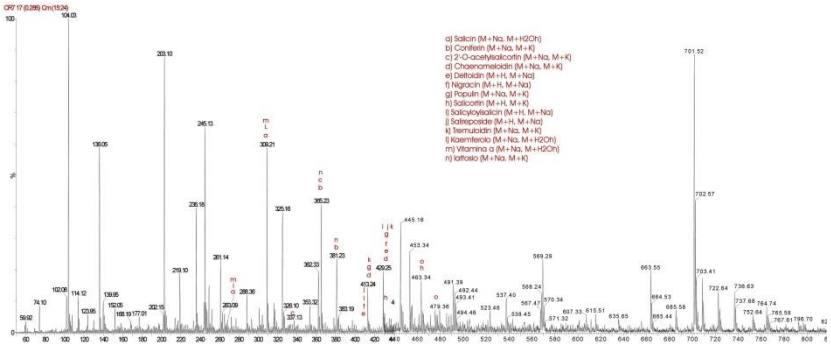

Fig. 12: LC-ESI$^+$ mass spectrum (direct infusion) of root methanol extract from *P. alba* with partial assignment of m/z peaks.

2.4.2. Mass Spectra Of Extracts (C++ Applications)

ESI-MS has been used primarily to confirm the metabolite assignment in NMR spectra. The two dimensional $^{1}H,^{1}H$ COSY and $^{1}H,^{13}C$ HSQC spectra allowed to draw partial structures of metabolites, and to suggest possible assignment candidates. For instance, salicin derivatives were hypothesized to be present in the extracts by the COSY pattern of the saligenin moiety (labelled 2 in Figure 3D). The HSQC spectrum contained signals which were compatible with the presence of salicin derivatives, but because of the lack of reference spectra we could not identify exactly the specific derivative amongst those that are known to be present in poplar leaves (Morse et al, 2007). Mass spectra were used to further refine the assignment, and to propose possible candidates (for instance the mass of salireposide was found). Mass spectra allowed to confirm the assignment of salicin, some saligenin containing phenolic derivatives and choline (see also Table 2). As the ensemble of metabolites that can be detected by ESI-MS are significantly different from that can be detected by NMR. Moreover, Peak intensities in NMR spectra are linearly proportional to the metabolite concentration, while MS peaks depends on both concentration and ionization efficiency (i.e. mass spectra do not allow a direct comparison of relative metabolite concentration). A large number of peaks in ESI-MS spectra could not be associated to NMR peaks. These MS signals are listed in Table 3 . We noted that most of the compounds that could be consistently assigned in NMR and MS spectra showed intense M+H and M+Na peaks, with lower

```
#define H_MASS 1.0
#define NA_MASS 22.9
#define K_MASS 38.96
#define H2OH_MASS -18.01

class tab_entry {
public:
    std::string name;
    int mz;
    int H;
    int Na;
    int K;
    int H2Oh;
};


int nsamples;



/**
 *  Ascii file parsing and data discretization
 */
int readFile(const std::string file_list, std::vector<double>& p) {
    double v1,v2;
    int n;

    std::ifstream in(file_list.c_str());

    if (not in.is_open()) {
        std::cerr << "Cannot read: " << file_list << std::endl;
        return 0;
    }

    p = std::vector<double>(nsamples, 0.);
    while (not in.eof()) {
```

Fig. 13: MS analysis application source code

intensity M+K peaks. Therefore, Table … di massa lists the exact mass of the compounds that show at least two of these m/z . Table .. di massa also reports possible assignment candidates. However, unambiguous assignment requires further analysis of the NMR spectra of extracts through comparison with true standards or further MS analysis with fragmentation techniques.

```
int analyze(std::vector<int>& peaks, std::vector<tab_entry>& tab, std::vector<tab_entry>& matches) {
    for (int i=0; i<(int)tab.size(); ++i) {
        int H = tab[i].H;
        int Na = tab[i].Na;
        int K = tab[i].K;
        int H2Oh = tab[i].H2Oh;
        int found = 0;

        tab_entry match;
        match.name = tab[i].name;
        match.H = -1;
        match.Na = -1;
        match.K = -1;
        match.H2Oh = -1;

        for (int j=0; j<(int)peaks.size(); ++j) {
            if (peaks[j] == H) {
                match.H = H;
                found++;
                break;

            } else if (peaks[j] > H) {
                break;
            }
        }

        for (int j=0; j<(int)peaks.size(); ++j) {
            if (peaks[j] == Na) {
                match.Na = Na;
                found++;
                break;
```

Fig. 14: MS analysis application source code

A simple application has been designed, implemented and used in order to perform automatically MS analysis. In this way, mass spectrum from different samples have been processed in order to detect the peaks, remove the outliers, remove the peaks due to the washing process and finally search for some specific masses in the selected data.

```
std::vector<int> getPeaks(std::string f, int win, double T, std::vector<double>& p) {
    std::vector<int> peaks;
    int n = readFile(f, p);

    if (n == 0) {
        std::cerr << "Failed to load: " << f << std::endl;
        exit(-1);
    }

    for (int i=0; i<nsamples; ++i) {
        if (p[i] > T) {
            if (win == 0) {
                peaks.push_back(i);

            } else {
                bool localMax = true;
                for (int j = -win; j<=win; ++j) {
                    if (j == 0 or i + j < 0 or i + j > nsamples - 1) continue;
                    localMax = localMax && p[i] > p[i + j];
                }

                if (localMax) {
                    peaks.push_back(i);
                }
            }
        }
    }


    return peaks;
}
```

Fig. 15: MS analysis application source code

The first routine implemented in the software is the one needed to load the data from an ascii (text file) file and to select the peaks. Input data is passed to the application using an ascii file in which each row refers to a sample in the data as a couple <mass, concentration>. Then, another function has been written in order to scan the input data and select only the samples with a concentration higher than a threshold T (for instance T=1E+05 or T=1E+06).

In this phase, also sampling is performed, in order to reduce the amount of data, transforming it in a discrete signal. Finally, the peaks corresponding to noise due to the washing procedures are masked. At this step the data is read to be processed in order to search for the masses combinations. In particular, four combinations have been searched: given a mass X, the combinations X+H, X+Na, X+K and X-H_2OH. To determine as found a molecule with mass X, at least two of these combination have two be detected.

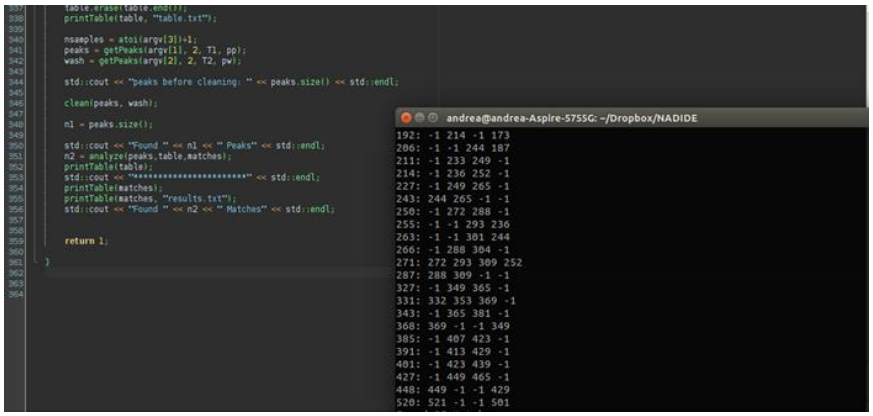

Fig. 16: MS analysis application source code

On the different datasets, CF7, CR7, CuF1 and CuR1, a first search has been performed, feeding the algorithm with a table containing the masses to be detected. The same procedure has been finally repeated looking for all the possible masses in a given range (es. 50-800).

The described software has been implemented in C++, using the standard mathematic libraries. On an average laptop, with a i7 quad core CPU, the whole process, consisting in data loading, data cleaning, peaks detection and mass search, took an average time of 63.25 ms.

						CF7			CR7			CuF1			CuR1		
		M	[M+H]	[M+Na]	M+K	[M+H]	[M+Na]	M+K	[M+H]	[M+Na]	M+K	[M+H]	[M+Na]	M+K	[M+H]	[M+Na]	M+K
1	Acido succinico	118,09	119,09	141,09	157,02										X		X
2	Arabinosio	150,13	151,13	173,13	189,06							X	X				
3	Acido citrico	192	193,124	215,124	231,054	X	X										
4	Maltosio	342,3	343,3	365,3	381,23		X	X		X	X		X	X		X	X
5	Acido folico	441	442,403	464,403	480,333					X	X						
6	Coniferin	343	344	366	381,93		X	X		X	X		X	X		X	X
7	Tremuloidin	390,38	391,38	413,38	429,31		X	X		X	X					X	X
8	Salireposide	406,38	407,38	429,38	445,31	X	X		X	X		X	X		X	X	
9	Salicyloylsalicin	407	408	430	445,93	X	X		X	X		X	X		X	X	
10	Salicortin	425	426	448	463,93	X		X	X		X	X		X	X		X
11	Populoside-C	463	464	486	501,93	X		X							X		X
12	Populoside-A	449	450	472	487,93	X	X										
13	Populin	391	392	414	429,93		X	X		X	X		X	X		X	X
14	Nigracin	407	408	430	445,93	X	X		X	X		X	X		X	X	
15	Deltoidin	407	408	430	445,93	X	X		X	X		X	X		X	X	
16	Chaenomeloidin	391	392	414	429,93		X	X		X	X		X	X		X	X
17	2'-O-acetylsalicortin	326,34	327,34	349,34	365,27		X	X		X	X		X	X		X	X
18	Tremulacin	529	530	552	567,93								X	X			
19	P-Coumaril-Alcol	151	152	174	189,93							X	X				
20	Unknown	129	130	152	167,93							X	X				
21	Unknown	135	136	158	173,93								X	X		X	X
22	Unknown	175	176	198	213,93	X	X					X	X				
23	Unknown	187	188	210	225,93					X	X		X	X			
24	Unknown	211	212	234	249,93		X	X		X	X		X	X		X	X
25	Unknown	214	215	237	252,93		X	X		X	X		X	X		X	X
26	Unknown	227	228	250	265,93		X	X					X	X		X	X
27	Unknown	230	231	253	268,93					X	X						
28	Unknown	243	244	266	281,93	X	X					X	X		X	X	
29	Unknown	250	251	273	288,93		X	X		X	X		X	X		X	X
30	Unknown	266	267	289	304,93		X	X		X	X		X	X		X	X
31	Unknown	271	272	294	309,93	X	X	X	X	X	X	X	X	X	X	X	X
32	Unknown	287	288	310	325,93	X	X		X	X	X	X	X		X	X	
33	Unknown	327	328	350	365,93					X	X		X	X		X	X
34	Unknown	315	316	338	353,93				X		X						
35	Unknown	331	332	354	369,93		X	X		X	X		X	X	X	X	X
36	Unknown	385	386	408	423,93		X	X		X	X		X	X		X	X
37	Unknown	391	392	414	429,93					X	X		X	X		X	X
38	Unknown	401	402	424	439,93		X	X					X	X		X	X
39	Unknown	427	428	450	465,93		X	X		X	X		X	X		X	X
40	Unknown	510	511	533	548,93	X	X		X	X							
41	Unknown	531	532	554	569,93	X	X		X	X							

Tab. 3: List of m/z candidates which have been found by the C++ application of ESI-MS spectra.

2.5.Principal Component Analysis (PCA)

Principal component analysis is one of the oldest and most widely used multivariate techniques (Hotellin, 1933). The concept behind PCA is to describe the variance in a set of multivariate data in terms of a set of underlying orthogonal variables (principal components). The original variables (metabolite concentrations) can be expressed as a particular linear combination of the principal components. PCA is a linear additive model, in the sense that each principal component (PC) accounts for a portion of the total variance of the data set. Often, a small set of principal components (2 or 3) account for a relevant proportion of the total variance, and in such circumstances, one can resynthesize the data from those few PCs and thus reduce the dimension of the data set. Plotting the data in the space defined by the two or three largest PCs provides a rapid means of visualizing similarities or differences in the data set, possibly allowing for improved discrimination of samples.

2.5.1. Leaves

To perform PCA on the ^{1}H-NMR spectra of methanol leaf extracts, spectra were bucketed in the region between 8.4-0.4 ppm with bucket size of 0.02 ppm, yielding 400 variables after exclusion of the solvent resonances (4.90-4.70 ppm and 3.40-3.25). The intensities of each bucket was scaled to the total spectrum intensity. PCA was carried out with no further scaling of the data and with the exclusion of small variances (cut-off 3%). Fig. 17 shows that the first principal component, explaining 70% of the system variance, separates the control sample (black) from copper treatment (blue). Such a separation is not complete, as there is a significant overlap between the two classes mostly due to two copper treated samples falling into the control class. Higher order PCAs do not cause a further separation between classes, and only 5 PCs are needed to explain > 95% of the total variance. The analysis of the loading plot along PC1 (superposed to a representative spectrum, sample CF7) allows to identify which spectral regions

contribute most to the separation between the classes. Positive loads along PC1 for copper treated samples indicate an increase of unsaturated fatty acid (namely, oleic and linolenic acid) in copper treated samples as compared to controls. Such an increase is correlated with a decrease of sugars (including sugar phosphates), that can be appreciated by the negative loadings of variables corresponding to the anomeric protons of mono-, di- and oligosaccharides as well as to bulk poly-alcoholic functions. The aromatic region has a smaller but significant contribution in defining the separation. As a matter of fact, PCA performed using only the spectral region between 8.4 and 6.0 ppm evidences the same classification of the sample as obtained by using the full spectrum, where a mild separation between the two groups is obtained along PC1, explaining 70 % of the total variance. By comparing the 1D loads plot (Figure 18F) with the NMR spectrum (Figure 18G), copper treated samples appear to have lower levels of benzoic acid (and its esters) and of salicortin (and analogues), and higher levels of cinnamic acid derivatives (ferulic acid, caffeic acid, etc).

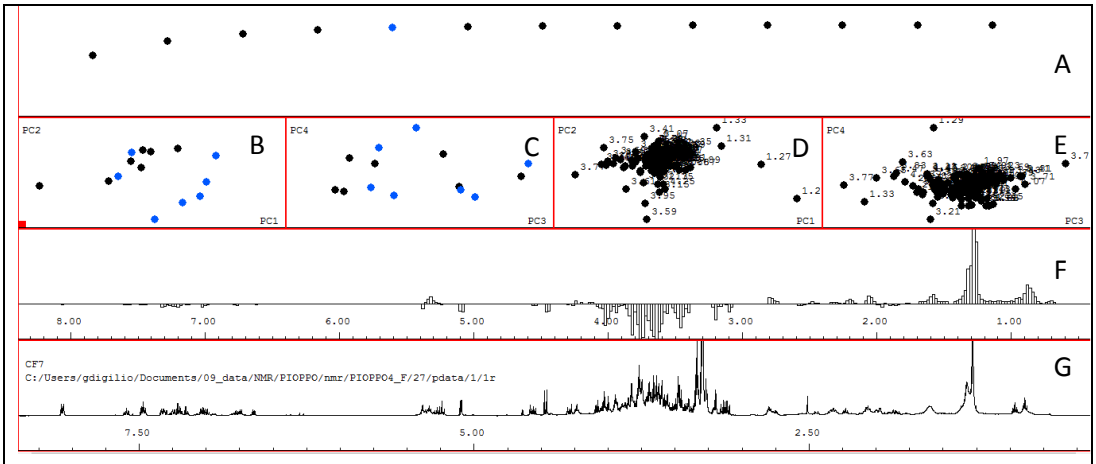

Fig. 17: PCA of the ^{1}H-NMR spectra of methanol extracts of leaves from *P. alba*. **A)** Plot of the explained variance (the point in blue represents a cumulative explained variance > 95%). **B)** PC1 *vs* PC2 score plot (blue: controls, *n*=7; black: copper treatment, *n*=7) **C)** PC3 *vs* PC4 score plot. **D)** PC1 *vs* PC2 loads plot; **E)** PC3 *vs* PC4 loads plot; **F)** 1D loads plot of PC1; **G)** Sample spectrum of leaf extract (control sample CF7.)

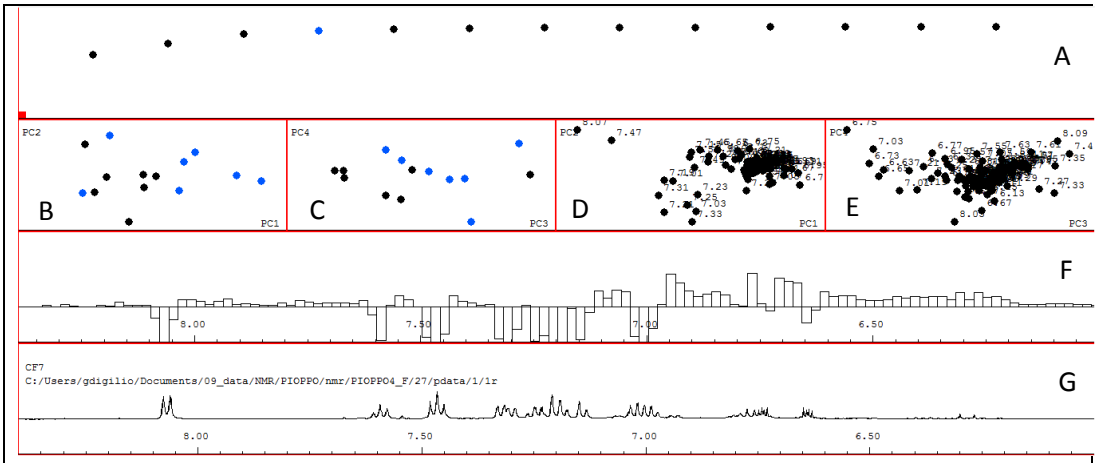

Fig. 18: PCA (aromatic region only) of the ^{1}H-NMR spectra of methanol extracts of leaves from *P. alba*. **A)** Plot of the explained variance (the point in blue represents a cumulative explained variance > 95%). **B)** PC1 *vs* PC2 score plot (blue: controls, *n*=7; black: copper treatment, *n*=7) **C)** PC3 *vs* PC4 score plot. **D)** PC1 *vs* PC2 loads plot; **E)** PC3 *vs* PC4 loads plot; **F)** 1D loads plot of PC1; **G)** Sample spectrum of leaf extract (control sample CF7.)

2.5.2. Roots

Spectra were processed for multivariate analysis exactly as leaves spectra were. As seen for leaves, the PCA of roots shows that PC1 (explaining 50% of total variance) can separate control and treated groups, even though such a separation appears less marked than in the case of leaves (an overlap between the groups still remains). Five PCs are needed to explain >95% of total variance. The analysis of 1D loads reveals the that copper-treated samples have increased levels of aliphatic methyl groups and fatty acids (but not unsaturated ones), that are correlated with the decrease of sugar resonances (Fig.19). Unlike leaves, the signals in the aromatic region do not contribute to the classification of samples. PCA analysis performed by bucketing only the aromatic region (8.4-6.0 ppm) failed to distinguish the treated from the untreated groups (Fig. 20). Although >95% of the

total variance could explained by three PCs, none of them caused an appreciable split into classes.

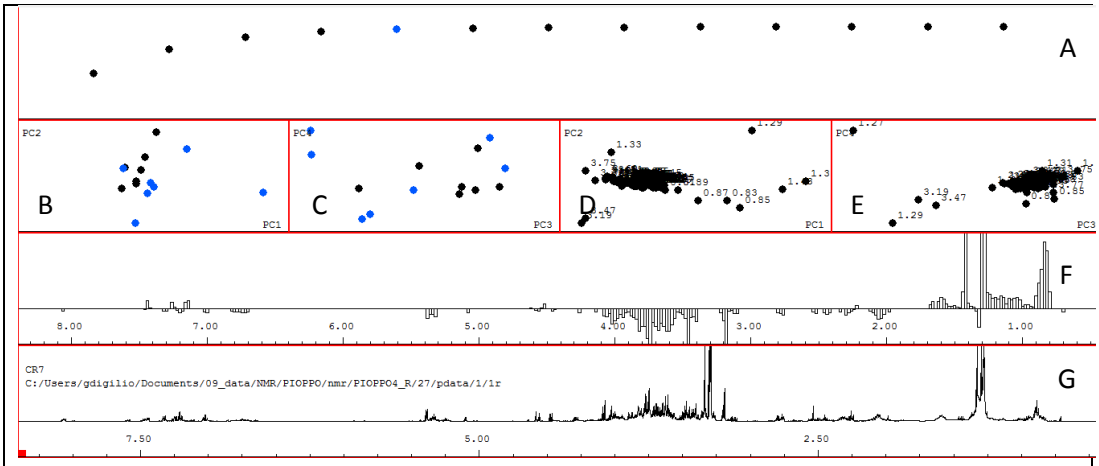

Fig. 19: PCA of the ^{1}H-NMR spectra of methanol extracts of roots from *P. alba*. **A)** Plot of the explained variance (the point in blue represents a cumulative explained variance > 95%). **B)** PC1 *vs* PC2 score plot (blue: controls, *n*=7; black: copper treatment, *n*=7) **C)** PC3 *vs* PC4 score plot. **D)** PC1 *vs* PC2 loads plot; **E)** PC3 *vs* PC4 loads plot; **F)** 1D loads plot of PC1; **G)** Sample spectrum of leaf extract (control sample CR7.)

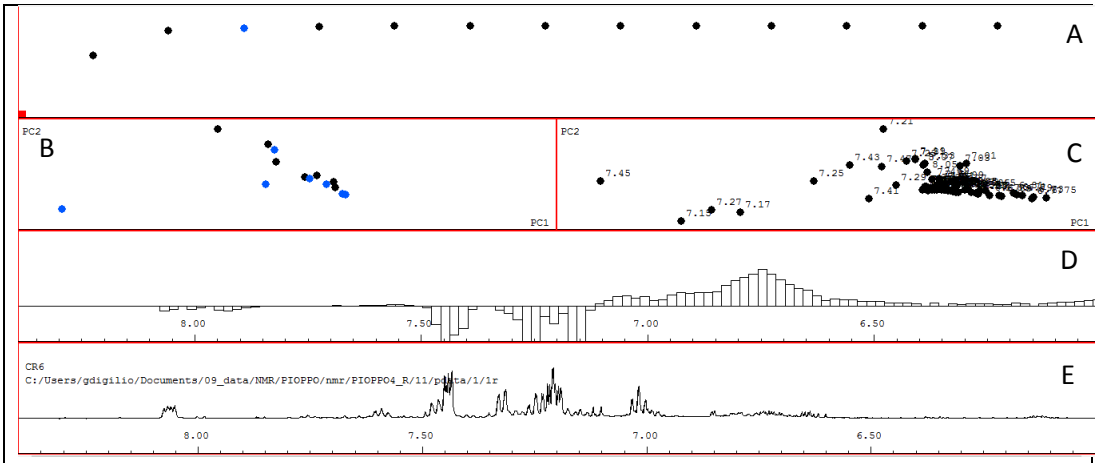

Fig. 20: "root 2" PCA of the ^{1}H-NMR spectra of methanol extracts of roots from *P. alba*. **A)** Plot of the explained variance (the point in blue represents a cumulative explained variance > 95%). **B)** PC1 *vs* PC2 score plot (blue: controls, *n*=7; black: copper treatment, *n*=7) **C)** PC1 *vs* PC2 loads plot; **D)** 1D loads plot of PC1; **E)** Sample spectrum of leaf extract (control sample CR7.)

2.6. Conclusions

To the best of our knowledge this is the first NMR characterization of extracts from poplar leaves and roots. The NMR spectra of methanol extracts of poplar leaves could be only partially assigned because of the lack of extensive databases of NMR spectra in methanol. Within this extract , major components were benzoic acid, salicin, saligenin, several saligenin phenolic glucosides, oleic acid, linolenic acid, several members of the hydroxycinnamic acids family, catechol, glucose di- and oligo-saccharides (including phosphates) and choline. These compounds were identified by evaluation of molecular connectivities as obtained from $^{1}H,^{1}H$ COSY spectra and $^{1}H,^{13}C$ HSQC spectra, and confirmed by *i)* spectral matching with the spectra of true standards and *ii)* detection of the corresponding *m/z* peaks in ESI-MS. In addition to these metabolites, the presence of lignin precursors could be inferred on the basis of HSQC spectra. Many more resonances and spin system were detected but not assigned, mostly because of the lack of reference standard spectra in methanol. Most of these compounds appear to be present at low to mid concentration levels in the extract of leaves. To further assign the spectrum, chromatographic separation followed by NMR of the fraction is needed, together with hyphenated mass analyses. The assignment of root extracts revealed as the main components the same metabolites found in leaves, but benzoic acid, salicin, saligenin, several saligenin phenolic glucosides, oleic acid, several members of the cinnamic acid family of secondary metabolites, catechol, catechin, glucose di- and oligo-saccharides (including phosphates) and choline. Most of the compounds that were assigned in leaves were also found in root extracts.

Most of literature data about metabolic profiles of plant extracts have been obtained by water or water/methanol extraction protocols (Verpoorte et al, 2007; Rehill et al, 2005). Metabolites typically identified in these studies include all amino acids, organic acids, p-hydroxy-benzoic acid, saturated and unsaturated fatty acids (mostly α-linolenic acid and its esters) sugars (glucose, sucrose and unspecified glycosides) and a number of secondary metabolites (kaempferol,

quercetin, sinapic acid, and hydroxycinnamic acid analogues such as ferulic acid, caffeic acid and chlorogenic acid). Of these compounds, only linolenic acid and sugars were found at high levels in addition to low levels of compounds belonging to the hydroxycinnamic acids family. The aromatic region in poplar extract was dominated by the resonances of benzoic acid saligenin-based compounds. No amino acid was unambiguously detected. Thus, the ensemble of metabolites obtained by our extraction protocol is very different from those that can be found in the literature, preventing a detailed comparative assessment between the metabolome between different species.

PCA has been used to evaluate the change of the metabolic fingerprint due to copper stress in poplar. Multivariate analysis showed that a mild separation into the treated vs untreated groups could be found both in leaves and roots. The NMR signals contributing to the classification were spread all over the spectrum in the case of leaves, whereas only the aliphatic region had a significant contribution in the case of the roots. The separation in classes was somewhat more clear by the analysis of leaves rather than roots. This is rather surprising, as copper has been administered to plants by dissolving copper salts into the water feeding the roots. In leaves, the most important determinant to define the effect of copper treatment is the increase of saturated and unsaturated fatty acids (namely, oleic and linolenic acid) and hydroxycinnamic acid derivatives that is correlated with a decrease of sugars (including sugar phosphates), benzoic acid, and saligenin based compounds. Although less apparent, also the metabolome changes in root indicate an increase of saturated (and, to a lesser extent, unsaturated) fatty acid together with a decrease of sugars.

2.7. Bibliography

Arisi A.C.M, Mocquot B., Lagriffoul A., Mench M., Foyer C.H., Jouanin L., (2000), Responses To Cadmium In Leaves Of Transformed Poplars Overexpressing Γ-Glutamylcysteine Synthetase, Physiologia Plantarum, 109: 143–149.

Beckonert O., Keun H. C., Ebbels T. M. D., Bundy J. G., Holmes E., Lindon J. C., Nicholson J. K., 2007, Metabolomic And Metabonomic Procedures For NMR Spectroscopy Of Urine, Plasma, Serum And Tissue Extracts. Nature Protocols, 11: 2692-2703.

Boeckler G.A., Gershenzon J. and Unsicker S.B., (2011) Phenolic Glycosides Of The Salicaceae And Their Role As Anti-Herbivore Defenses, Phytochemistry, 72: 1497–1509.

Bradshaw H.D., Ceulemans R., Davis J. and Stettler, R.F., (2000) Emerging Model Systems In Plant Biology. Journal Of Plant Growth Regulation 19: 306–313.

Cakmak I, Engels C., (1999), Role Of Mineral Nutrients In Photosynthesis And Yield Formation, Crop Nutrition, 141-168.

Cobbett C., Goldsbrough P., (2002), Phytochelatins And Metallothioneins: Roles In Heavy Metal Detoxification And Homeostasis, Plant Biology, 53: 159–182.

Di Baccio D., Navari-Izzo F., Izzo R., (2004), Seawater Irrigation: Antioxidant Defence Responses In Leaves And Roots Of A Sunflower (*Helianthus Annuus* L.) Ecotype, Journal Of Plant Physiology,161: 1359–1366.

Di Baccio D., Kopriva S., Sebastiani L., Rennenberg H., (2005), Does Glutathione Metabolism Have A Role In The Defence Of Poplar Against Zinc Excess?, New Phytologist, 167: 73-80.

Faust M.B. and Christians N.E., (2000) Cu Reduces Shoot Growth And Root Development Of Creeping Bentgrass,. Crop Science, 40: 498-502.

Foyer C.H., Descourvieres P., Kunert K.J., (1994), Protection Against Oxygen Radicals: An Important Defense Mechanism Studied In Transgenic Plants, Plant, Cell & Environment,17: 507–523.

Foyer C.H., Rennenberg H., (2000), Regulation Of Glutathione Synthesis And Its Role In Abiotic And Biotic Stress Defence. In: Brunold C, et al., ed. Sulfur Nutrition and Sulfur Assimilation in Higher Plants, 127–153.

Gathy, P. (1970) Plaidoyer Pour Une Essence Oubliee: Le Peuplier Blanc (*Populus Alba* L.). Bulletin de la Société Royale Forestière de Belgique, 6: 265–271.

Hotellin, H. (1933) Analysis Of A Complex Of Statistical Variables Into Principal Components. Journal Of Educational Psychology 24: 417–441.

Isebrands, J.G., Dickson, R.E., Rebbeck, J. and Karnosky, D.F. (2000) Interacting Effects Of Multiple Stresses On Growth And Physiological Processes In Northern Forest Trees. In: Mickler, R.A., Birdsey, R.A. And Hom, J. (Ed) Responses of Northern US Forests to Environmental Change. Springer-Verlag, 149–180.

Isebrands J.G. And J. Richardson, (2012), Poplars And Willows Trees For Society And The Environment.

Kamenova-Jouhimenko S., Georgieva V., Tzonev T.Z., Gecheva V., (2003) The Influence Of Surplus Of Cd And Cu On Photosynthesis, Transpiration And Bioproductivity Of Pea. Ecology And Future, 2: 25-28.

Kuzovkina, J., (2010), Willows Beyond Bioenergy: Salix For Ecological Engineering And As A Specialty Crop In Low Input Systems. In: Scarascia-Mugnozza, G. And Stanton, B.,(Ed) Book Of Abstracts. Fifth International Poplar Symposium. Poplars And Willows: From Research Models To Multipurpose Trees For A Bio-Based Society, Research Council for Agriculture, 9.

Le Gall G., Colquhoun I.J., Davis A.L., Collins G.J., Verhoeyen M.E., (2003), Metabolite Profiling Of Tomato (*Lycopersicon Esculentum*) Using 1H NMR

Spectroscopy As A Tool To Detect Potential Unintended Effects Following A Genetic Modification. J AgriFood Chem 51: 2447–2456.

Marschner H., (1995), Mineral Nutrition of Higher Plants, Ed.:2, Academic Press.

Milton Gordon, 1998, Phytoremediation Of Trichloroethylene With Hybrid Poplars. Environmental Health Perspectives Supplements, p:5.

Mirck, J. and Volk, T.A., (2010), Response Of Three Shrub Willow Varieties (Salix Spp.) To Stormwater Treatments With Different Concentrations Of Salts. Bioresource Technology 101: 3484–3492.

Morse A.M., Tschaplinski T.J., Dervinis C, Pijut P.M., Schmelz E.A., Day W., Davis J.M., (2007), Salicylate And Catechol Levels Are Maintained In *nahG* Trasgenic Poplar, Phytochemistry, 68: 2043-2052.

Nan Z.R., Zhao C.Y., Li J.J., Chen F.H., Sun W., (2002), Relations Between Soil Properties And Selected Heavy Metal Concentrations In Spring Wheat (Triticum Aestivum L. Grown In Contaminated Soils, Water Air And Soil Pollut, 133: 205–213.

Nelson, N.D., (1984), Poplars Are Not Inherently Low In Photosynthetic Capacity. Photosynthetica 18, 600–605.

Rauser W.E., (1999), Structure And Function Of Metal Chelators Produced By Plants: The Case For Organic Acids, Amino Acids, Phytin And Metallothioneins, Cell Biochemistry And Biophysics, 31: 19–48.

Rehill B., Clauss A., Wieczorek L., Thomas W., Lindroth R., (2005), Foliar Phenolic Glycosides From *P Fremontii, P. Angustifolia* And Their Hybrids, Biochemical Systematics And Ecology, 33: 125-131.

Rennenberg H., Brunold C., (1994), Significance Of Glutathione Metabolism In Plants Under Stress, Progress In Botany, 5: 142–155.

Rock S.A., (1997), Phytoremediation, The Standard Handbook Of Hazardous Waste Treatment And Disposal, Ed:2.

Roy M., Couillard D.,(1998), Metal Leaching Following Sludge Nylon Membrane Vs. Porous Ceramic Cup, J. Environ. Qual., 32:1642–1652.

Stettler, R.F., Bradshaw, H.D. Jr, Heilman, P.E. And Hinckley, (1996) T.M. (Ed) Biology Of *Populus* And Its Implications For Management And Conservation. National Research Council Of Canada Research Press.

Schützendübel A, Polle A., (2002), Plant Responses To Abiotic Stresses: Heavy Metal-Induced Oxidative Stress And Protection By Mycorrhization, Journal Of Experimental Botany, 372: 1351–1365.

Toler H.D., Morton J.B., Cumming J.R., (2005), Growth And Metal Accumulation Of Mycorrhizal Sorghum Exposed To Elevated Copper And Zinc. Water, Air And Soil Pollution, 164: 155-172.

Vangronsveld J. And Clijsters J.H., (1994), Toxic Effect Of Metals. In (Ed). ME Farago (Ed.). "Plants And Chemical Elements. Biochemestry, Uptake, Tolerance And Toxicity",. VCH Publishers, 150-177.

Verpoorte R., Choi YH., Kim HK., (2007), NMR-Based Metabolomics At Work In Phytochemistry, Phytochemistry, 6: 3-14.

Woolhouse H.W. And Walker S. (1981), The Physiological Basis Of Copper Toxicity And Copper Tolerance In Higher Plants. (Ed) "Copper In Soils And Plants", P. Academic Press, 235-262.

Ye Z.H., Baker A.J.M., Wong M.H., Willis A.J. (1997) Copper And Ni Uptake, Accumulation And Tolerance In *Typha Latifolia* With And Without Iron Plaque On The Root Surface. Plant Physiology, 136: 481-488.

Xiang C., Oliver D.J., (1999), Glutathione And Its Central Role In Mitigating Plant Stress. In: Pessarakli M, Ed. Handbook Of Plant And Crop Stress, 697–707.

Biological Magnetic Resonance (BMRB) Data Bank – Metabolomics (http://www.bmrb.wisc.edu/metabolomics/)

Human Metabolome Database (HMDB) (http://www.hmdb.ca/)

Chapter 3.: Rice

3.1 Rice Introduction

Oryza sativa commonly known as rice, is a cereal from Asia. It is a spermatophyta (seed plants), belonging to the Monocotyledons class (Shao et al, 2007).

Its origins are not clear, but it is estimated that the first exemplars of rice should be appeared about fifteen thousand years ago, in the Himalaya area. Rice is renowned for being easy to be genetically manipulated, property that makes it a model for cereal biology (Zhang et al, 2008).

Rice can be classified in two major subspecies, japonica or sinica varieties, cultivated on dry fields and indica, that grows submerged (Oka, 2012).

Carnaroli; is a medium grained rice grown in the northern provinces of Italy. It is characterized by an high amylose concentration (Julio and Villareal, 1993).

3.1.1. Dietary And Economic Relevance Of Rice

FAO statistics assert that in 39 countries rice is the staple food, with an unbalanced distribution that has a major consumption localized in Asia. Rice consumption in South and Southeast Asia is higher than the energy dependence on any other staples in other regions. About 2700 millions of people, in Asia, have a diet composed, in terms of caloric intake, at the 35-39 percent of rice.

In South and Southeast Asia, the contribution of rice to protein in the diet is estimated between 50 and 70 percent, higher than in any other region of the world.

Rice consumption continues to increase following the population growth in the poorest countries, mainly for its large availability and accessibility in terms of price.

FAO esteemed, for the 2014, a world production of about 764 millions of tons of rice, with China, India, Indonesia and Bangladesh as major producers. In Europe, the major rice producer is Italy, with a cultivated surface of about 220.000 hectares and a total production of about 1.35 millions of tons. In Italy, while in terms of agricultural production rice has a significant relevance, it covers less than the 1% of the total turnover of the food industry.

Rice has a nutrient content of approximately 79% carbohydrate, about 7% protein (mostly lost during refinement) and about 0.6% in lipid; these nutritional properties make rice the most complete cereal in alimentation.

3.1.2. Arsenic

Arsenic (atomic number 33) is a silver-grey brittle crystalline solid with atomic weight of 74.9, specific gravity 5.73, melting point 817°C (at 28 atm), boiling point 613°C, and vapour pressure 1 mm Hg at 372°C. Arsenic is a semimetallic element with the chemical symbol "As". Arsenic is odourless and tasteless. Arsenic can combine with other elements to form inorganic and organic arsenicals (NGWA, 2001). In the environment, arsenic is combined with oxygen, chlorine, and sulphur to form inorganic arsenic compounds. Inorganic arsenic compounds are mainly used to preserve wood. Organic arsenic compounds are used as pesticides, primarily on cotton plants (U.S. H&H Services, 2005).

Arsenic exists in the −3, 0, +3, and +5 oxidation states, and in a variety of chemical forms in natural waters and sediments (Hasegawa et al, 2009). Environmental forms include arsenious acid (H_3AsO_3), arsenites, arsenates, methylarsenic acid, dimethylarsinic acid, and arsine. Two most common forms in natural waters arsenite and inorganic arsenate, referred as As^{3+} and As^{5+}. From both the biological and the toxicological points of view, arsenic compounds can be classified into three major groups. These groups are inorganic arsenic compounds, organic arsenic compounds, and arsine gas (WHO, 2000).

Trivalent arsenites are hard acids and preferentially complexes with oxides and nitrogen. Trivalent arsenites predominate in moderately reducing anaerobic environments such as groundwater. The most common trivalent inorganic arsenic compounds are arsenic trioxide, sodium arsenite, and arsenic trichloride (WHO, 2000). As^{5+} arsenates include $As(OH)_3$ and $AsO_2OH_2^-$ (Mohan and Pittman, 2007). Arsenites (AsO_3^{3-} ortho-arsenite, a polymeric chain anion meta-arsenite $[AsO^{2-}]_n$, a polymeric chain anion, $As_2O_5^{4-}$, $As_3O_7^{5-}$, $As_4O_9^{6-}$, $[As_6O_{11}^{4-}]_n$) is predominant in reduced redox potential conditions (Hasegawa et al, 2009).

Arsenic is one of the contaminants found in the environment which is notoriously toxic to man and other living organisms (Chutia et al, 2009). It is a highly toxic element that exists in various species, and the toxicity of arsenic depends on its species. The pH, redox conditions, surrounding mineral composition, and microbial activities affect the form (inorganic or organic) and the oxidation state of arsenic. It is generally accepted that the inorganic species, arsenite [As^{3+}] and arsenate [As^{5+}], are the predominant species in most environments, although the organic ones might also be present (Andrianisa et al, 2008).

In general, inorganic compounds of arsenic are regarded as more highly toxic than most organic forms which are less toxic (NGWA, 2001; Chutia et al, 2009; Ampiah-Bonney et al, 2007; Vaclavikova et al, 2008). The trivalent compounds (arsenites) are more toxic than the pentavalent compounds (arsenates) (Ampiah-Bonney et al, 2007; Vaclavikova et al, 2008). It has been reported that As^{3+} is 4 to 10 times more soluble in water than As^{5+}. However, the trivalent methylated arsenic species have been found to be more toxic than inorganic arsenic because they are more efficient at causing DNA breakdown (Vaclavikova et al, 2008). Although As^{5+} tends to be less toxic compared to of As^{3+}, it is thermodynamically more stable due to the fact that it predominates under normal conditions and becomes the cause of major contaminant in ground water (Chutia et al, 2009). Arsenate which is in the pentavalent state [As(V)] is also considered to be toxic and carcinogenic to human (Yusof et al, 2009).

3.1.2.1. Arsenic As A Soil Pollutant

Arsenic can be naturally found on earth in form of arsenic sulphide, metal arsenates or arsenites. Different human activities, mainly industrial ones, make use of Arsenic, like pharmaceutical and glass industries, agrochemical production, wood preservatives and others.

Examples of areas in which As contamination have been proved and studied can be found all around the world; many of the states surrounding Texas, including New Mexico, Oklahoma, Arkansas, and Louisiana, have a significant number of freshwater aquifer wells that produce water with arsenic concentrations that exceed the new EPA national standard of 10 µg/L (Tinker et al, 2005).

In the environment of central India (for example Ambagarh, Chauki, Chhattisgarh) in all type of waters, the arsenic levels exceeded the permissible limit, 10 µg/L. The most toxic and mobile inorganic species i.e. As(III) and As(V) are predominantly present in water of this region. The soils have relatively higher contents of arsenic and other elements such as Mg, Al, Si, K, Ca, Ti, V, Cr, Mn, Fe, Co, Ni, Cu, Zn, As, Ga, Zr, Sn, Sb, Pb and U. The most of people living in this region are suffering with arsenic borne diseases (i.e. melanosis, keratosis, skin cancer, etc.) (Patel et al, 2005).

In Italy high levels of arsenic have been detected in groundwaters in many municipalities of Emilia Romagna and Lombardy [3,4], in some municipalities of Veneto and in the Campi Flegrei area (Naples), as well as in spring waters and lakes of northern Lazio (Barbieri et al, 2014).

In Sardinia (Italy), some relevant soil pollution problems have been recognized as a direct consequence of intense mine activities. In Barraxiutta, located in south-western Sardinia, in the 1700s and 1800s, huge accumulations of mineral waste were visible close to the old flotation area, and high concentrations of lead (around 10–14%) and silver (around 60%) were persistent. The extraction of mineral continued until 1967 and stopped definitively 3 years later in 1970 because of the mine depletion. As a consequence of the previous mine activities,

Barraxiutta is described and is identified by experts through the “Piano di Caratterizzazione di Barraxiutta” as an area of potential pollution, a specific site where residuals mineral materials are collected in high concentrations. These mineral materials are dispersed by means of wind and rain, and cause widespread contamination of the soil, surface and underground water. In this area, recent studies, involving machine learning technique based on symbolic quasi-optimal learning, have detected strong pattern and cause-effect relations between high As concentrations and the presence of other chemicals due to intense mine activities (Manca and Cervone, 2013).

Arsenic effects on human health are observable in a long-term exposure and one of the first studied case of arsenic contamination has been registered in south-east Asia, where arsenic sediments where deposited millions years ago near to the Gange river. Studies about the areas around the arsenic deposit have estimated that about 30 million people may be in risk of arsenic related diseases due to contaminated water (Li et al, 2009).

Humans are generally subjected to arsenic by food, mainly fish, shellfish, meat and cereals.

The way arsenic is stored in soil depends on the soil characteristics, like its pH and biological activity. Of course, soil arsenic pollution, can affect the rice yield as well as the grain quality (Raymond and Okieimen, 2011). From the human health point of view, an arsenic contaminated soil can be a threat for people affecting, mainly, the food chain. Arsenic exposure has been demonstrated to be involved in several diseases and pathologies like diabetes, heart, neurological, gastrointestinal and liver damages, cancer, bone marrow and blood diseases.

On the plants, arsenic contaminations show reduced plant growth, partial or total sterility and incomplete grain development.

3.1.3. Arsenic And Rice: Uptake, Accumulation And Responses By The Plant

Independently from the As concentration in the soil, the uptake of arsenic in rice depends on some soil parameters like pH, texture, presence of iron, aluminium, oxide minerals and organic matter. The activity of some biotic an abiotic factors can cause the oxidation-reduction of the As species (Atkinson and Urwin, 2012).

As a flooded cultivation, rice fields present often anaerobic soils. In these conditions, rice roots spread oxygen, resulting in an iron hydroxide plaque formation on the root surface. This iron plaque, has a strong affinity with As(V) and impacts on the arsenic uptake by rice.

3.1.3.1. Uptake And Behaviour Of Arsenic In Plant

Through exposure to drinking water, people are exposed to arsenic also due to ingestion of vegetation which has been contaminated by irrigation with arsenic-contaminated water.

Moreover, even the cattle and their products, are indirectly exposed to this risk.

Understanding how Arsenic is taken up by plants and is subsequently transformed is essential for the evaluation of the risks posed by arsenic-contaminated soils for the people and wildlife in these regions where livestock have been fed on arsenic-contaminated vegetation and elsewhere (Meharg and Hartley-Whitaker, 2002).

Arsenic is released into the environment in both inorganic and organic forms: Arsenate [As(V) $(AsO_4)^{3-}$] and arsenite [As(III) $(AsO_3)^{3-}$] are the inorganic, phytoavailable forms of arsenic in soil solution. However, microbes, which can methylate and demethylate arsenic species in soils, may transform inorganic arsenic species to organic species and vice versa (Xu et al, 2008).

We must consider, anyway, that most of the plants so far investigated, have more than one species of arsenic in their tissues (Meharg and Hartley-Whitaker, 2002).

As-contaminated groundwater is used to irrigate rice paddies during the dry season, then, rice plant is inherently efficient in the uptake of As (Su et al, 2010), which is further elevated when arsenic is present in the water (Meharg and Rahman, 2003).

If arsenate (the main arsenic species found in aerobic soils), is taken up by rice plant roots via phosphate transporters, (Su et al, 2010) arsenite is the dominant form in submerged paddy field conditions (anaerobic soils) (Xu et al, 2008; Su et al, 2010) and enters in rice root cells through a transporter for silicic acid (Yamaji, 2009).

This protein, is localized in the exodermis and endodermis, where the Casparian strips are formed (Welch et al, 2000) and it is permeable to a range of small neutral (undissociated) molecules, including arsenite and methylated As species (Welch et al, 2000; Xu et al, 2008; Su et al, 2010).

Arsenate is reduced to arsenite within the rice root (Xu et al, 2008). Arsenite may be detoxified through complexation with thiol-rich peptides followed by sequestration into vacuoles (Zhang et al, 2008).

Methylated As species are taken up by rice roots much less efficiently than inorganic species, that appear to be translocated within the plant more efficiently. However, the transport and unloading of As to/into the grain, which are key processes in terms of human exposure to this contaminant, are far from being fully understood; but, anyway, irrespective of soil arsenic concentrations, in rice tissues, arsenic concentration followed this trend: root> straw> grain. (Li et al, 2009).

Once in the plant, (for example in maize plant, *Oryza Sativa*.) As can disturb plant metabolism, as arsenate decouples phosphorylation in mitochondria and arsenite inactivates many enzymes by reacting with sulphydryl groups of proteins (Dixon, 1997). Obviously, the increase in rate of As availability in the soil solution due to flooding results in higher As uptake by the plants. As a result, Arsenic is more available in soil water due to flooding. Under aerobic soil conditions, instead, it is

considered that most As remains bound to iron oxides and fortunately unavailable to plants.

3.1.4. Arsenic Interactions With Other Elements And In Particular Phosphorous

Phosphorus (P) is one of the major macronutrients for plant growth and development. The acquisition process of inorganic phosphate (Pi) by plant roots is accomplished through its active uptake carried by the Pi transporters into the epidermal and cortical cells of the root. Once in the root cortical cells, Pi must eventually be loaded into the apoplastic space (Gonzalez-Chavez et al, 2002). As a chemical analogue of phosphate, arsenic competes with P in the soil, and during plant uptake (Meharg et al, 2003). Physiological and electrophysiological studies showed that arsenate (the main arsenic species found in aerobic soils) and phosphate share the same transport pathway in plants (Meharg and Hartley-Whitaker, 2002). Once inside the cytoplasm, arsenate competes with phosphate, for example replacing phosphate in ATP to form unstable ADP-As, and leads to the disruption of energy flows in cells (Meharg et al, 2003).

A number of researchers have found that arsenic compounds tend to reduce the effects of selenium (Hill, 1975; Howell and Hill, 1978; Kraus and Ganther, 1989; Levander 1977; Miyazaki et al, 2003; Schrauzer, 1987; Schrauzer et al, 1978). Likewise, selenium can decrease the effects of arsenic, including clastogenicity (Beckman and Nordenson, 1986; Biswas et al, 1999; Sweins, 1983), delayed mutagenesis (Rossman and Uddin, 2004), cocarcinogenesis (Uddin et al, 2005), cytotoxicity (Babich et al, 1989; Rössner et al, 1977; Styblo and Thomas, 2001), and teratogenicity (Holmberg and Ferm, 1969). The mechanism of this mutual inhibition of effects is not known, but may be related to the formation of a selenium-arsenic complex (seleno-bis [S-gluthionyl] arsinium ion; Gailer et al, 2002) that is excreted more rapidly than either arsenic or selenium alone (Cikrt et al, 1988; Hill, 1975; Levander, 1977; Levander and Baumann, 1966) or due to

selenium-induced changes in arsenic methylation (Styblo and Thomas, 2001; Walton et al, 2003). There is little direct evidence that variations in selenium exposure in humans lead to significant increases or decreases in arsenic toxicity, although copper smelter workers who developed lung cancer had lower tissue levels of selenium than workers who did not develop lung tumours (Gerhardsson et al, 1985). This suggests that selenium deficiency could significantly increase the risk of lung cancer following inhalation exposure to arsenic, but it is difficult to distinguish cause from effect in such a study. However, there is evidence that administration of selenium can facilitate recovery from arsenic poisoning. In residents living in an area of Inner Mongolia with high levels of arsenic in drinking water, administration of 100–200 μg selenium/day in the form of selenium yeast and exposure to arsenic-free water for 14 months resulted in a greater improvement in clinical signs and symptoms, liver function, and EKG readings as compared to residents administered arsenic-free water only (Wuyi et al, 2001; Yang et al, 2002). An improvement in skin lesions was observed in 67 and 21% of the subjects in the selenium-supplemented and control groups (Yang et al, 2002). Additionally, the levels of arsenic in blood, hair, and urine were significantly lower after the 14-month period only in the selenium supplemented group. Suggestive evidence of a positive interaction between arsenic and benzo(a)pyrene has also been noted for induction of lung adenocarcinomas in hamsters (Pershagen et al, 1984). Studies of rats exposed to arsenic, lead, and cadmium, alone or in combination, have revealed mainly additive or subadditive effects on body weight, hematological parameters, and enzymes of heme synthesis (Mahaffey and Fowler 1977; Mahaffey et al, 1981). Similarly, studies of the tissue levels of arsenic in rats fed arsenic with or without lead or cadmium revealed only limited evidence of any toxicokinetic interactions (Mahaffey et al, 1981). Pretreatment of rats with a nontoxic dose of cadmium had no effect on the lethality of a high dose of arsenic and did not reduce arsenic-induced hepatotoxicity (Hochadel and Waalkes, 1997). These data do not suggest that arsenic toxicity is likely to be significantly influenced by concomitant exposure to these metals. However, supplementation with zinc or chromium may be useful in

reducing chronic arsenism. Arsenic has been shown to cause an increase in total plasma cholesterol; co-administration of chromium(III) counteracts this effect (Aguilar et al, 1997). Pretreatment of mice with zinc, at least 24 hours before injection with arsenic-73, reduced arsenic retention compared to controls that did not receive the zinc pretreatment or received it only a short time before the administration of arsenic (Kreppel et al, 1994). Zinc is an inducer of metallothionein, but this induction does not appear to be the mechanism that reduces arsenic toxicity because other inducers of metallothionein did not reduce arsenic toxicity and arsenic elimination was increased by the zinc pretreatment. Since methylation of arsenic is a detoxification mechanism, it is possible that chemicals that interfere with the methylation process could increase toxicity. This is supported by studies in animals in which reagents that inhibit methylation enzymes (e.g., periodate-oxidized adenosine) caused an increase in tissue levels of inorganic arsenic (Marafante and Vahter, 1986; Marafante et al, 1985). Similarly, cellular glutathione levels appear to play a role in the methylation process, and treatment with reagents (e.g., phorone) that decrease glutathione levels increases arsenic toxicity (Buchet and Lauwerys, 1987). Inadequate dietary intake of methionine, choline, or protein may also exacerbate arsenic toxicity. Rabbits pretreated with diets low in choline, methionine, or protein showed a significant increase in tissue retention of arsenic and a significant decrease in the excretion of dimethylarsinic acid (Vahter and Marafante, 1987).

The role of soil P availability in the As tolerance of some plants species is also unknown, indeed, while As uptake can be fatal by eventually disrupting ATP formation (Bai et al, 2008), the presence of commensurate P availability in the soil has been shown prevent cell death by competing with As for P binding sites in the roots. Reduced uptake of arsenic can then allow the plant time to detoxify (Woolson et al, 1971; Meharg et al, 2003). for this defence mechanism to be successful, sufficient supply of P is required in the soil.

In rice plant, competitive inhibition of uptake with phosphate showed that arsenite and arsenate were taken up by different uptake systems; especially arsenate

absorption was strongly suppressed in the presence of phosphate (Su et al, 2010). Addition of phosphate to the soil might enhance downward movement of As, leading to increased leaching from the topsoil (Su et al, 2010). Also it has been reported that application of P enhanced the As accumulation in grain and straw of rice grown in flooded condition (Nriagu et al, 1988).

Some researches establish that As concentration in grain (husked) and straw clearly showed that irrespective of tillage options and P levels, rice straw contained much higher concentrations of As than grain. However, aerobic soil reduce arsenic uptake compared to anaerobic conditions for all phosphorus levels (Su et al, 2010).

3.1.5. Effects Of Heavy Metals On The Uptake Of Nutrients By Plants

Metals are natural components in soil (Lasat et al, 2000). Some of these metals are micronutrients necessary for plant growth, such as Zn, Cu, Mn, Ni, and Co, while others have unknown biological function, such as Cd, Pb, and Hg (Shtangeeva et al, 2004). Metal pollution has harmful effect on biological systems and does not undergo biodegradation.

Plants have evolved highly specific and very efficient mechanisms to obtain essential micronutrients from the environment, even when present at low ppm levels. Plant roots, aided by plant-produced chelating agents and plant-induced pH changes and redox reactions, are able to solubilize and take up micronutrients from very low levels in the soil, even from nearly insoluble precipitates. Plants have also evolved highly specific mechanisms to translocate and store micronutrients. These same mechanisms are also involved in the uptake, translocation, and storage of toxic elements, whose chemical properties simulate those of essential elements. Thus, micronutrient uptake mechanisms are of great interest to phytoremediation (Robinson et al, 2000).

The range of known transport mechanisms or specialized proteins embedded in

the plant cell plasma membrane involved in ion uptake and translocation include **i)** proton pumps (″-ATPases that consume energy and generate electrochemical gradients), **ii)** co- and antitransporters (proteins that use the electrochemical gradients generated by ″-ATPases to drive the active uptake of ions), and **iii)** channels (proteins that facilitate the transport of ions into the cell). Each transport mechanism is likely to take up a range of ions. A basic problem is the interaction of ionic species during uptake of various heavy metal contaminants. After uptake by roots, translocation into shoots is desirable because the harvest of root biomass is generally not feasible. Little is known regarding the forms in which metal ions are transported from the roots to the shoot. Plant uptake-translocation mechanisms are likely to be closely regulated. Plants generally do not accumulate trace elements beyond near-term metabolic needs. And these requirements are small ranging from 10 to 15 ppm of most trace elements suffice for most needs (Sebastiani et al, 2004).

The exceptions are "hyperaccumulator" plants, which can take up toxic metal ions at levels in the thousands of ppm. Another issue is the form in which toxic metal ions are stored in plants, particularly in hyperaccumulating plants, and how these plants avoid metal toxicity. Multiple mechanisms are involved. Storage in the vacuole appears to be a major one (Djingova et al, 1999).

Water, evaporating from plant leaves, serves as a pump to absorb nutrients and other soil substances into plant roots. This process, termed evapotranspiration, is responsible for moving contamination into the plant shoots as well. Since contamination is translocated from roots to the shoots, which are harvested, contamination is removed while leaving the original soil undisturbed. Some plants that are used in phytoextraction strategies are termed "hyperaccumulators." They are plants that achieve a shoot-to-root metal-concentration ratio greater than one. Nonaccumulating plants typically have a shoot-to-root ratio considerably less than one. Ideally, hyperaccumulators should thrive in toxic environments, require little maintenance and produce high biomass, although few plants perfectly fulfil these requirements (Salido et al, 2003).

3.2 Materials And Methods

A large pot experiment was conducted in a glasshouse. The duration of the experiment was about 120 days from transplanting to the harvest.

Humidity and temperature were not controlled, but the glasshouse prevented the plants from rain exposure, allowing to provide controlled nutrition and precise amounts of As to the plants. Plants were also protected from high irradiation and from animal predation.

3.2.1. Sand And Soil Preparation

Quartz sand, an inert material, was used a substrate for plant growth. It was sterilized in an oven for 3 hours at 180 °C.

Plants were watered with deionized water three times per week and they'd been treated with $Na_2HAsO_4.7H_2O$ solution.

Three different concentration of As had been used 32 µM, 64 µM, 128 µM.

For this survey has been used:

- 32 large pots (30x30x15 cm)

- 8 small pots (25x25x12 cm)

(Plastic pots were before sterilized in a solution with water and bleach 5:1)

Large pots were filled with sand up to 12 cm and were added 3,5 L of water before the seedlings; small pots, instead, filled up to 5 cm and 1,3 L of water were added before the seedlings.

Large basins had been used with two different concentrations of As (As1 and As2) and 2 different concentrations of P (P1 and P2). Each group had 8 pots.

As0 = without As

As2 = As 0,8 mg/L

P1 = $[PO_4^{3-}]$ 32 µM

P2 = $[PO_4^{3-}]$ 64 µM

Small basins were used with 4 different concentrations of As and 3 different concentrations of P.

	P1	P2	P3
As0			1
As1	1	1	1
As2			1
As3	1	1	1

Tab. 4: Number of experimented treatments

As0 = without As

As1 = As 0,4 mg/L

As2 = As 0,8 mg/L

As3 = As 1,6 mg/L

P1[(PO_4)]$^{3-}$ 32 µM

P2[(PO_4)]$^{3-}$ 64 µM

P3[(PO_4)]$^{3-}$ 128 µM

Macronutrients and micronutrients were provided through a Long Ashton nutrient solution (Hewitt, 1966).

The sterilized mother solutions are composed by:

- 5 solutions for macronutrients (250x)

- 1 solution for micronutrients (250x)

Mother solutions were autoclaved at 121°C x 15'

RT= Room Temperature

N° test tube	Substance	Final Conc.	g/L	g/250 ml	Preserve at:	Take out(ml)
MACRONUTRIENTS						
1	$Ca(NO_3)_2 \times 4H_2O$	2 mM	118 g/L	29.5 g	4°C	20
2	$MgSO_4 \times 7H_2O$	0,75 mM	46.218 g/L	11.555 g	RT	20
3	KNO_3	2 mM	50.554 g/L	12.639 g	RT	20
4	NaH_2PO_4	32 mM 64 mM 128 mM	9.6 g/L (80mM)	2.4 g	RT	2 4 8
5	FeNaEDTA	50 mM	4.588 g/L	1.147 g	RT	20
MICRONUTRIENTS						
6	$MnSO_4 \times H_2O$	10 mM	0.4226 g/L	0.1056 g	RT	20
	$CuSO_4 \times 5H_2O$	1 mM	0.0624 g/L	0.0156 g		
	H_2BO_3	40 mM	0.6184 g/L	0.1546 g		
	$ZnSO_4 \times 7H_2O$	2 mM	0.1438 g/L	0.0360 g		
	$NaMoO_4 \times 2H_2O$	0,5 mM	0.0302 g/L	0.00755 g		
	NaCl	100 mM	1.4620 g/L	0.3655 g		

Tab. 5: Long Ashton nutrient solution (Hewitt, 1966).

3.2.2. Rice Variety And Seedling Transplantation

A high yielding variety of rice (*Oryza sativa* L.) Carnaroli was selected for the experiment. All seeds were sterilized in Sodium hypo chloride solution (NaClO) Seedlings 28 days old were uprooted carefully from seedbed and transplanted on the day after flooded condition. Five seedlings, almost 10 cm apart from each other, were transplanted in each pot.

3.2.3. Sample Preparation

Once picked up roots and shoots samples, these, were crumbled in a ceramic container by means of a little ceramic mortar. It's been previously needful for when several sample was still too fresh., to heat up biomass in the stove, to allow us to crumble it easily.

Material used (ceramics) were first washed with ultrapure water, and later dried in the oven at ~80 °C, in order to prevent the possible contamination of different samples, pounded using the same container and mortar.

After grinding the biomass, samples were put in small containers, according to the different concentrations of phosphorus and As.

3.3. Analysis

For analyzing samples have been used three different instruments which are:

- Microwave Digestion System
- ICP-MS
- ICP-OES
- Elemental Analyser

3.3.1. Microwave Digestion System

The samples of roots and stem were subjected to acid digestion with HNO_3 69% after being further sieved at 0.2 mm. The digestion was conducted with a microwave system. This technique was usually accomplished by exposing a sample to a strong acid in a closed vessel and raising the pressure & temperature through microwave irradiation. This was increased in temperature and pressure of the low pH sample medium increases both the speed of thermal decomposition of the sample and the solubility of heavy metals in solution. Once these heavy metals was in solution, it is possible to quantify the sample through elemental techniques.

The program involved in two steps:

- 15 min to reach 180 °C (Pmax = 1200 W) ;

- 15 min at 180 °C (Pmax = 1200 W) .

The mineralized solutions were taken with ultrapure water and properly diluted.

From the first series of analyses a loss of the instrumental performance was observed with the progress of the analytical sequence, probably due to the characteristics of the solution. In order to a semi-quantitative analysis was performed to estimate the content of the elementary sample, and it was confirmed the presence of high amounts of salts of Na , Mg, Al, K and Ca, which were not a target of this survey.

We proceeded, therefore, the preparation of an analytical blank, 1% HNO_3, containing the estimated quantities of Na, Mg, Ca (5 mg/l), K (1 mg/l). This solution was used to prepare the calibration standards and submit the instrument under the same conditions in both the calibration phase that analysis of unknown samples.

3.3.2. ICP-MS

The analysis of As were performed using a mass spectrometer with inductively coupled plasma Thermo Scientific *XSeries 2*. This instrument is capable of detecting metals and several non-metals at concentrations as low as one part in 10^{-12} (part per trillion). This is achieved by ionizing the sample with inductively coupled plasma and then using a mass spectrometer to separate and quantify those ions.

Each analytical sequence was preceded by the optimization of the instrumental parameters in order to obtain the best possible response in the analysis phase. This procedure involves the specific optimization of the signal of As (m/z = 75).

The calibration curve is forced through the signal of the analytical blank and weighted by the standard deviation of the absolute calibration solutions.

The As was determined using the CCT- KED mode, provided by the introduction before the mass analyser of a gas flow (typically 5.0 ml/min of a mixture H_2/He 8/92) and setting of an energy barrier (through the application of an appropriate potential difference of hexapole and octapole lenses). It was considered to be the average of three scans performed on the same solution.

The stability of the instrument response time is controlled through the use of an internal standard that is introduced continuously into the spray system together with the sample. The internal standard solution is composed of In 1.0 g/L in 1% HNO_3.

After the analysis of each solution the instrument performs a rinse cycle with 1% HNO_3 to avoid contamination and memory effect between samples.

3.3.3. ICP-OES

Phosphorous and sulphur concentrations were determined by means of a Spectro Genesis ICP-OES spectrometer (Spectro Analytical Instruments, Kleve, Germany), equipped with a crossflow nebulizer and a Scott spray chamber.

Plasma was generated by Argon and the power was of 1400 W.

The flow conditions were: coolant flow = 12.00 L/min, auxiliary flow = 0.60 L/min and nebulizer flow = 1.00 L/min. This instrument is an atomic emission spectrometer with inductively coupled plasma, used for the detection of trace metals. It is a type of emission spectroscopy that uses the inductively coupled plasma to produce excited atoms and ions that emit electromagnetic radiation at wavelengths characteristic of a particular element.

The calibration curve is forced through the signal of the analytical blank and weighted by the inverse of the concentration.

The elements were determined considering the spectral line that provides the best results in terms of signal intensity, precision and accuracy; precisely for phosphorus (P) was considered the 213.618 μm line and for sulphur (S) the 182.034 μm line. It was considered to be the average of three scans performed on the same solution.

The stability of the instrument response time is controlled by the repeat sequence at the end of the analytical blank and a calibration standard.

After the analysis of each solution the instrument performs a rinse cycle with 1% HNO_3 to avoid contamination and memory effect between samples.

3.3.4. Elemental Analyser

Elemental analysis uses combustion to convert the sample elements to simple gasses, i.e. CO_2, H_2O, & N_2. Upon entering the analyser, the sample is combusted in pure oxygen environment at temperatures in the range of 1200-1500 F. The product gasses are separated under steady state conditions, and measured as a function of thermal conductivity (Elemental Analysis, Inc.). This analysis were carried out by means of EA3000 CHN Elemental Analyser (EuroVector, Milano, Italy). Acetanilide, purchased by EuroVector (Milano, Italy) was used as calibration standard (C % = 71.089, H % = 6.711, N % = 10.363). The instruments settings are shown in the table below.

Carrier (He)	120 kPa	Front Furnace	1050 °C
Purge	80 mL/min	Rear Furnace	900 °C
Oxygen	20 mL	GC Oven	85 °C
$\Delta P\ O_2$	35 kPa	Retention time	
Oxidation time	8.8 s	N	45 s
Sample delay	6 s	C	75 s
Run time	400 s	H	170 s

Tab. 6: Instruments Settings Of Elemental Analyzer

3.3.5. Data Analysis

Data with normal distribution were subjected to one-way ANOVA, considering treatments as factors; means were compared with appropriate post-hoc tests (either Fisher's PLSD or Tukey's HSD) and differences were considered to be significant for $p < 0.05$. Data with non-normal distributions were subjected to Kruskal-Wallis test, followed by Mann-Whitney for the comparison of means; again, differences were considered to be significant for $p < 0.05$. Analyses were performed with Statview and R 3.0.2 packages of software.

Principal component analysis on the whole dataset were performed with Statistica 7.

3.4. Results And Discussions

3.4.1. Morphological Plant Measures

Table 1 reports significance levels for the four parameters taken in account, according to the Kruskal-Wallis test. As can be observed, the four parameters are substantially affected by factors “arsenic” and “Treatment” (combining P and As levels). Factor “phosphorus” shows lower significance levels and does not affect “fresh roots weight”.

Factor	Fresh Roots Weight	Fresh Shoots Weight	Dry Roots Weight	Dry Shoots Weight
As	**	***	***	***
P	N.S.	*	***	**
Treatment	**	***	***	***

Tab. 7: Arsenic, Phosphorus and treatment significance levels on morpholofigical parameters, according to Kruskal-Wallis test. N.S. = Not significant. *, **, *** = significant with probability 0,05, 0,01, 0,001, respectively.

Results referring to fresh roots weight are reported in Fig. 2. In absence of As, increase P in the nutritive solution causes a root fresh biomass enhancement, resulting crucial in the comparison between the first and third P level. At the first and second As level, it can be observed a reduction of the fresh root biomass enhancement in correspondence of the increase of P concentration, but differences are significant only at the first As level and for the comparison between the basal P level and the successive two levels. At the maximum As level there are no noticeable differences in the fresh root biomass with respect to variation in the phosphatic nutrition. At the same P level in the nutrient solution (comparisons reported with capital letters), some significant differences correlated to As concentration, emerge; at the first phosphorus level, plants grown with 0,4 or 0,8 mg/L of As shown an increment in the fresh root biomass with respect to the control samples and the plants grown with 1,6 mg/L of As. At the second P level there are no significant variations corresponding to changes in As concentration.

At the third P level, plants treated with As show fresh root biomass values always lower than the control group samples (but significant only for the first As level). Curiously, with the increase of P concentration a progressive fresh root biomass enhancement is observed.

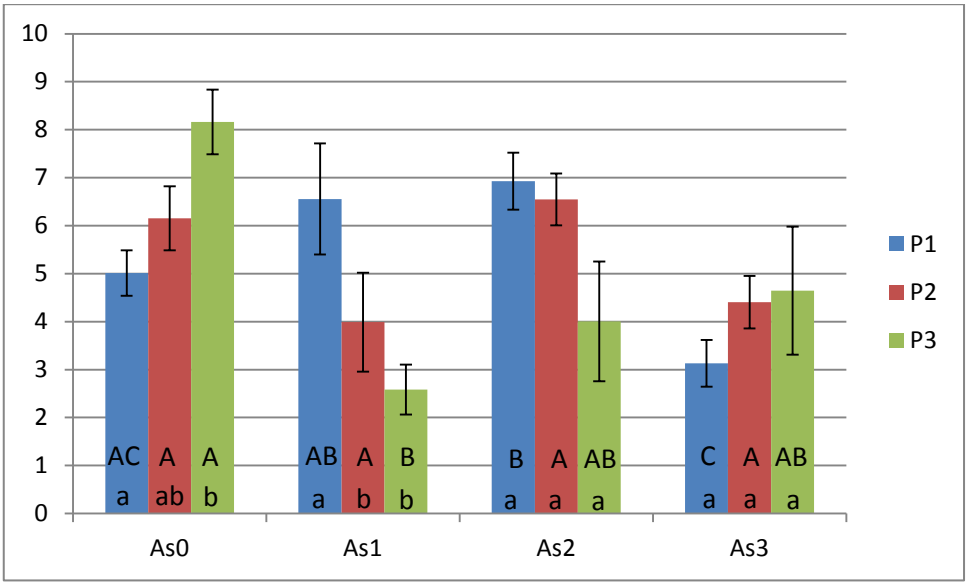

Fig. 21 – Fresh root weight (in grams) of rice plant at the repot. Each column report the mean value and the standard error bar. P1: 32 µM of P in the nutrient solution; P2: 64 µM; P3: 128 µM. As0: without added As; As1: 0,4 mg/L of As added as arsenate once a week; As2: 0,8 mg/L di As; As3: 1,6 mg/L di As. Statistically significant differences in the same As level (three column group) are reported with different lowercase letters; statistically significant differences between treatments with the same P level (columns with the same color) are reported with different capital letters.

Fig. 22 shows results about fresh shoot weight. Considering the effects of P variations in the nutrient solutions for each arsenic level (comparisons reported with capital letters); it can be observed that, at 0 and 1 As levels, P concentration variations do not produce significant variations. At the second As level it can be noticed a significant decrease in the fresh epigeal biomass due to the higher P concentration. At the third As level, finally, an increase in the fresh epigeal biomass is observable, in correspondence of the increase of P concentration.

At the same P level in the nutrient solution (comparison reported with capital letters), some significant differences in correspondence with As concentration changes are observable; at the first P level, only the plants growth with the highest As value show a n important reduction in the fresh epigeal mass. At the second P level, As concentration variation promote some effects that cannot be considered as a simple linear model because the fresh epigeal biomass decreases (with respect to the control group, without metalloid) at the first and third As level, but it does not show any important variation at the second As level. Similarly as for what observed on the roots, fresh epigeal biomass values are lower than the ones shown by control and the increase of phosphorus concentration lead to a progressive increase of fresh root biomass.

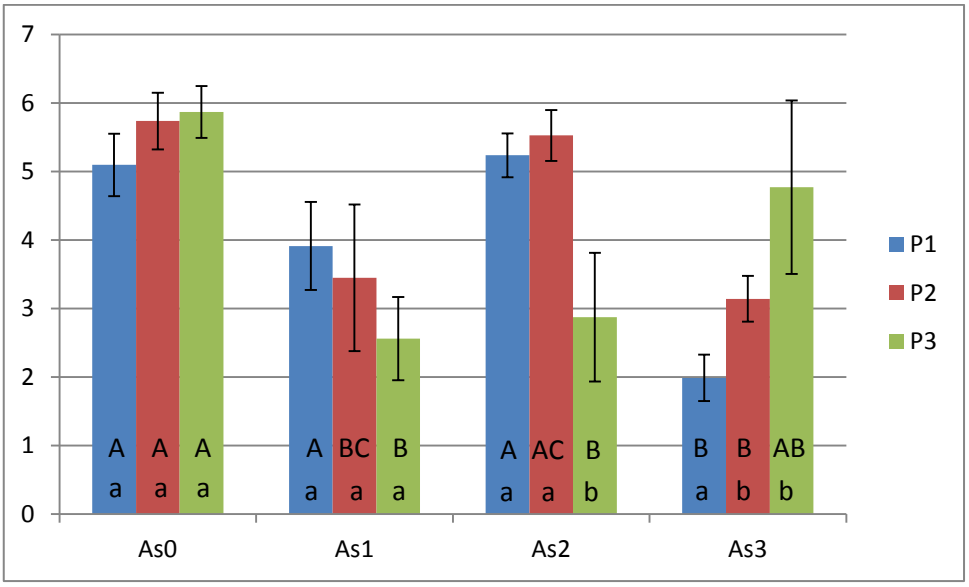

Fig. 22 – Fresh shoot weight (in grams) of rice plants at repot. Each column reports mean value and standard error bar. P1: 32 μM of phosphate in the nutrient solution; P2: 64 μM; P3: 128 μM. As0: without added As; As1: 0,4 mg/L of As, added as arsenate once a week; As2: 0,8 mg/L di As; As3: 1,6 mg/L of As. Statistically significant differences in the same arsenic level (three columns group) have been reported with different lowercase letters; statistically significant differences between treatments with the same phosphorus level (columns with the same colour) have been reported with different uppercase letters.

In Fig. 23 the results about roots dry roots weight. Considering the effects of the P variations in the nutrient solutions, for each As level (comparisons reported with lowercase letters), it can be observed that, in absence of As and at the third level of As, variations of P concentration do not promote any significant variation. At the first As level it is noticeable a clear trend in the decrease of the dry root biomass in correspondence with the increase of P concentration, with significant differences between the first and the next two levels of P. At the second As level, only the higher P level induces an important dry root biomass reduction.

At the same P level in the nutrient solution (comparisons reported with uppercase letters), some important differences in correspondence with variations of As concentrations; at the first P level it is observable a reduction of the dry root biomass with the increasing of the As concentration, but the differences are significant only in the comparison between the first and the third As level.

At the second P level, all the As treatment show dry root biomass values lower than the ones relative to the control group, with important differences between the first and the third As level. Even at the highest P concentration, As treatments result in lower values with respect to the control group, mainly at the first and the second As level, while not at the third.

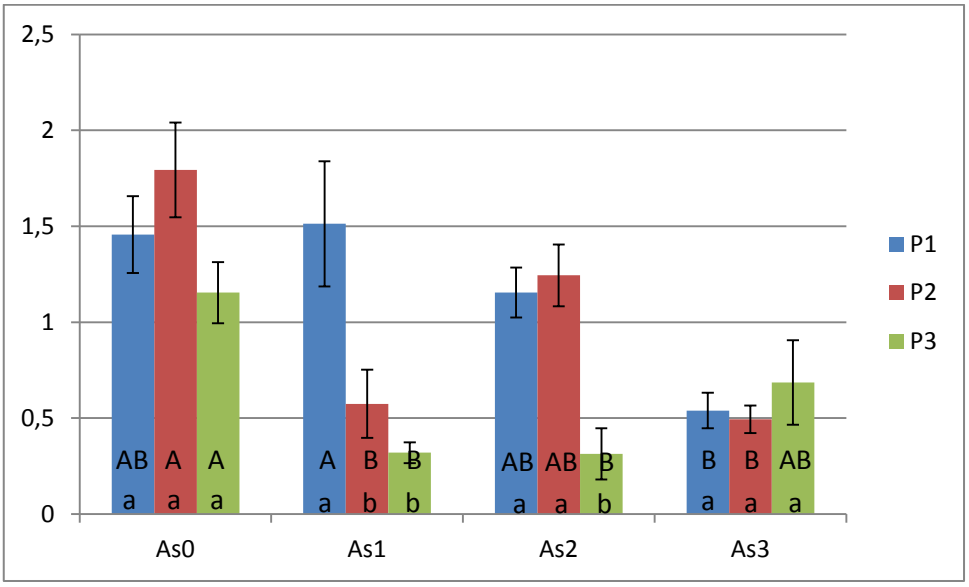

Fig. 23 – Dry root weight (in grams) of rice plants at repot. Each column reports the mean value and the standard error bar..P1: 32 μM of phosphate in the nutrient solution; P2: 64 μM; P3: 128 μM. As0: without added As; As1: 0,4 mg/L of As added as arsenate once a week; As2: 0,8 mg/L of As; As3: 1,6 mg/L of As. Statistically significant differences inside the same As level (three columns group) have been reported with different lowercase letters; statistically significant differences between treatments with the same phosphorus level (column with the same colour) have been reported with capital letters.

In Fig. 24 results about dry shoot weight have been reported. Considering the effects of the P variations in the nutrient solutions, for each As level (comparison reported with lowercase letters), it is observable that in absence of As, or at the third As level, variations in P concentration do not promote significant alterations.

At the first As level, it is evident a clear reduction in the dry root biomass in correspondence of the increase of P concentration, with significant differences between the first and the third P level. At the second As level, the highest P concentration induces a noticeable reduction in the dry root biomass.

At the same P level in the nutrient solution (comparisons reported with capital letters), some significant differences can be observed, with respect to changes in the As concentration; at the first P level, an important dry epigeal biomass reduction can be noticed for the third As level, with respect to the control and the second As level. At the second P level, all the As treatments show dry root

biomass values lower than the control, with significant differences between the first and the third As level. Even in the highest P concentration, all the As treatment result clearly lower than the control, the first and the second As level but not for the third.

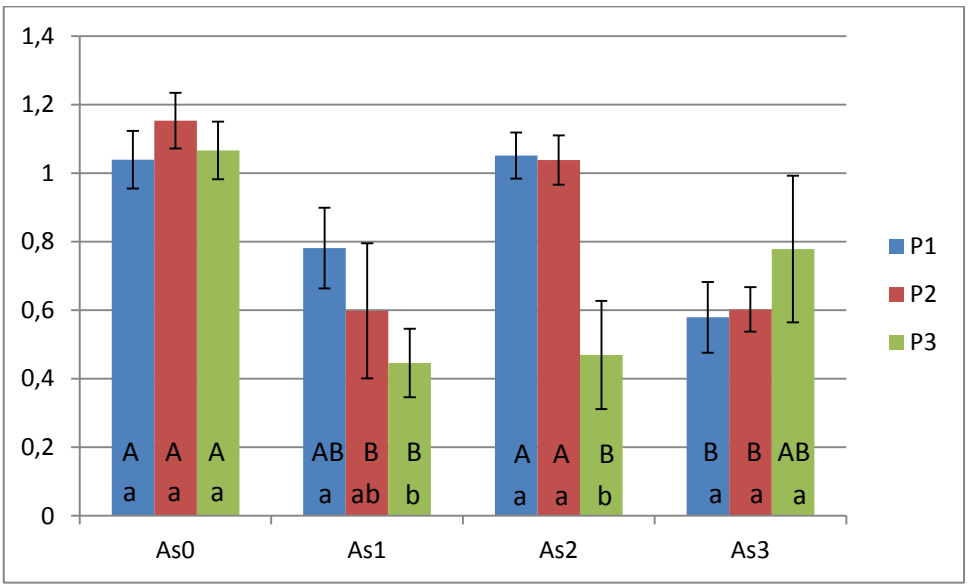

Fig. 24 – Dry shoot weight (in grams) of rice plants at repot. Each column reports mean value and the standard error bar. P1: 32 μM of phosphate in the nutrient solution; P2: 64 μM; P3: 128 μM. As0: without As added; As1: 0,4 mg/L of As added as arsenate once a week; As2: 0,8 mg/L of As; As3: 1,6 mg/L of As. Statistically significant differences in the same As group (three columns group) have been indicated with lowercase letters; statistically significant differences between treatment with the same P level (column labeled with the same colour) have been indicated with capital letters.

3.4.2. Uptake Results Of Shoot Samples

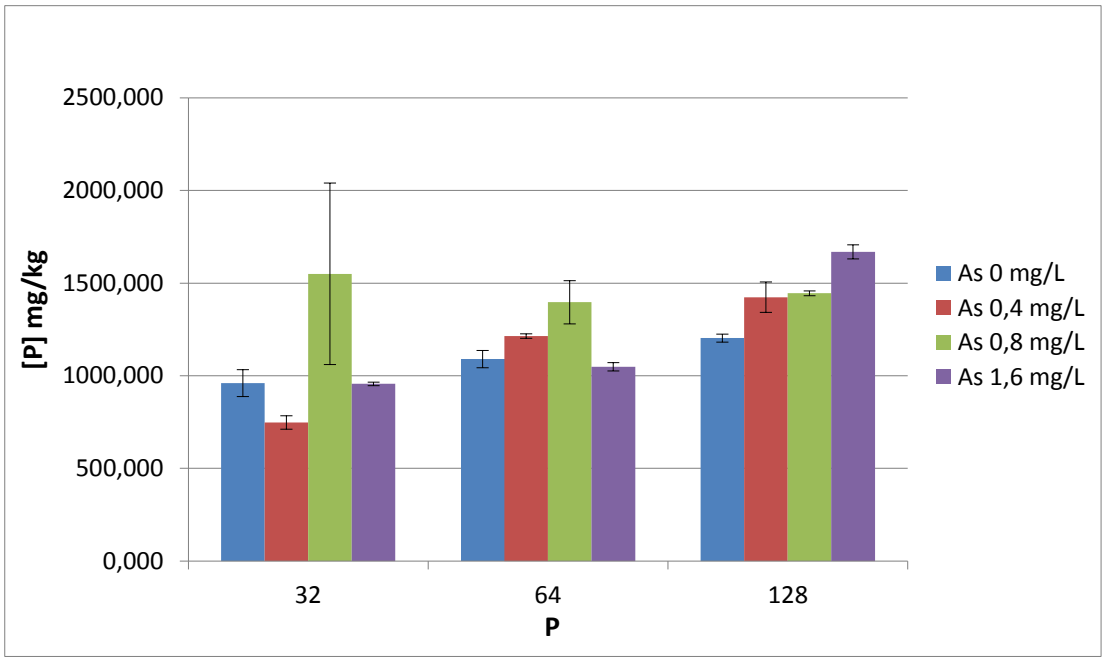

Fig. 25: P uptake of shoot samples subjected to different treatments. For each treatment, mean value and standard errors are reported.

Fig. 25 shows Phosphorus uptake by shoot samples in function of the As and P treatment they have been subjected. On the x axis the different concentrations of P (P1, P2, P3) are reported. For each P concentration, three different As treatment have been experimented: As1, corresponding to an As concentration of 0.4 mg/l, As2, corresponding to a concentration of 0.8 mg/l and finally As3, the treatment with the higher concentration of As, corresponding to 1.6 mg/l.

A last bin can be observed, As0, the blue one, that represents the samples that have not been subject to As treatment.

Observing the As0 bins projections on the P uptake axis, it can be noticed that, in absence of As, the phosphorus absorbed by the samples, grows almost linearly with the concentrations they have been subjected.

Another observable evidence is that, the maximum P uptake has been registered

on the samples subjected to the highest concentrations of P and As, corresponding, in the plot, to the last violet bin on the right.

It is also interesting to notice that, the lowest P uptake has been registered for the samples with low phosphorus (P1) and As (As1) concentration, while, when subjected to P1As2 treatment, the shoot samples show a much higher phosphorus uptake, reported in the first red bin.

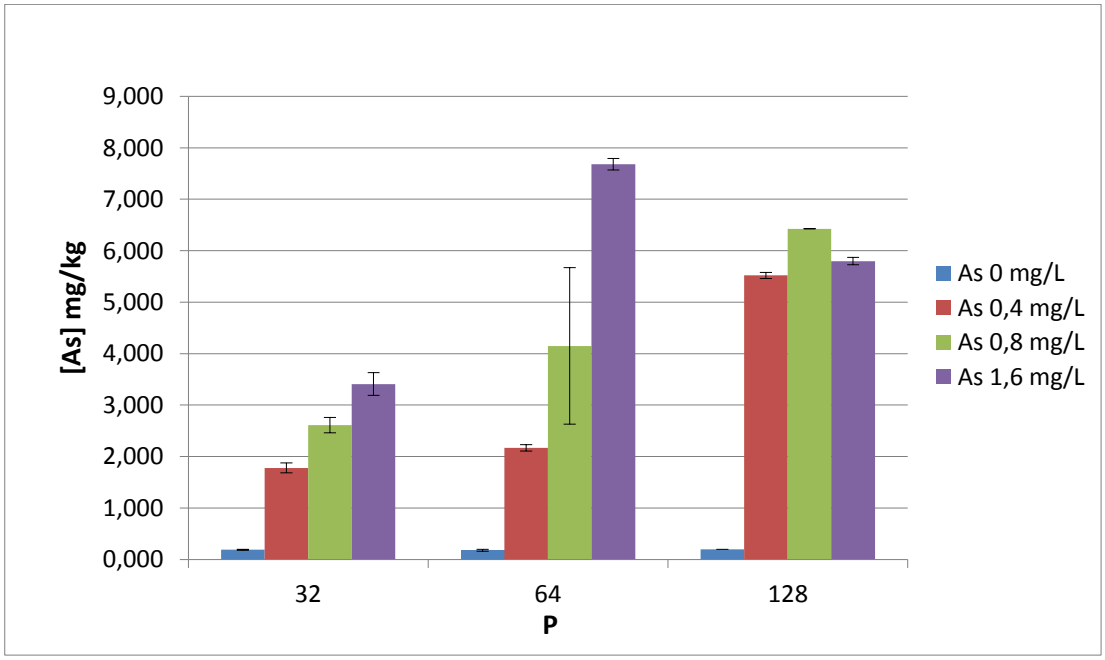

Fig. 26: As uptake of shoot samples subjected to different treatments**.** For each treatment, mean value and standard errors are reported.

Fig. 26 reports the As uptake observed on the shoot samples in relation with the treatment performed. Obviously, all the blue bins have null values, since they correspond to non-As treatments. As predictable, generally, the As uptake registered grows with respect to the As concentration of the treatments performed, with a maximum As absorption observable for the samples subjected to P2As3. This can be justified by the chemical similarity of P and As, that causes an increasing As uptake in presence of lower concentrations of P.

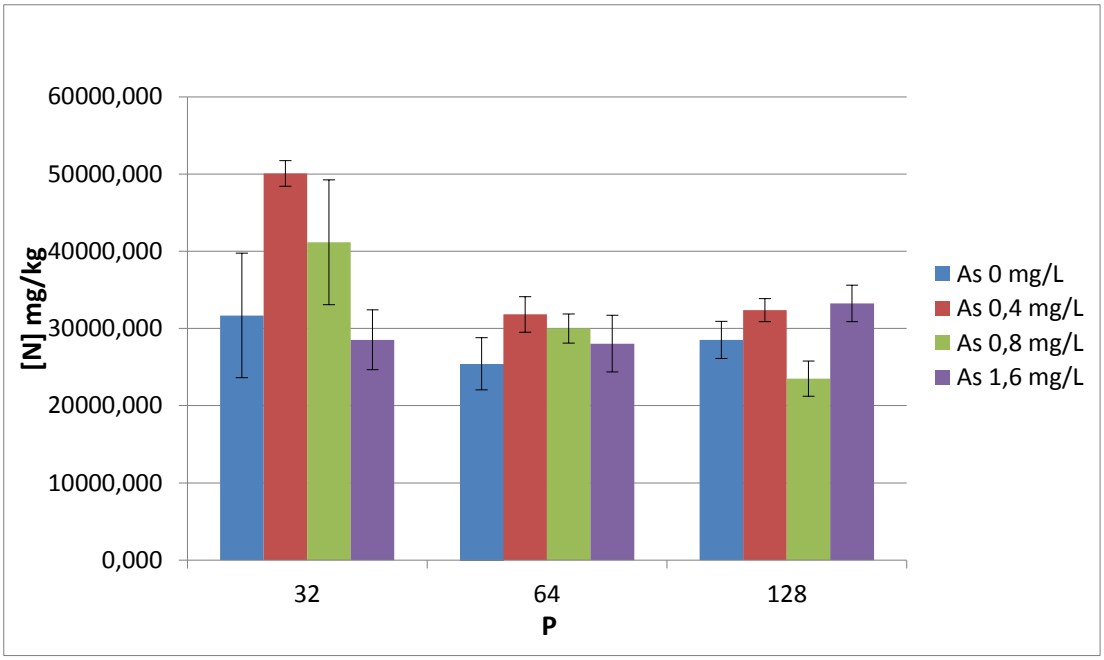

Fig. 27: N uptake of shoot samples subjected to different treatments. For each treatment, mean value and standard errors are reported.

Fig. 27 shows the nitrogen absorption observed in relation with the different treatments. It can be noticed that the higher values correspond to samples threated to As1P1 and As2P1, while the samples subjected to higher concentrations of phosphorus shows N values that are almost similar.

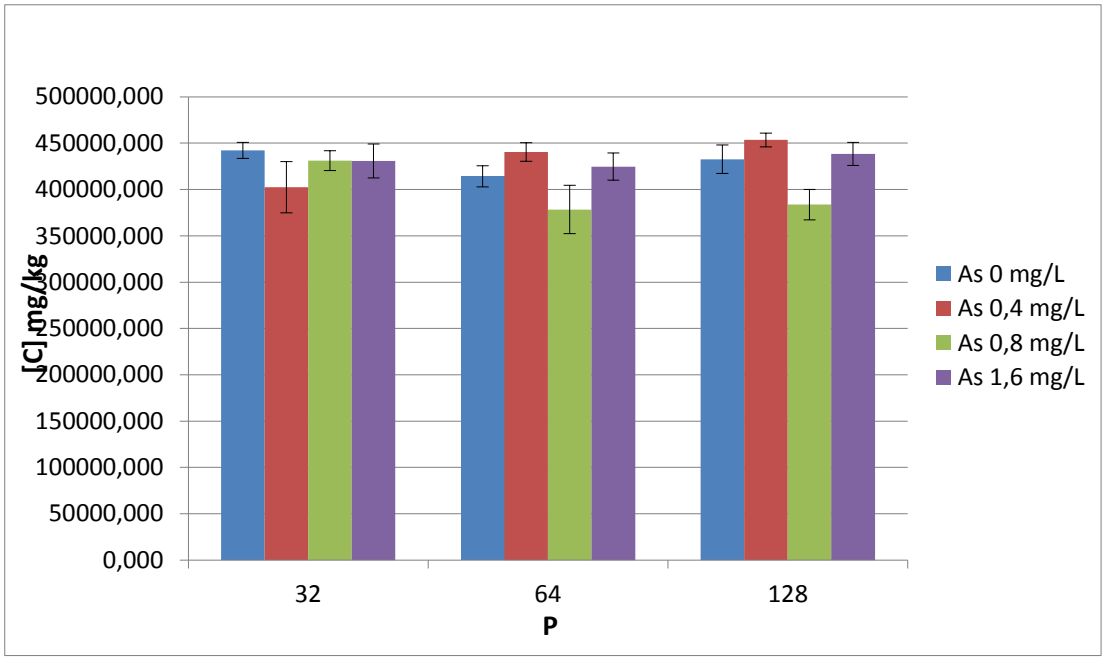

Fig. 28: C uptake of shoot samples subjected to different treatments. For each treatment, mean value and standard errors are reported.

Fig. 28 reports the carbon uptake registered from the different threated samples. In this case it looks that the C absorption has been influenced much by the different treatment with exception for the samples exposed to the higher phosphorus concentrations: in particular, treatments As2P2 and As2P3 have caused the lower C uptakes.

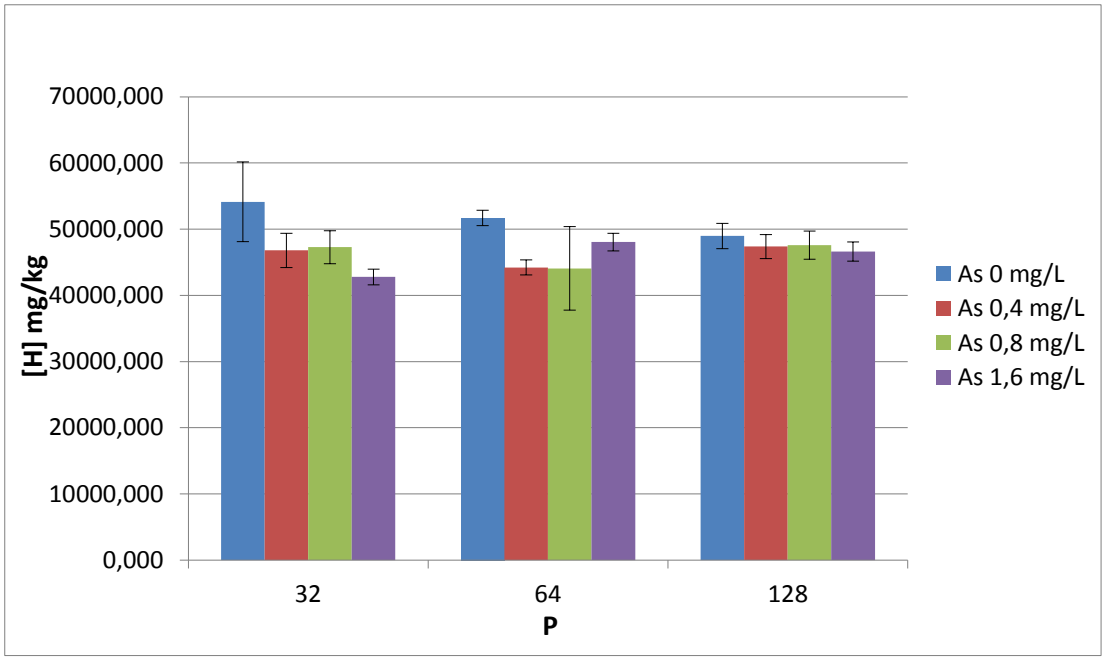

Fig. 29: H uptake of shoot samples subjected to different treatments. For each treatment, mean value and standard errors are reported.

Observing Fig. 29 it can be noticed that the hydrogen uptake has not been significantly biased by the different treatments experimented. For all the samples, the H absorption registered lies in a range between 400000 mg/l and more than 500000 mg/l, with a maximum value observable on the first bin, the one relative to samples threated with the lower concentrations of P and As.

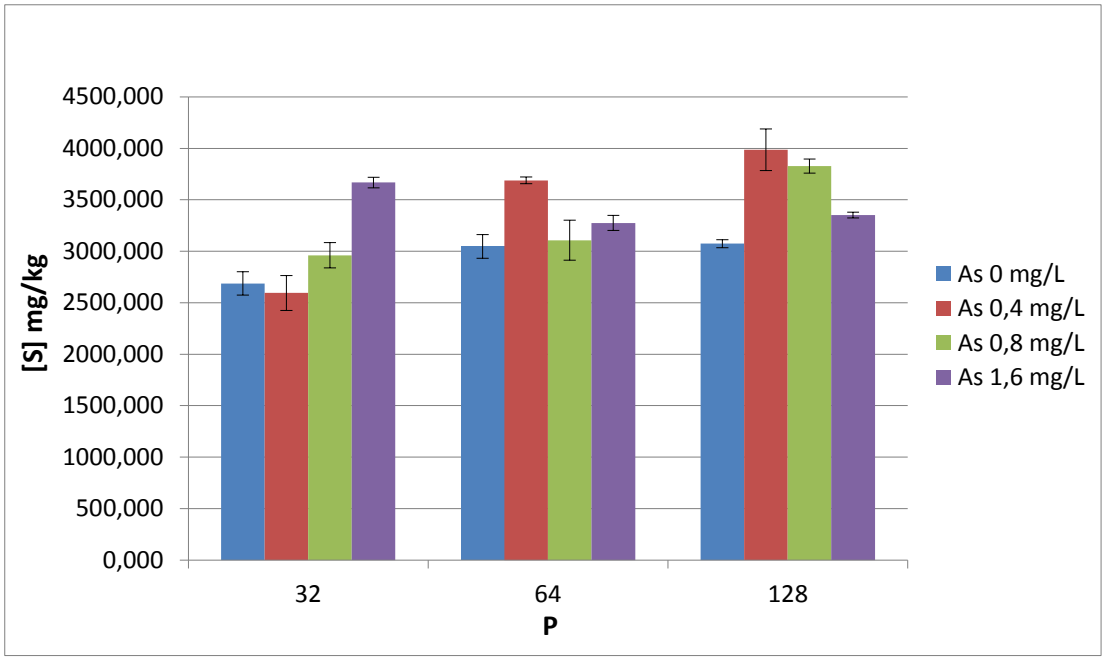

Fig. 30: S uptake of shoot samples subjected to different treatments. For each treatment, mean value and standard errors are reported.

In Fig. 30, the last plot shows the results obtained in terms of sulphur uptake: also in this case it can be noticed that the different treatments have not influenced strongly the S absorption but, it is interesting to see, that higher phosphorus concentrations have caused the maximum S uptake (As1P3, As2P3).

3.4.3. Uptake Results Of Root Samples

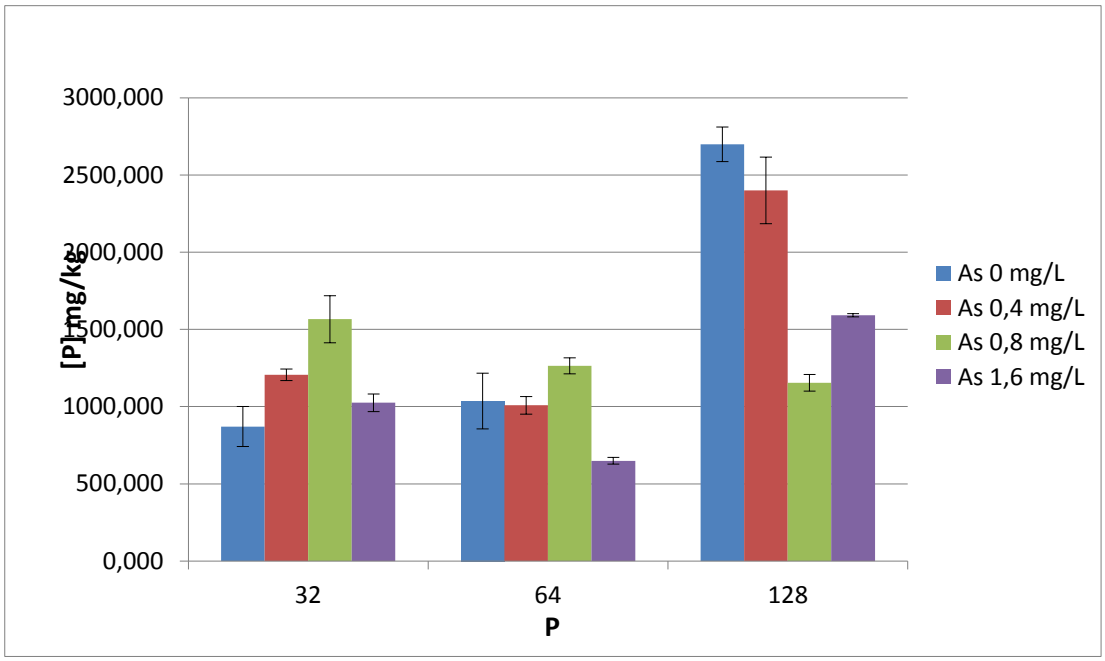

Fig. 31: P uptake of samples subjected to different treatments. For each treatment, mean value and standard errors are reported.

Fig. 31 shows the phosphorus uptake, observed on the root samples, in function of the As and P treatments. As predictable, the higher values have been registered on the samples threated with the higher concentrations of P (As0P3, As1P3, As3P3). It is interesting to notice that, differently from what observed on the shoot samples, the uptake values are much higher on roots.

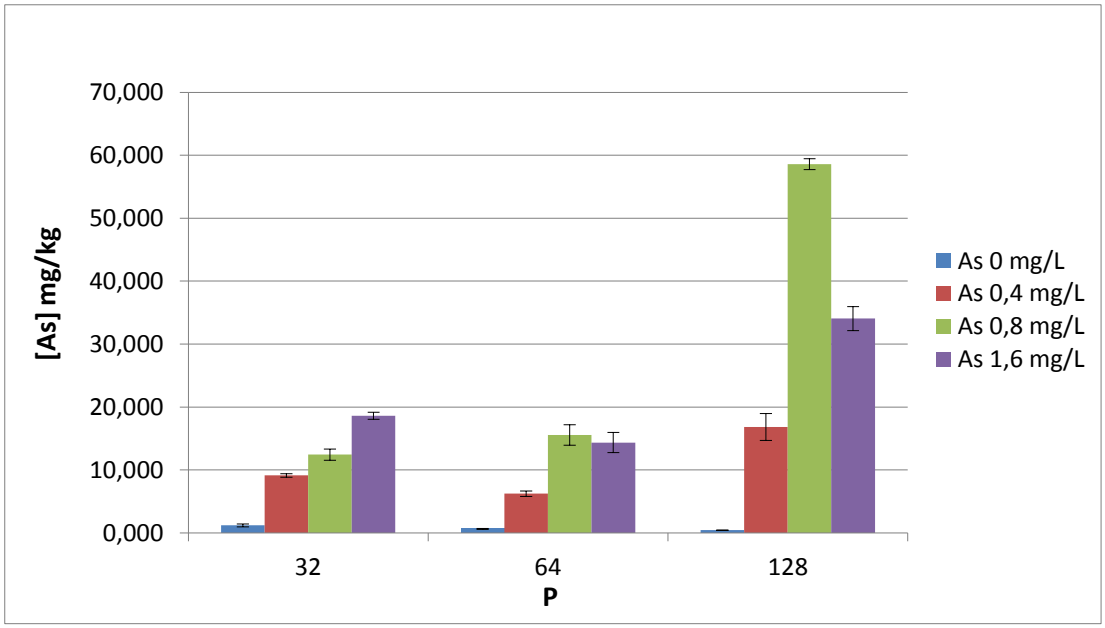

Fig. 32: As uptake of root samples subjected to different treatments. For each treatment, mean value and standard errors are reported.

Fig. 32 shows the root samples As uptake with respect to the different treatments. Obviously, blue bins, corresponding to As0 treatments, shows a null As uptake. It can be noticed that the higher As uptakes have been observed on the samples threated with the higher P concentrations (P3) and that, in particular, the treatment As2P3 is the one which shows a major As absorption by the roots.

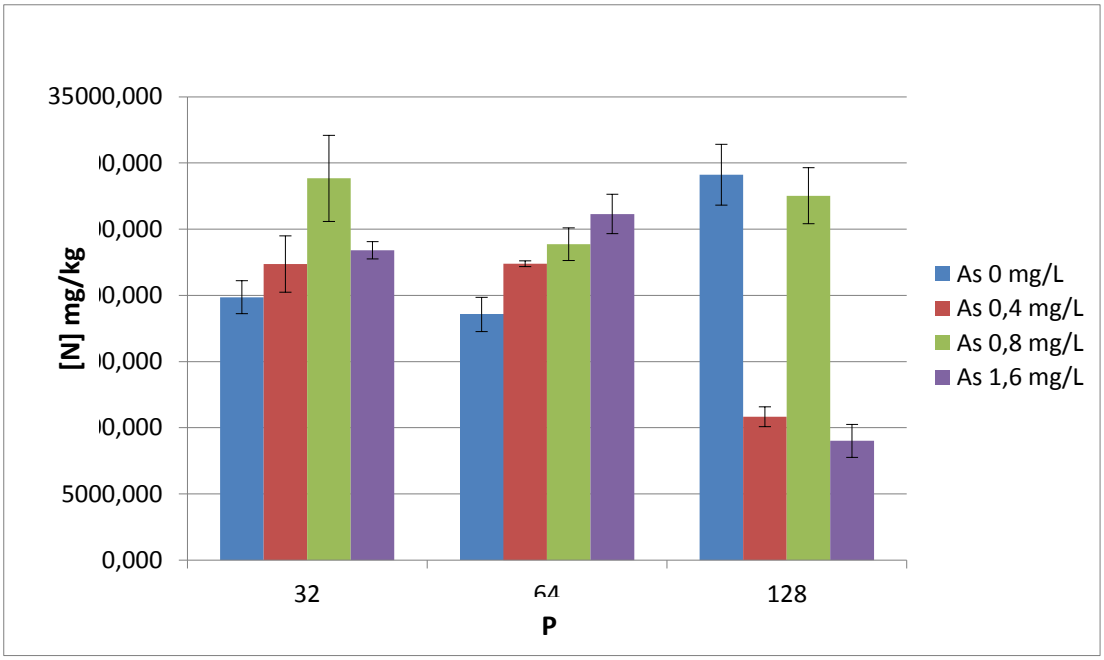

Fig. 33: N uptake of root samples subjected to different treatments. . For each treatment, mean value and standard errors are reported.

Fig. 33 reports the values registered in terms of nitrogen absorption; while, in general, the uptake values seems not strongly related with the different treatments, it can be noticed that root samples subjected to As1P3 and As3P3 shows a minimum nitrogen absorption.

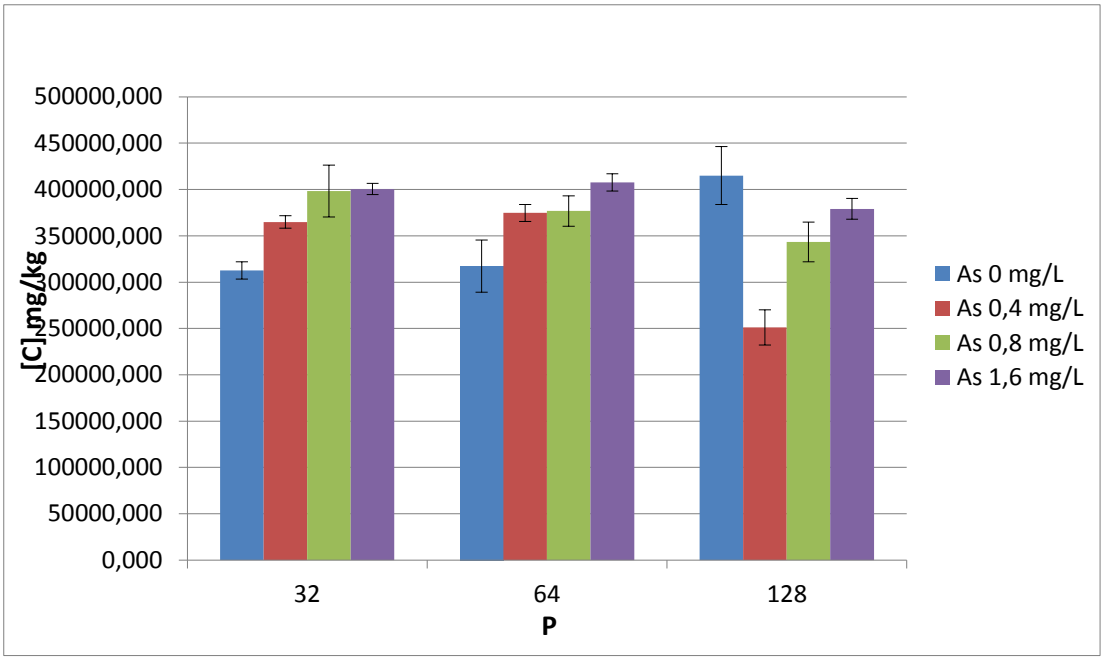

Fig. 34: C uptake of root samples subjected to different treatments. For each treatment, mean value and standard errors are reported.

Similarly to what observed in Fig. 33, Fig. 34 shows that the carbon uptake by the root samples is not so strongly related with the different treatments. Also in this case it can be observed that the samples subjected to As1P3, had a minor carbon uptake.

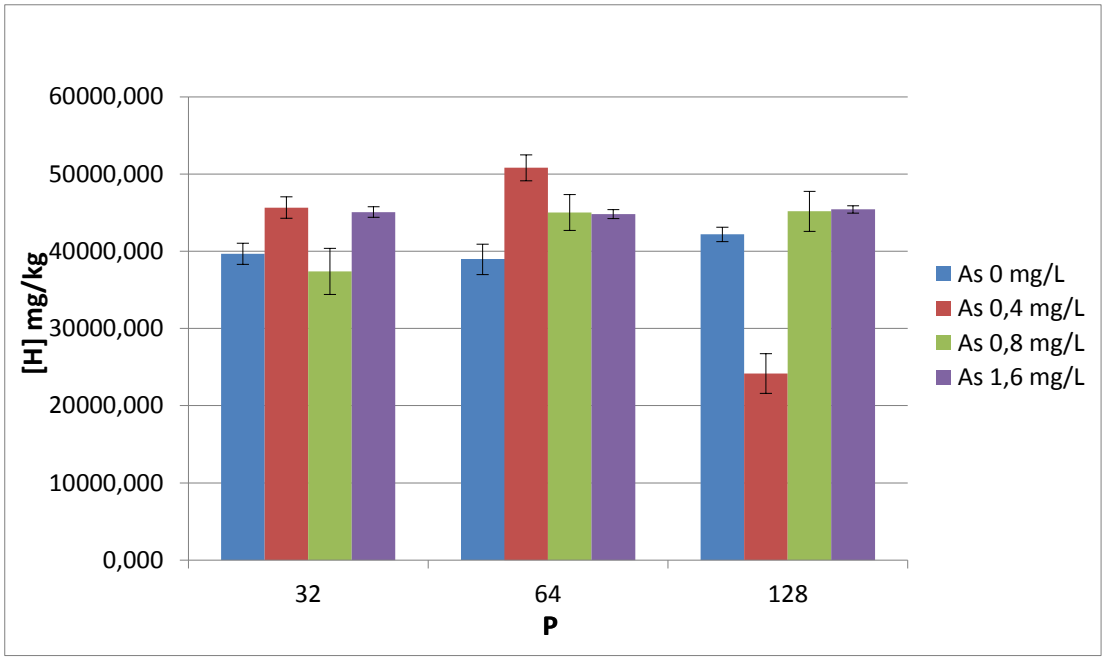

Fig. 35: H uptake of root samples subjected to different treatments.

Fig. 35, reports the hydrogen uptake values registered on the different root samples. One more time, as observed for carbon and nitrogen, the samples that show a minor hydrogen uptake are the one subjected to As1P3 treatment.

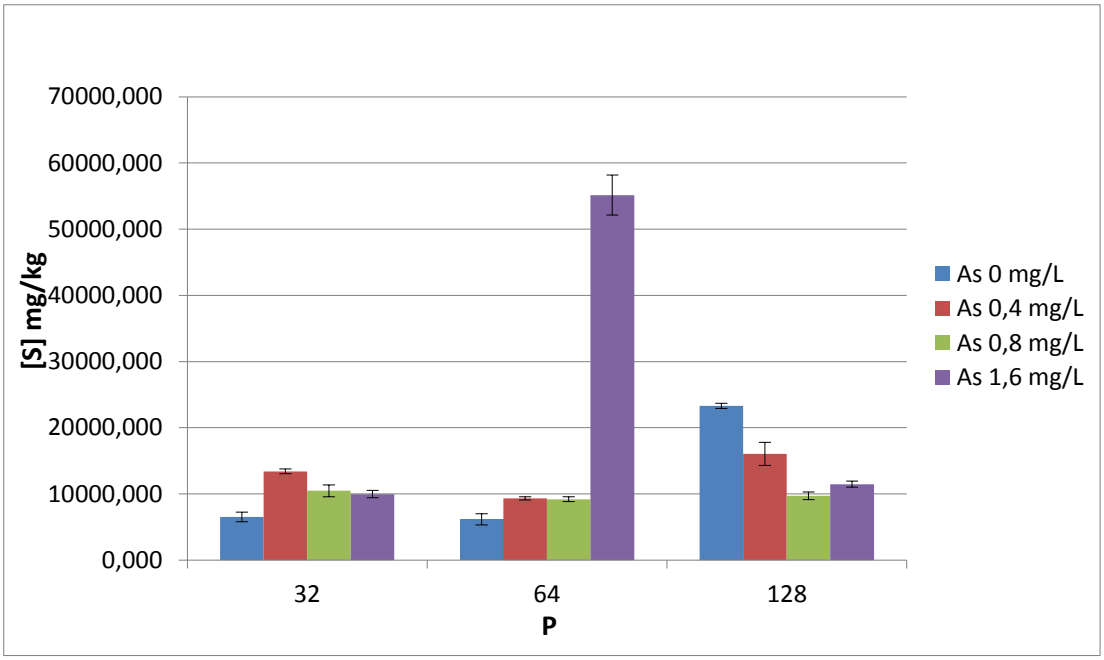

Fig. 36: S uptake of root samples subjected to different treatments. For each treatment, mean value and standard errors are reported.

In Fig. 36,the last plot, Plot S, reports the sulphur uptake values registered for the root samples subjected to different As and P concentrations. In this plot, a relevant peak, in term of sulphur uptake, can be observed for the treatment As3P2: on the samples subjected to this treatment, the sulphur values registered are more than three time higher than the values registered on all the other samples.

3.5. PCA Analyses

The original dataset is characterized by eight different features (As, P, C, N, H, S, lenght, DW, FW). A principal component analysis has been performed (ignoring the "lenght" feature) defining seven principal component. Fig. 37 reports the PC scree plot: each element on the x axis corresponds to a principal component and its value on the y axis indicates the corresponding variance. From the scree plot can be observed that the first three components (PC1, PC2, PC3) contain about the 60% of the overall variance.

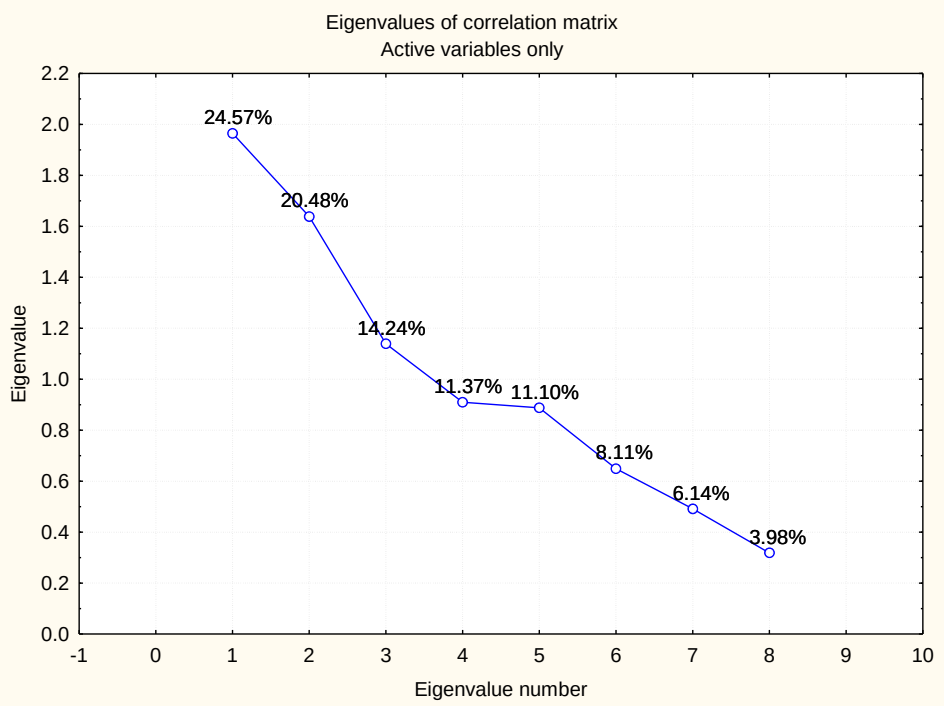

Fig. 37: Principal Components Scree Plot

Fig. 38 reports the loading plot PC1-PC2. In a loading plot each axis corresponds to a principal component. Projecting the original features in this new space, it is possible to show how a feature contributes to a specific PC and to get an overall idea of the meaning of the new variable defined by the component. From Fig. 38 it is evident that features As, P and S give an important contribution to PC1; from this observations we can interpret PC1 as a new variable representing the uptake of the elements by the plants. In the same way we can observe that the two

variables, DW, FW, both regarding the weight of the samples, have an important role in the PC2 composition: we can interpret this component as a variable reporting an information about the growth stage of the plant.

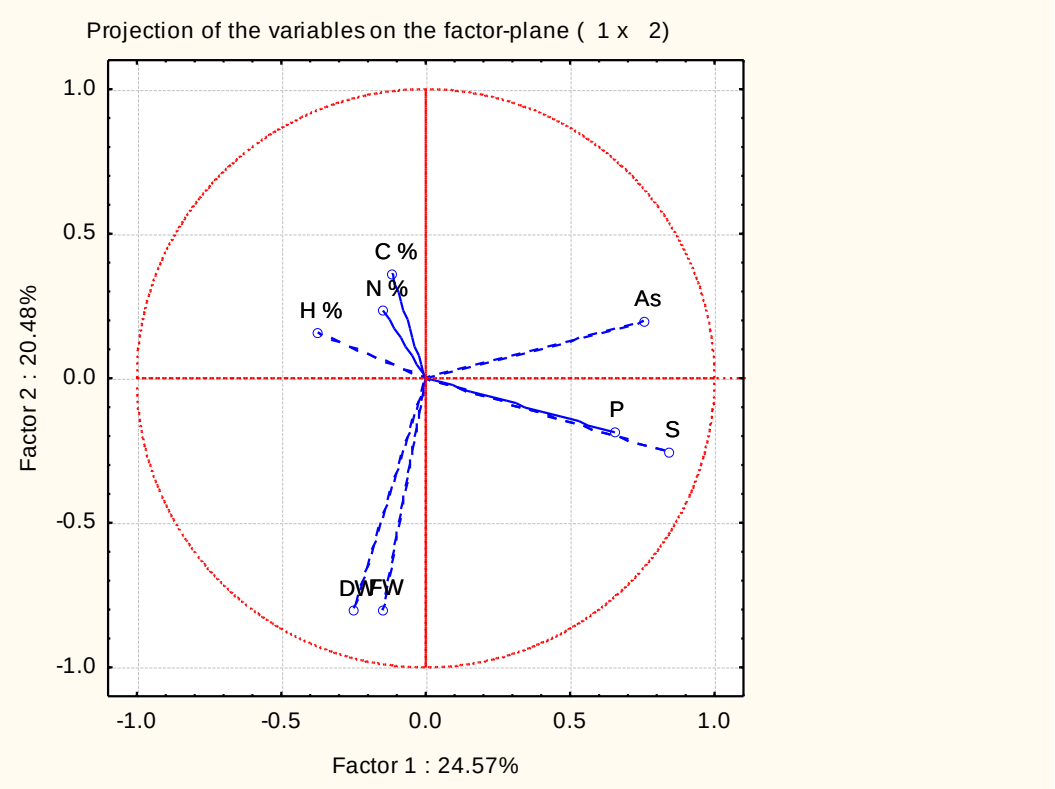

Fig. 38: PC1 vs PC2 loading plot

Fig. 39 shows the loading plot PC1-PC3. On the y axis the contribution for PC3 are reported: as can be observed, the more important feature for this component are the percentage values of C and N, and to a minor extent of H. From the plot it is also evident that H and C are correlated while N is anticorrelated.

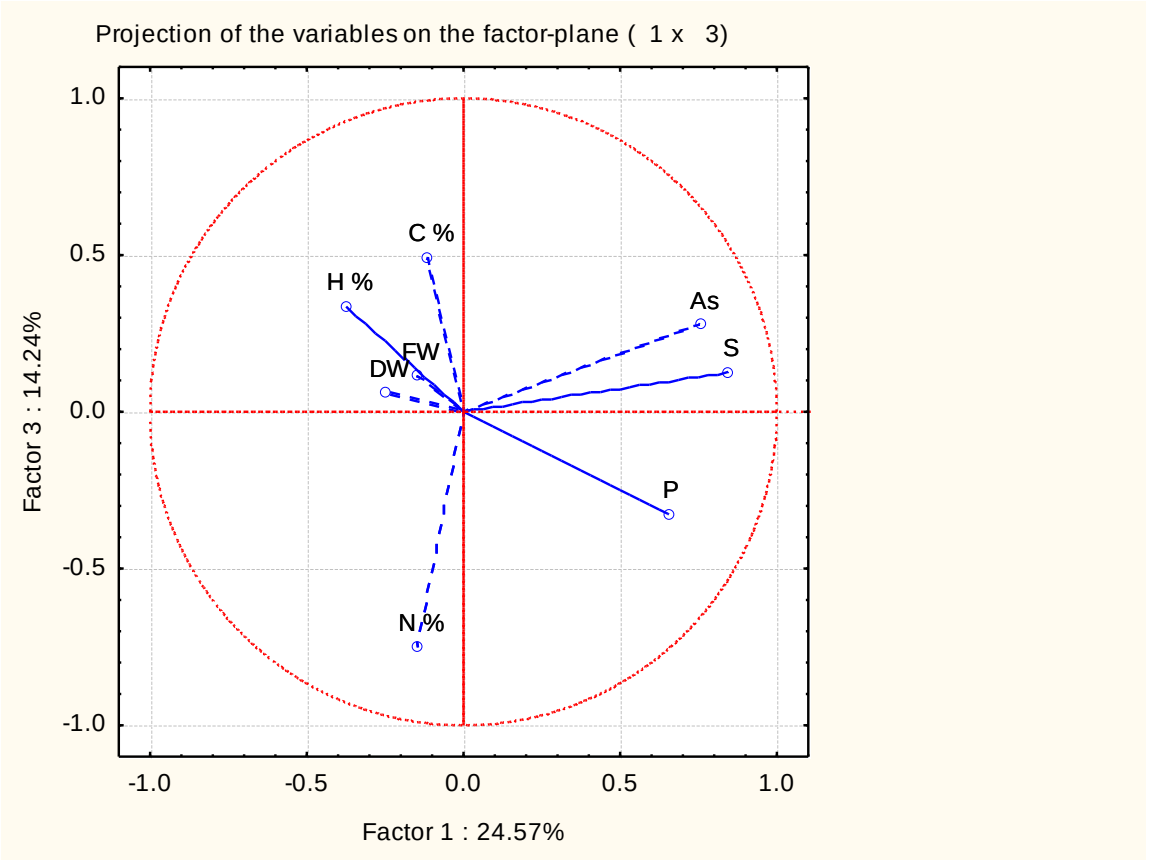

Fig. 39: PC1 vs PC3 loading plot

Fig. 40 shows the score plot for PC1-PC2. The points in the plot correspond to samples, marked with different colours in relation to the treatment, in terms of As and P exposure, they have been subjected.

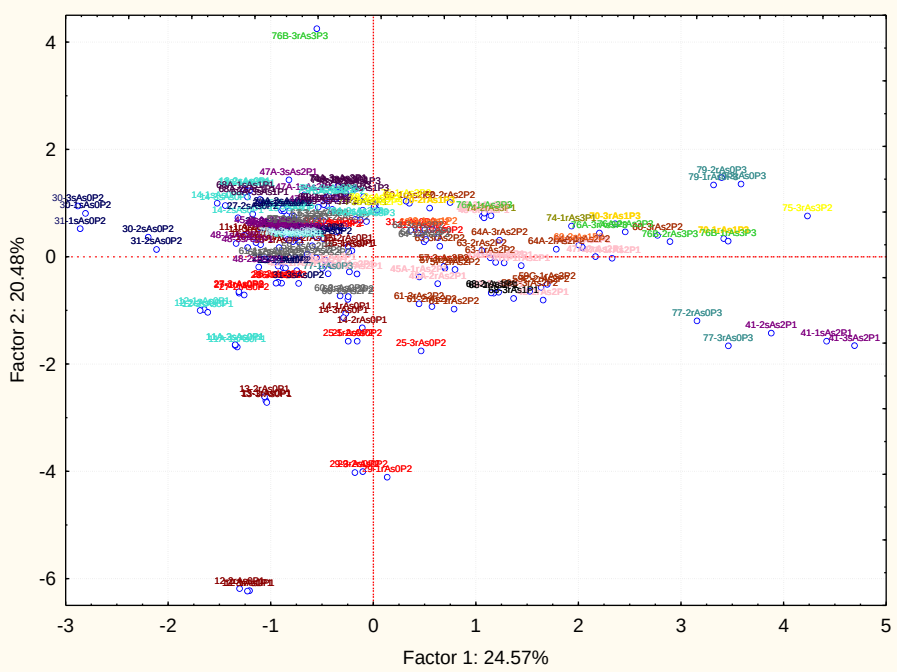

Fig. 40: PC1 vs PC2 score plot

In Fig. 41, data reported in Fig. 40 have been roughly classified in root samples (red label) and shoot samples (blue label). Samples from shoots and roots are pretty well separated with respect to PC1: it can be inferred that root samples show an higher As and P uptake, represented by higher values on the PC1 axis. From this results some important considerations can be taken: it seems that As is accumulated in the plant but that roots absorb it in a much higher way, while shoots and the edible parts, do not absorb particularly it. This can be important from a health point of view.
At the same time, samples are not so strongly separated by PC2: it can be reasonable to think that plants growth has not been influenced by the different treatments performed.

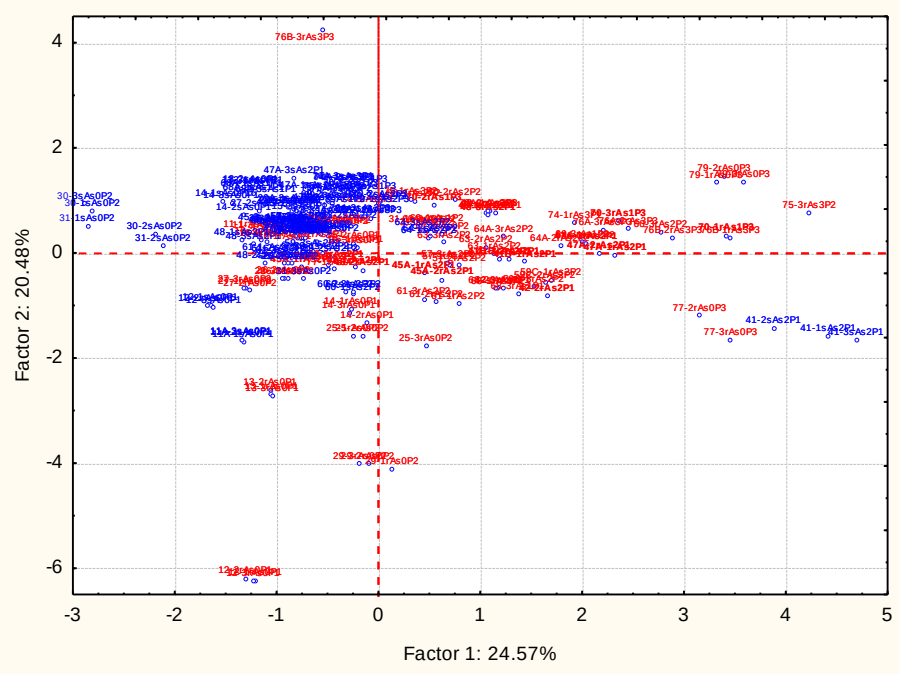

Fig. 41: PC1 vs PC2 score plot with labelled data: blue marks correspond to shoot samples, red ones to roots.

Fig. 42 reports the same score plot as Fig. 41, but with samples marked with different colours, depending on the As exposure they have been subjected.

It can be noticed that some clusters, composed by samples subjected to the same treatments, emerge. As told for Fig. 41, here again is possible to notice that roots and shoots absorb differently As: for instance, the green samples have been

treated with high concentration of As; while the roots samples show higher values for PC1, the shoots samples, in bold green, all lie near to the zero. Once more it seems that the aerial part of the plants do not absorbs significantly As.

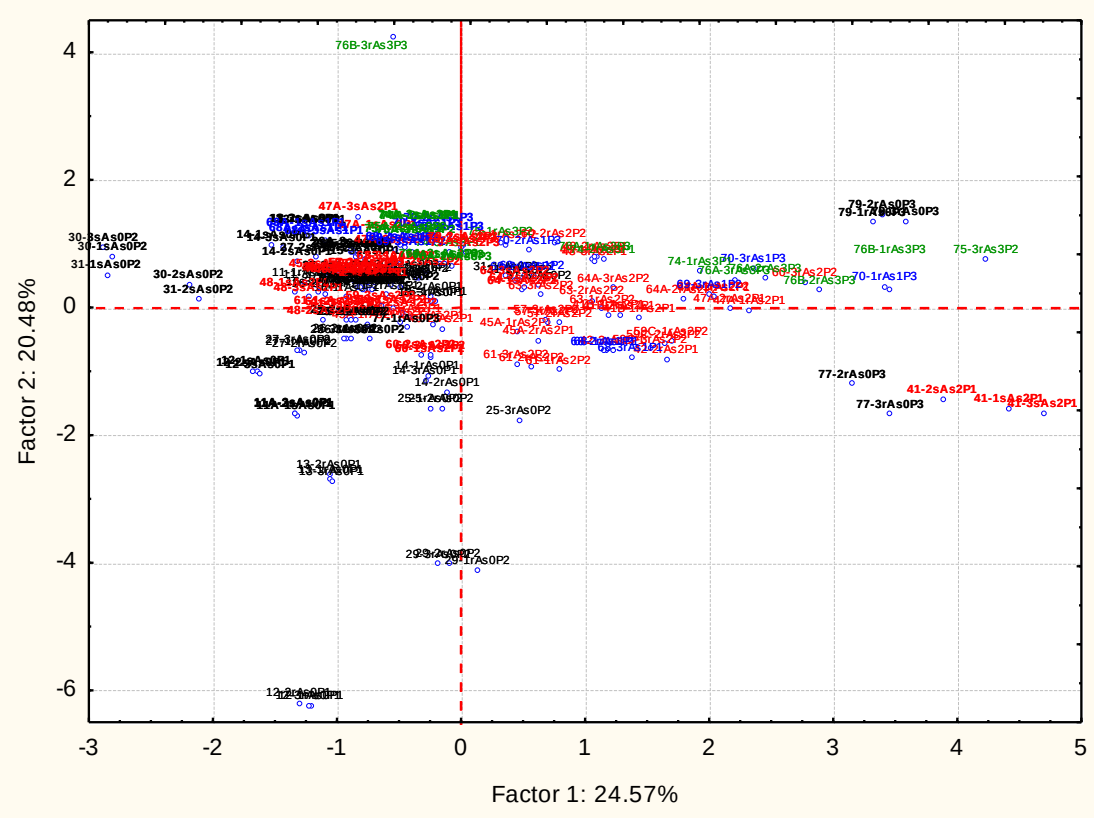

Fig. 42: PC1 vs PC2 score plot: samples have been marked with different labels corresponding to the As treatment they have been subjected

From the above plots it can be observed that the treatments performed have produced relevant effects that are not so easy to be rationalized. In order to get more precise conclusions it is needed to remove progressively outliers from the whole dataset, concentrating the analysis on the most informative data.

The score plot reported in Fig. 42 has been used to detect and remove some outliers (#75B3r, 121r, 2r,3r). On the remaining data, PCA has been performed again.

Fig. 43-44-45 show the results obtained applying PCA on the cleaned data: in Fig.

46 another outlier sample (752r) is easily observable. Once detected, it has been removed from the dataset and PCA has been performed one more time.

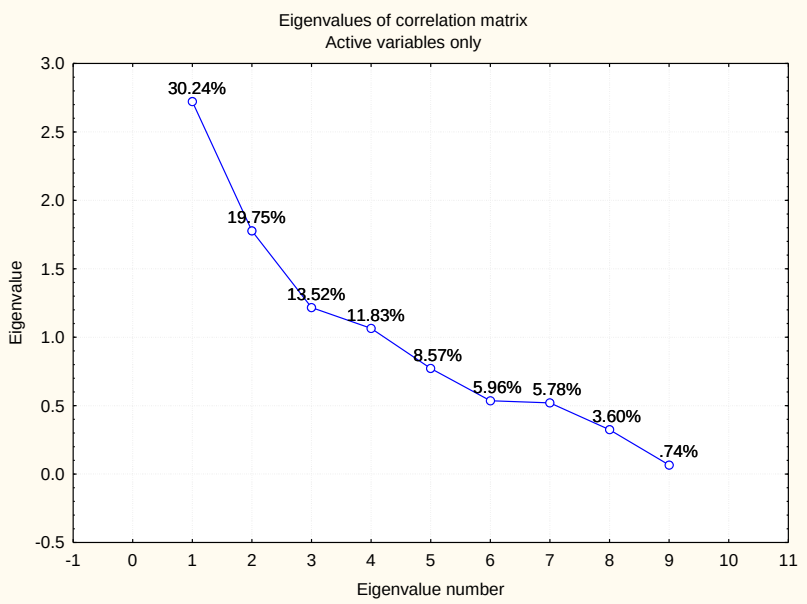

Fig. 43: Principal Components scree plot obtained on the new dataset

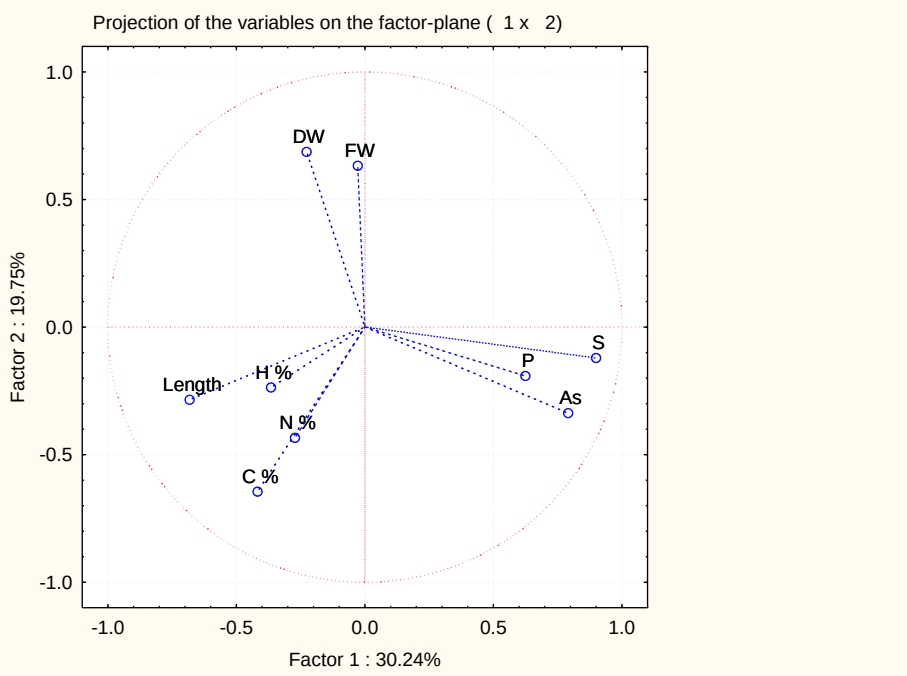

Fig. 44: PC1 vs PC2 loading plot obtained on the new dataset

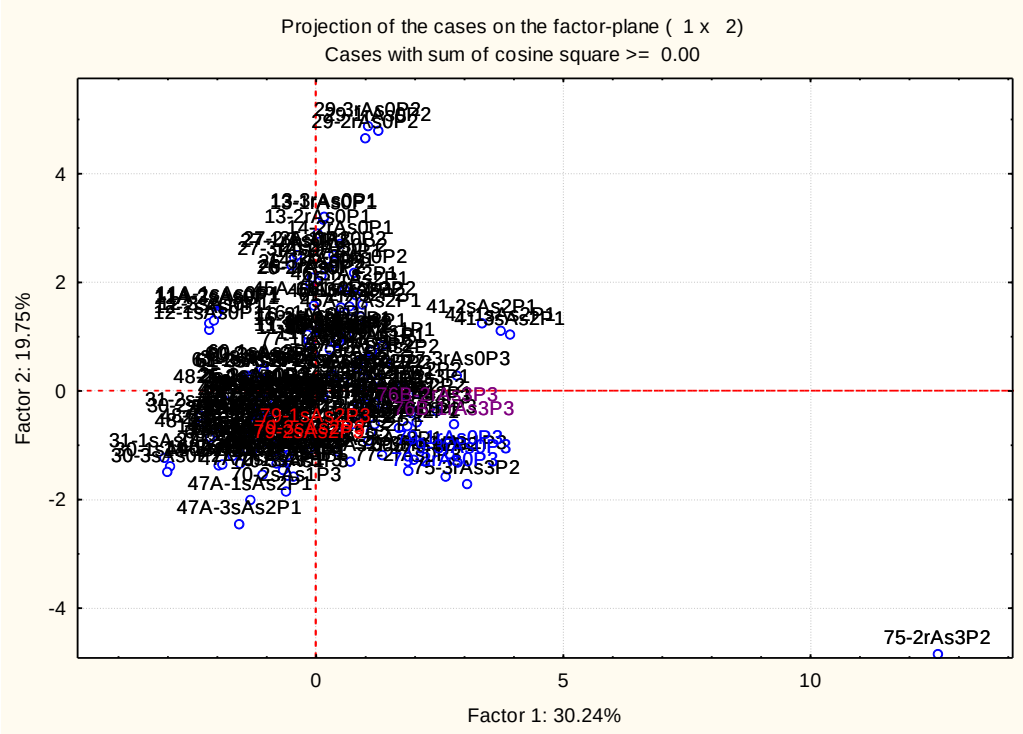

Fig. 45: PC1 vs PC2 score plot obtained using the new dataset

The PCA obtained on this new dataset is shown in Fig. 46-47-48; the loading plot reported in Fig. 48 reports clearly a strong separation between root and shoot samples. This is due to the stronger principal components obtained from the cleaned data. The minor uptake on the edible part of the plant is confirmed in this new results.

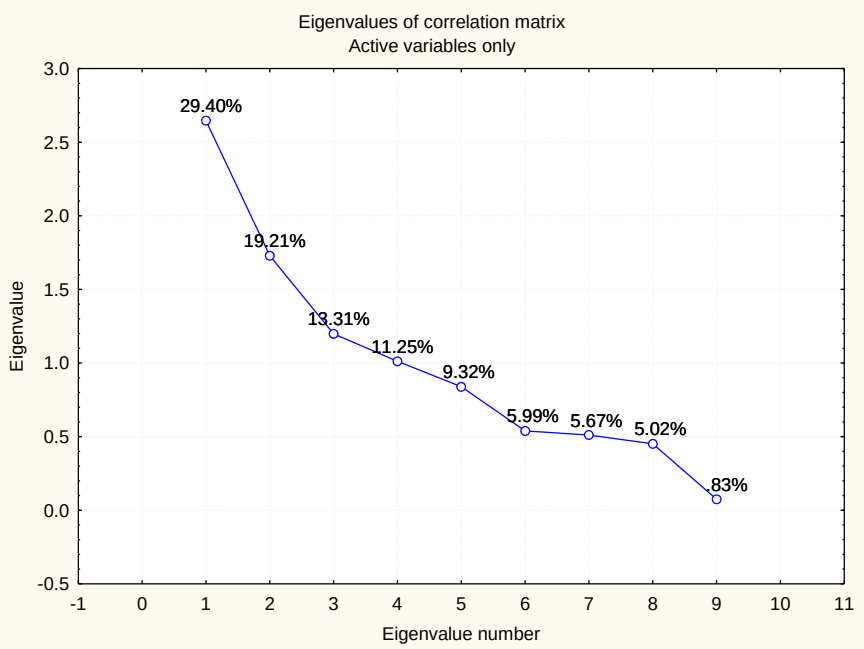

Fig. 43: another scree plot on cleaned data

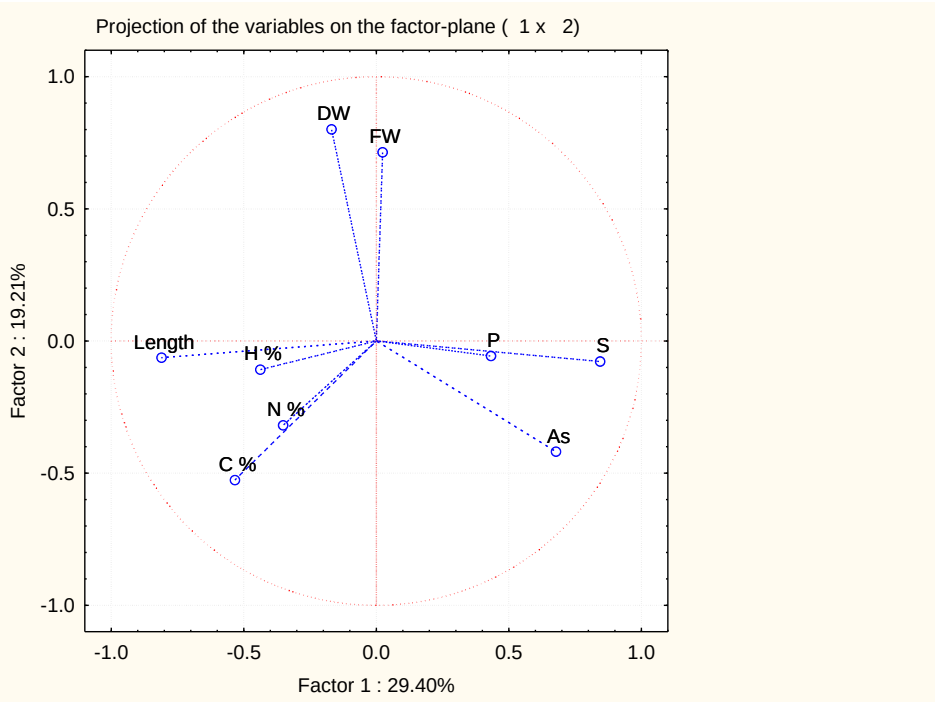

Fig. 44: PC1 vs PC2 new loading plot

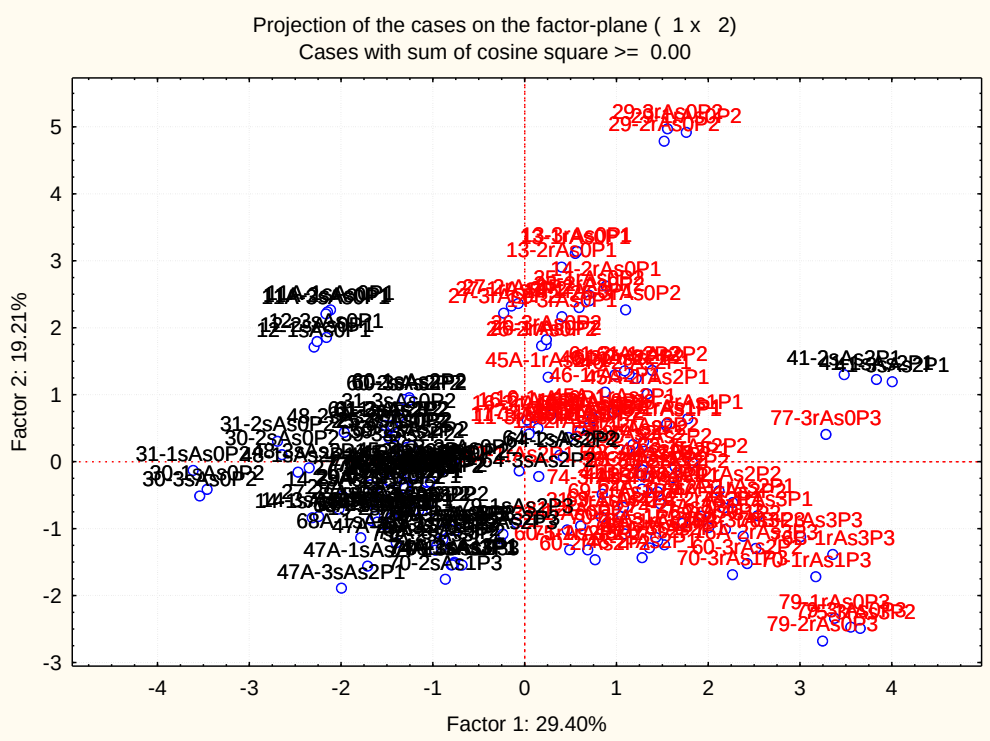

Fig. 45: in black shoot samples, in red roots

In Fig. 46, a score plot for the cleaned data is reported. Samples have been marked with different colours depending on the As and P treatment they have been subjected. Observing the data distribution, orange samples, the ones with As=0 and P=2, and red samples (As=0, P=1) show the highest values on the PC2 axis. At the same time samples marked with dark green (As=0, P=3) and grey (As=1, P=3) show the min values in terms of PC2.

From this observations it seems reasonable to say that high exposure of P has influenced negatively the plants growth while the samples with the best growth are the ones from the control set. Anyway, the overall growth variance shown by the samples is not so large.

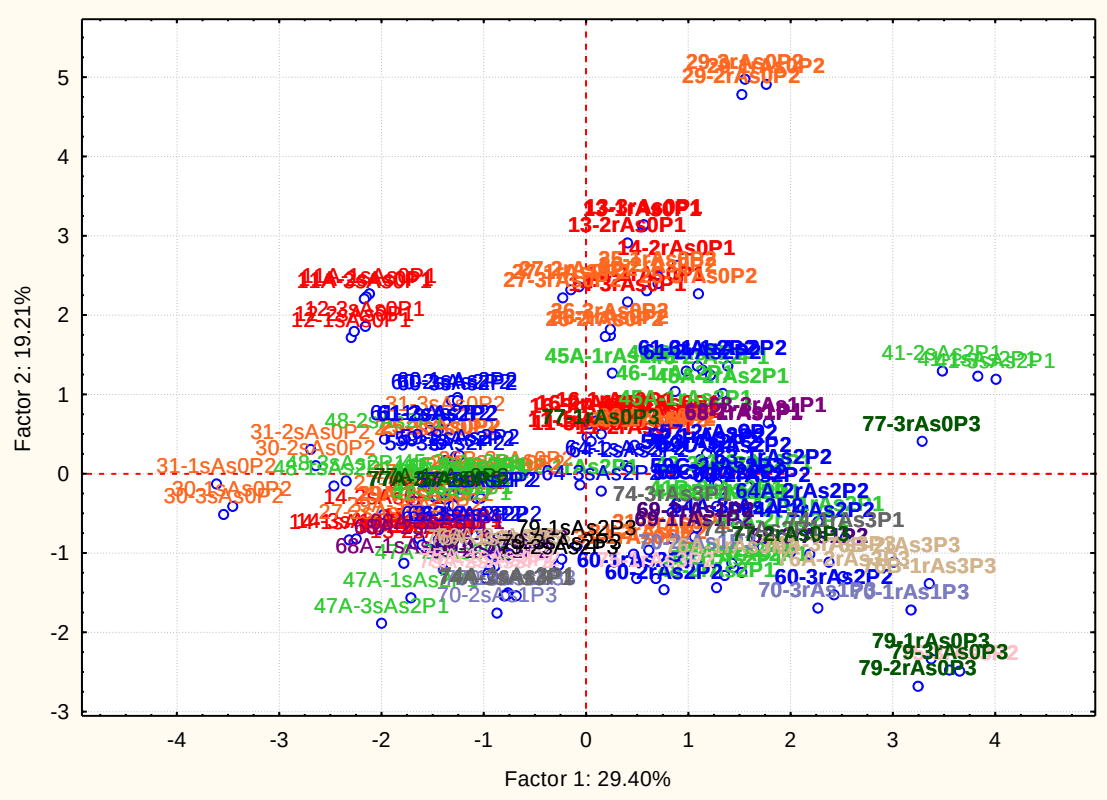

Fig. 46: each samples have been colored with a different color with respect to the treatment performed

Fig. 47 shows a loading plot PC1-PC3. From this plot the contributions of the various initial variables in PC3 are observable.

From the score plot in Fig. 48 it can be noticed that PC3 does not separate properly the different samples: in this plot root samples are marked in red while shoot samples are black.

Fig. 49a-49b show better the score plot from the PC3 axis point of view: it can be observed again that this component does not separate the samples. Some samples that can be considered outliers are also visible from this plots.

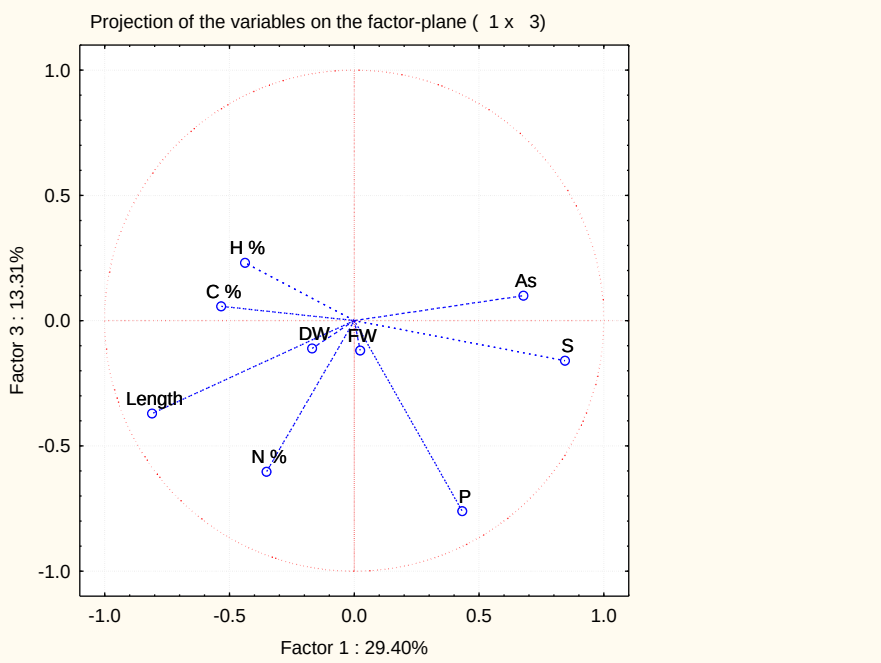

Fig. 47: PC1 vs PC3 loading plot for the cleaned dataset

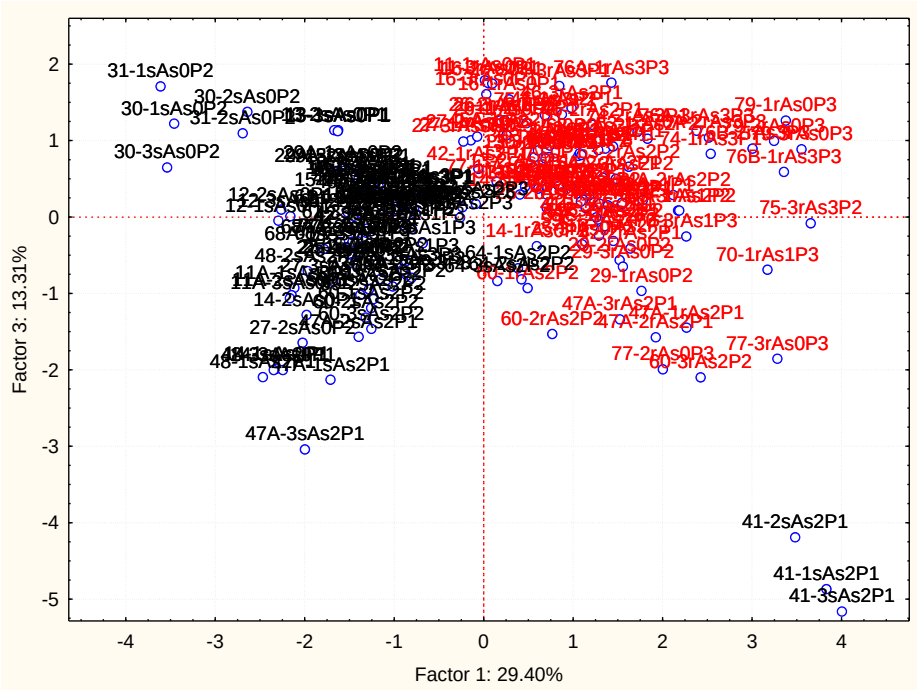

Fig. 48: PC1 vs PC3 score plot

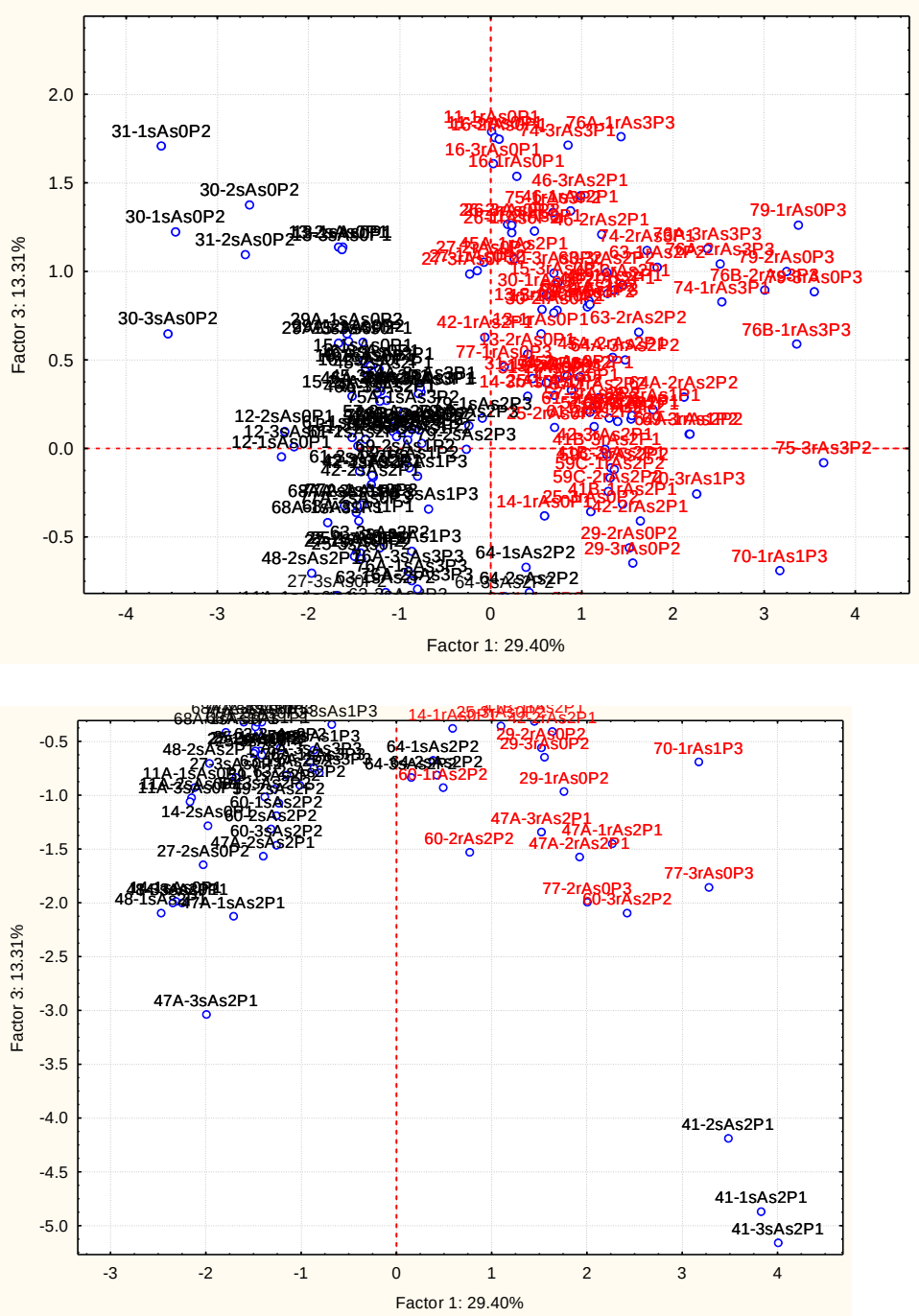

Fig. 49a-49b: PC1 vs PC3 score plot at a different scale

The last round of analysis has been performed on a dataset in which root and shoot samples have been coupled. Each new sample, in this new dataset, contains informations from root and shoots parts and is described by 18 features.

The Principal Components obtained on this data are shown in the plots reported in

Fig. 50-51-52.

In Fig. 52 the score plot PC1-PC2 for this dataset is reported, with samples subjected to As treatment marked in black and other samples marked in red.

A pretty evident separation between samples exposed to As and samples with As=0 is observable along both the axes. In the end, some outliers (75-2r and 41-1,2,3r) are visible. They have been removed from this dataset and the PCA process have been repeated.

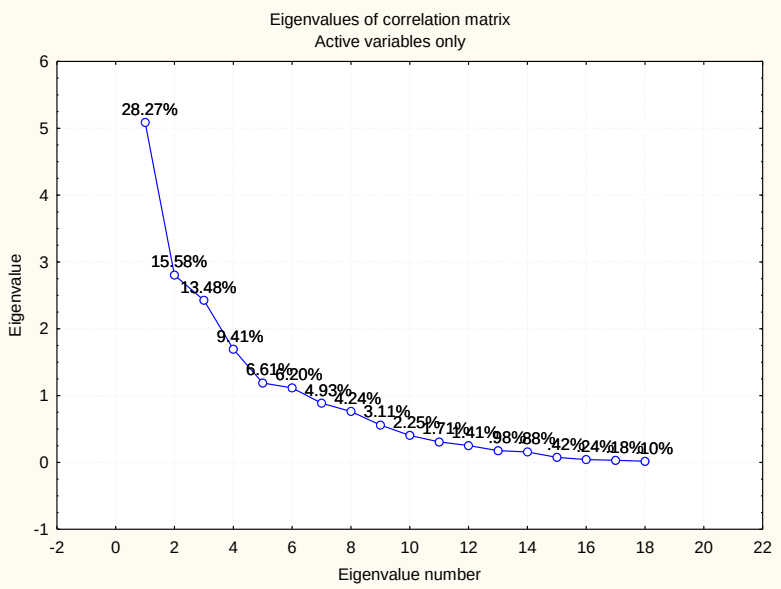

Fig. 50: coupled data scree plot

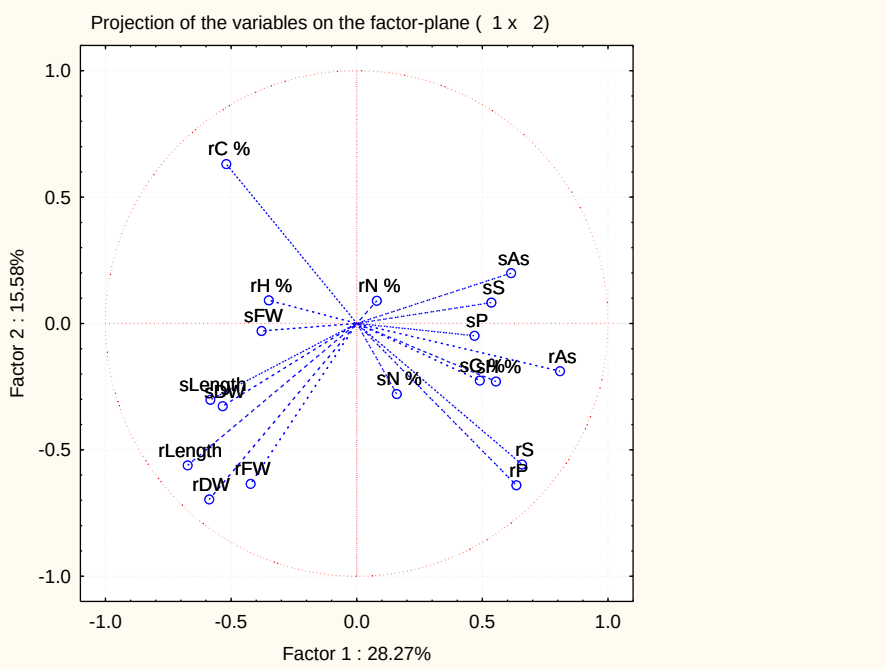

Fig. 51: coupled data PC1 vs PC2 loading plot

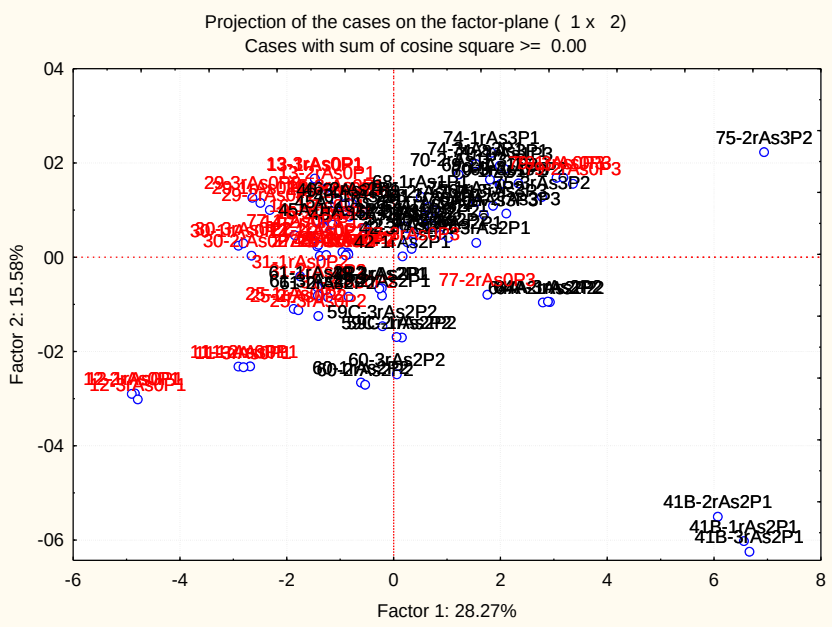

Fig. 52: marked PC1 vs PC2 scree plot

The principal components have been computed again on this new dataset, cleaned from outliers and with coupled samples (root+shoot). As for the previous

experiments Fig. 53 and Fig. 54 report the PC obtained and the corresponding PC1-PC2 load plot.

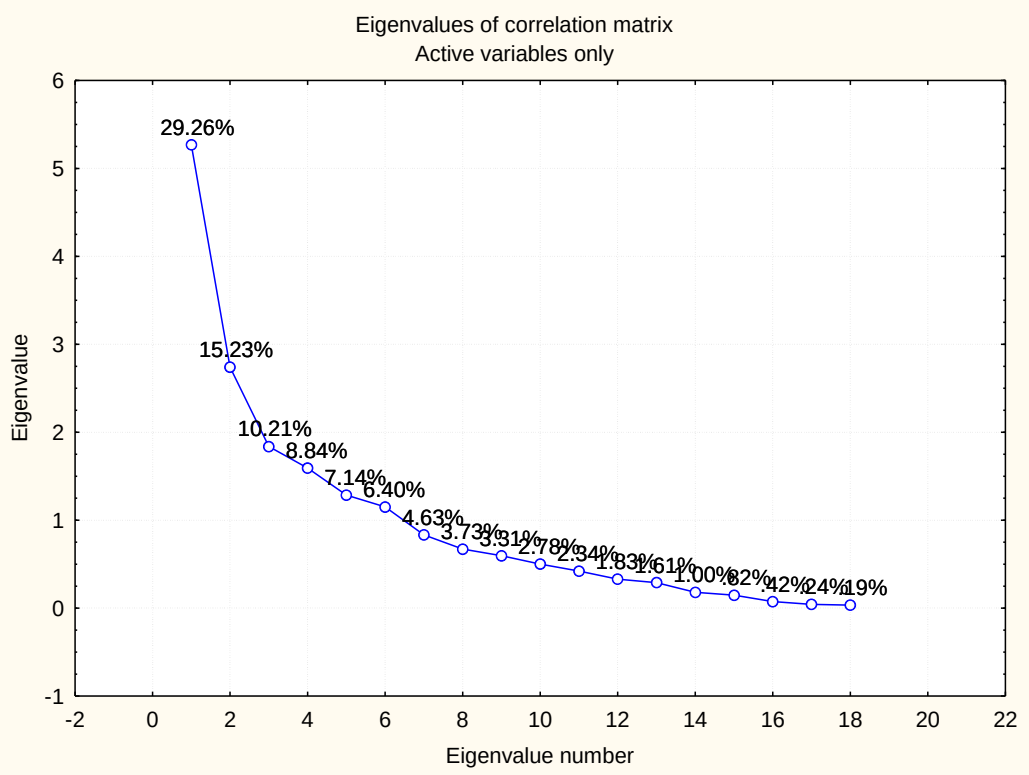

Fig. 53: scree plot of the final dataset

The score plot reported in Fig. 55 shows samples classified as treated or not with As. Samples marked in red have not been treated with As (As = 0) while samples in blue have been exposed to As. Observing data from the PC1 axis is evident that only samples subjected to As treatment show a major uptake while, only the red samples with three different concentrations of P have high values of PC1, since such an exposure to P can be toxic for the plant (Bhatti and Loneragan, 1970).

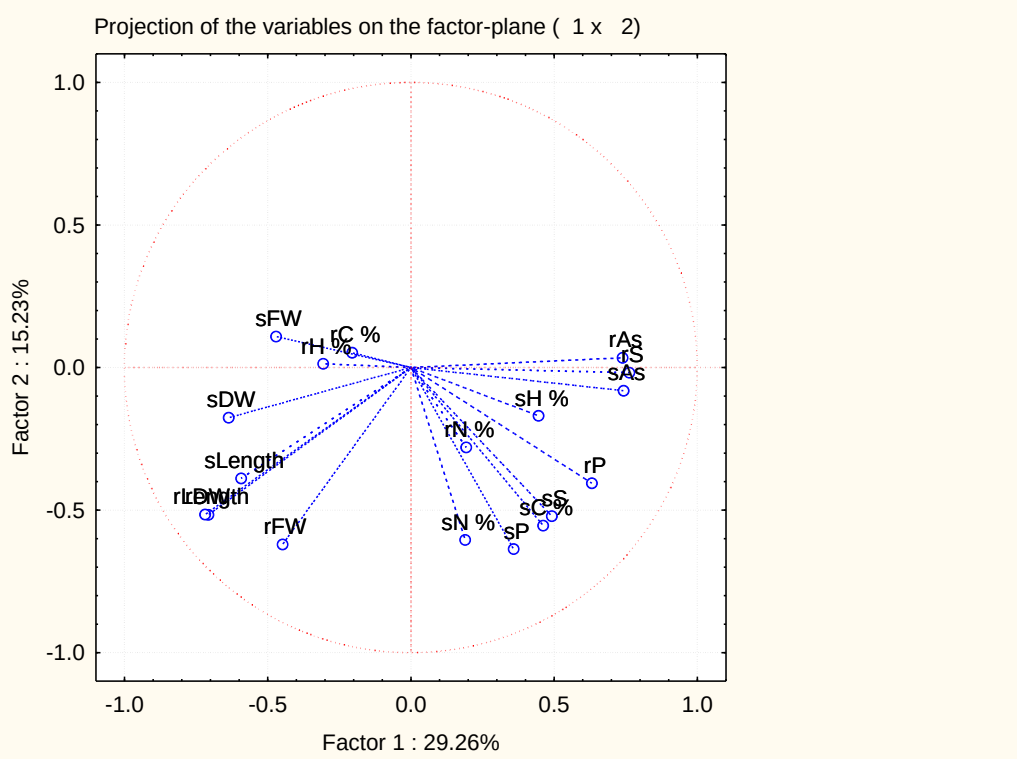

Fig. 54: PC1 vs PC2 loading plot for the final dataset

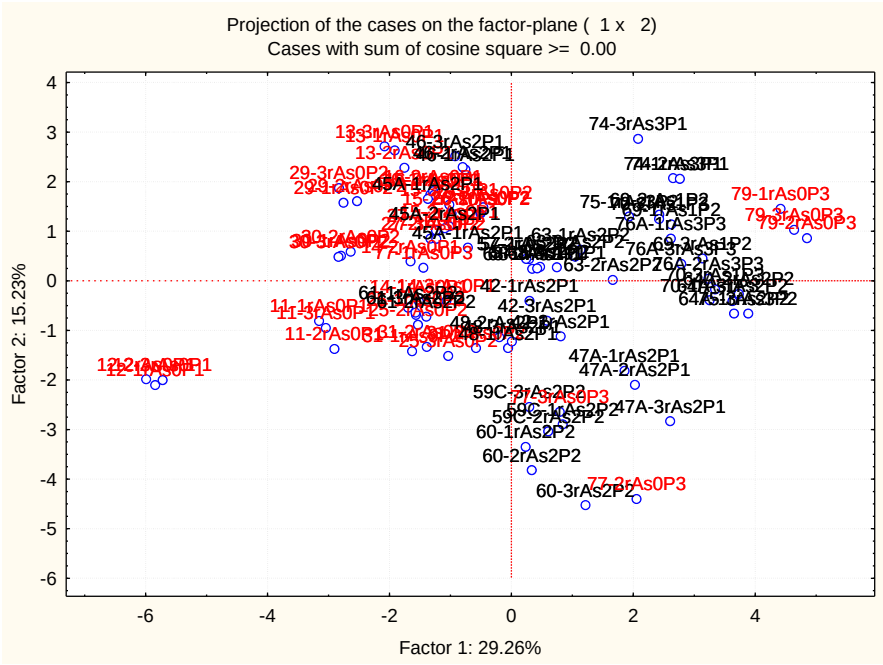

Fig. 55: PC1 vs PC2 score plot; shoot and root samples marked with different colors

3.5.1. Conclusions Of The PCA Analysis

The results obtained on the different datasets allow to make some important consideration concerning the impact of the As presence in rice culture:

i) As observable from the score plots involving PC2, the plants growth is not significantly affected by As exposure while samples treated with the highest concentration of P show a slightly reduced growth process;

ii) The PCA analysis demonstrated that the uptake is different in the various parts of the plant: regardless of the As and P exposure, roots have a major uptake, while aerial parts have lower As concentration.

3.6. Conclusions

Heavy metals uptake by plants, using phytoremediation technology, seems to be a prosperous way to remediate heavy-metals-contaminated environment. It has some advantages compared with other commonly used conventional technologies. Several factors must be considered in order to accomplish a high performance of remediation result. The most important factor is a suitable plant species which can be used to uptake the contaminant. Even the phytoremediation technique seems to be one of the best alternative, it also has some limitations.

Prolong research needs to be conducted to minimize this limitation in order to apply this technique effectively. In case of deficiency of P which is an essential macronutrient for plants; As substitutes the position of P because of chemical similarity (they are both group VA elements). Plants have adapted two broad strategies that enhance P acquisition and use: (a) those directed toward improved acquisition or uptake and (b) those targeted to conserve use (Lajtha and Harrison, 1995). Strategies that lead to better uptake or acquisition include expanded root surface area through increased root growth and root hair development (Lynch and Brown, 1998; Gilroy and Jones, 2000), organic acid synthesis and exudation (Marschner et al, 1986; Gilbert et al, 1998), enhanced expression of phosphate

transporters (Raghothama, 1999), and mycorrhizal associations (Marschner and Dell, 1994). Strategies aimed at conserving P involve internal remobilization of P, a decreased growth rate (Raghothama, 1999), more growth per unit P taken up (Lynch and Brown, 1998), and a modified carbon metabolism (Plaxton and Carswell, 1999). Negative effects by As on plant development have been reported in many studies and can be considered markers of toxicity. As it explained before; if it consider the negative effect of As to both human health and plants; deficiency of P has an important role of the century.

A study of shoot inorganic As(III) and organic-As species concentrations relative to those of the grain would be useful in explaining the high stability grain iAsIII concentration.

Seeds germinated on media containing different concentrations of As shows a decline in germination and retardation in the growth of the seedlings during the days of observation.

In our study, we observed toxic effects of As with a significant decline in the length and weight of roots. Reduced plant growth in response to arsenic exposure has also been reported by numerous investigators in other plants (Liu et al, 2005).

In shoot part, can be consider that in our study uptake of N,S,C,H not influenced from different concentration of As treatments. On the contrary in root part uptake of As effects the absorption of other elements. For instance uptake of P is influenced negatively from high concentration of As.

Future studies should be directed towards identifying the As-binding compounds in rice and improving As species recovery from the rice grain.

3.7. Bibliography

Aguilar M.V., Martínez-Para M.C., Gonzalez M.J., (1997), Effects Of Arsenic(V)-Chromium(III) Interaction On Plasma Glucose And Cholesterol Levels In Growing Rats, Ann. Nutr. Metab. 41: 189-195.

Ampiah-Bonney R. J., Tyson J. F., Lanza G. R., (2007), Phytoextraction Of Arsenic From Soil By *Leersia Oryzoides*, International Journal Of Phytoremediation, 9: 31–40.

Andrianisa H. A., Ito A., Sasaki A., Aizawa J., Umita T, (2008), Biotransformation Of Arsenic Species By Activated Sludge And Removal Of Bio-Oxidised Arsenate From Wastewater By Coagulation With Ferric Chloride, Water Research, 42: 4809–4817.

Arao, T., Kawasaki, A., Baba, K., Mori, S., Matsumoto, S., (2009), Effects Of Water Management On Cadmium And Arsenic Accumulation And Dimethylarsinic Acid Concentrations In Japanese Rice, Environmental Science And Technology, 43: 9361-9367.

Atkinson N.J., Peter E.U., (2012), The Interaction Of Plant Biotic And Abiotic Stresses: From Genes To The Field, Journal Of Experimental Botany, 63: 3523-3543.

Baiocchi A., Lotti F., Piscopo V., (2012), Conceptual Hydrogeological Model and Groundwater Resource Estimation in a Complex Hydrothermal Area: The Case of the Viterbo Geothermal Area (Central Italy). Journal of Water Resource and Protection.

Babich H., Martin-Alguacil N., Borenfreund E., (1989), Arsenic-Selenium Interactions Determined With Cultured Fish Cells, Toxicol. Lett., 45: 157-164.

Bai J.F., Lin X.G., Yin R., Zhang H.Y., Wang J.H., Chen X.M., Luo Y.M., (2008), The Influence Of Arbuscular Mycorrhizal Fungi On As And P Uptake By Maize (*Zea Mays* L.) From As Contaminated Soils, Appl. Soil Ecol., 38: 137–145.

Beckman L., Nordenson I., (1986), Interaction Between Some Common Genotoxic Agents, Hum. Hered., 36: 397-401.

Bhatti A., Loneragan J.F., (1970), Phosphorus Concentrations In Wheat Leaves In Relation To Phosphorus Toxicity, Agron. J., 1970.62: 288–290.

Bienvenido J.O., Villareal C. P., (1993), Grain Quality Evaluation Of World Rices, Int. Rice Res. Inst.

Biswas S., Talukder G., Sharma A., (1999), Prevention Of Cytotoxic Effects Of Arsenic By Short-Term Dietary Supplementation With Selenium In Mice In Vivo, Mutat. Res., 441: 155-160.

Buchet J.P., Lauwerys R., (1987), Study Of Factors Influencing The In Vivo Methylation Of Inorganic Arsenic In Rats, Toxicol. Appl. Pharmacol., 91: 65-74.

Chutia P, Kato S., Kojima T., Satokawa S., (2009), Arsenic Adsorption From Aqueous Solution On Synthetic Zeolites, Journal Of Hazardous Materials, 162: 440–447.

Cikrt M., Mravcová A., Malátová I., (1988), Distribution And Excretion Of 74As And 75Se In Rats After Their Simultaneous Administration: The Effect Of Arsenic, Selenium And Combined Pretreatment, J. Hyg. Epidemiol. Microbiol. Immunol. 32: 17-29.

Djingova R., Wagner G., Kuleff I., (1999), Screening Of Heavy Metal Pollution In Bulgaria Using *Populus Nigra* 'Italica', Science Of The Total Environment, 234: 175–184.

Gailer J., George G.N., Pickering I.J., (2002), Biliary Excretion Of [(GS)2asse]-After Intravenous Injection Of Rabbits With Arsenite And Selenate, Chem. Res. Toxicol., 15: 1466-1471.

Gaur A., Adholeya A., (2004), Prospects Of Arbuscular Mycorrhizal Fungi In Phytoremediation Of Heavy Metal Contaminated Soils, Current Science, 86: 528–534.

Gerhardsson L., Brune D., Nordberg I.G.F., (1985) Protective Effect Of Selenium On Lung Cancer In Smelter Workers, Br. J. Ind. Med., 42: 617-626.

Gerhardsson L., Brune D., Nordberg I.G.F., (1988), Multielemental Assay Of Tissues Of Deceased Smelter Workers And Controls, Sci Total Environ, 74: 97-110.

Gilbert G.A., Vance C.P., Allan D.L., (1998), Regulation Of White Lupin Metabolism By Phosphorus Availability, American Society of Plant Physiology, 1: 92-103.

Gilroy S., Jones D.L., (2000), Through Form To Function: Root Hair Development And Nutrient Uptake, Trends Plant Sci., 5: 56-60.

Gonzalez-Chavez C., Harris P.J., Dodd J., Meharg A.A., (2002), Arbuscular Mycorrhizal Fungi Conferenhanced Arsenate Resistance On Holcus Lanatus, New Phytol. 155, 163–171.

Hasegawa H., Rahman M.A., Matsuda T., Kitahara T., Maki T., Ueda K., (2009) Effect Of Eutrophication On The Distribution Of Arsenic Species In Eutrophic And Mesotrophic Lakes, Science Of The Total Environment, 407: 1418–1425.

Hewitt E.J., (1966), Sand And Water Culture Methods Used In The Study Of Plant Nutrition, Commonwealth Agricultural Bureau, Ed.: 2.

Hill C.H., (1975), Interrelationships Of Selenium With Other Trace Elements, Fed. Proc., 34: 2096-2100.

Hochadel J.F., Waalkes M.P., (1997), Sequence Of Exposure To Cadmium And Arsenic Determines The Extent Of Toxic Effects In Male Fischer Rats, Toxicology 116: 89-98.

Holmberg R.E., Ferm V.H., (1969), Interrelationships Of Selenium, Cadmium And Arsenic In Mammalian Teratogenesis, Arch. Environ. Health, 18: 873-877.

Howell G.O., Hill C.H., (1978), Biological Interaction Of Selenium With Other

Trace Elements In Chicks, Environ Health Perspect, 25: 147-150.

Kraus R.J., Ganther H.E., (1989), Synergistic Toxicity Between Arsenic And Methylated Selenium Compounds, Biol. Trace Elem. Res., 20: 105-113.

Kreppel H., Liu J., Liu Y., (1994), Zinc Induced Arsenite Tolerance In Mice, Fundam. Appl. Toxicol. 23: 32-37.

Lajtha K., Harrison A.F., (1995), Strategies Of Phosphorus Acquisition And Conservation By Plant Species And Communities. In H Tiessen, Wiley11: 140-147.

Lasat M.M., (2000), Phytoextraction Of Metals From Contaminated Soil, Journal Of Hazardous Substance Research, 2: 1–25.

Levander O.A., Baumann C.A., (1966), Selenium Metabolism: Effect Of Arsenic On The Excretion Of Selenium In The Bile, Toxicol. Appl. Pharm., 9:106-115.

Levander O.A., (1977), Metabolic Interrelationships Between Arsenic And Selenium, Environ Health Perspect, 19: 159-164.

Li R.Y., Stroud J.L., Ma J.F., McGrath S.P., Zhao F.J., (2009), Mitigation Of Arsenic Accumulation In Rice With Water Management And Silicon Fertilization, Environmental Science Technology, 43: 3778–3783.

Liu, X., Zhang, S., Shan, X., Zhu, Y.G., (2005), Toxicity Of Arsenate And Arsenite On Germination, Seedling Growth And Amylolytic Activity Of Wheat, Chemosphere, 61: 293–301.

Lynch J.P., Brown K.M., (1998), Regulation Of Root Architecture By Phosphorus Availability, American Society Plant Physiology, 19: 136-147.

Mahaffey K.R., Fowler B.A., (1977), Effects Of Concurrent Administration Of Lead, Cadmium And Arsenic In The Rat, Environ. Health Perspect., 19: 165-171.

Mahaffey K.R., Capar S.G., Gladen B.C., (1981), Concurrent Exposure To Lead, Cadmium And Arsenic Effects On Toxicity And Tissue Metal Concentrations In

The Rat, J. Lab. Clin. Med., 98(1):463-481.

Manca G., Cervone G., (2013), The Case Of Arsenic Contamination In The Sardinian Geopark, Italy, Analyzed Using Symbolic Machine Learning. Environmetrics, 24: 400–406.

Marafante E., Vahter M., (1986), The Effect Of Dietary And Chemically Induced Methylation Deficiency On The Metabolism Of Arsenate In The Rabbit, Acta Pharmacol. Toxicol., 59: 35-38.

Marafante E., Vahter M., Envall J., (1985), The Role Of The Methylation In The Detoxication Of Arsenate In The Rabbit, Chem Biol Interact, 56: 225-238.

Marschner H.V., Dell B., (1994), Nutrient Uptake In Mycorrhizal Symbiosis, Plant Soil 159: 89-102.

Marschner H.V., Romheld V., Horst W.J., Martin P., (1986), Root-Induced Changes In The Rhizoshpere: Importance For The Mineral Nutrition Of Plants, Zeitschrift Fur Pflanzenernaehrung Und Bodenkunde, 149: 441-456.

Meharg, A.A., Hartley-Whitaker, J., (2002), Arsenic Uptake And Metabolism In Arsenic Resistant Plant Species, New Phytol., 154: 29-43.

Meharg, A.A., Rahman, M., (2003), Arsenic Contamination Of Bangladesh Paddy Soils: Implications For Rice Contribution To Arsenic Consumption, Environmental Science And Technology, 37: 229-234.

Miyazaki K., Ushijima K., Kadono T., (2003), Negative Correlation Between Urinary Selenium And Arsenic Levels Of The Residents Living In An Arsenic-Contaminated Area In Bangladesh, J. Health Sci., 49: 239-242.

Mohan D., Pittman C.U.J., (2007), Arsenic Removal From Water/Wastewater Using Adsorbents, Journal Of Hazardous Materials, 142: 1–53.

National Ground Water Association, Copyright, (2001), Arsenic: What You Need To Know

http://www.ngwa.org/ASSETS/A0DD107452D74B33AE9D5114EE6647ED/Arsenic.pdf

Nosheen M., Qaisar M., Maroof S.M., Pervez A., Sultan S., Plants As Useful Vectors To Reduce Environmental Toxic Arsenic Content, The Scientific World Journal, 10: 1155-1166.

Nriagu, J.O., Pacyna, J.M., (1988), Quantitative Assessment Of Worldwide Contamination Of Air, Water, And Soils By Trace Metals, Nature, 333: 134–139.

Oka H.I., Origin Of Cultivated Rice, Elsevier, 2012.

Oremland, R.S., Stolz, J.F., (1975), The Ecology Of Arsenic, Science, 300: 939–944.

Patel K.S., Shrivas K., Brandt R., Jakubowski N., Corns W., Hoffmann P., (2005), Arsenic Contamination In Water, Soil, Sediment And Rice Of Central India, Environ. Geochem. Health, 27: 131-45.

Pershagen G., Nordberg G., Bjorkland N.E., (1984), Carcinomas Of The Respiratory Tract In Hamsters Given Arsenic Trioxide And/Or Benzo[a]Pyrene By The Pulmonary Route, Environ. Res., 34: 227-241.

Plaxton W.C., Carswell M.C., (1999), Metabolic Aspects Of The Phosphate Starvation Response In Plants, Plant Responses To Environmental Stress: From Phytohormones To Genome Reorganization, Marcel-Dekker, 350-372.

Raghothama K.G., (1999), Phosphate Acquisition, Plant Physiol. Plant Mol. Bio., 50: 665-693.

Raymond A., Okieimen W. and Okieimen F.E., (2011), Heavy Metals in Contaminated Soils, Ecology, 10: 5402-5422.

Robinson B.H., Mills T.M., Petit D., Fung L.E., Green S.R., Clothier E. (2000),. Natural And Induced Cadmium-Accumulation In Poplar And Willow: Implications For Phytoremediation, Plant And Soil, 227: 301–306.

Rossman T.G., Uddin A.N., (2004), Selenium Prevents Spontaneous And Arsenite-Induced Mutagenesis, Int. Congr. Ser., 1275: 173-179.

Rössner P., Bencko V., Havránková H., (1977), Effect Of The Combined Action Of Selenium And Arsenic On Suspension Culture Of Mice Fibroblasts, Environ Health Perspect, 19: 235-237.

Salido A.L., Hasty K.L., Lim J.M. Butcher D.J., (2003), Phytoremediation Of Arsenic And Lead In Contaminated Soil Using Chinese Brake Ferns (*Pteris Vittata*) And Indian Mustard (*Brassica Juncea*), International Journal Of Phytoremediation, 5: 89–103.

Schrauzer G.N., White D.A., McGinness J.E., (1978), Arsenic And Cancer: Effects Of Joint Administration Of Arsenite And Selenite On The Genesis Of Adenocarcinoma In Inbred Female C3H/St Mice, Bioinorg Chem, 9: 245-253.

Schrauzer G.N., (1987), Effects Of Selenium Antagonists On Cancer Susceptibility: New Aspects Of Chronic Heavy Metal Toxicity, Journal Of UOEH, 9: 208-215.

Sebastiani L., Scebba F., Tognetti R., (2004), Heavy Metal Accumulation And Growth Responses In Poplar Clones Eridano (*Populus Deltoides* × Maximowiczii) And I-214 (*P.* × Euramericana) Exposed To Industrial Waste, Environmental and Experimental Botany, 52: 79–88.

Shao G, Chen M, Wang W, Mou R, Zhang G, (2007), Iron Nutrition aVects Cadmium Accumulation And Toxicity In Rice Plants, Plant Growth Regul., 53: 33–42.

Sharma B., Singh S., Siddiqi N.J., Biomedical Implications Of Heavy Metals Induced Imbalances In Redox Systems, BioMed Research International, 2014: 10-36.

Shtangeeva I., Laiho J.V.P., Kahelin H., Gobran G.R., (2004), Phytoremediation Of Metal-Contaminated Soils, Symposia Papers Presented Before The Division

Of Environmental Chemistry, American Chemical Society.

Styblo M., Thomas D.J., (2001), Selenium Modifies The Metabolism And Toxicity Of Arsenic In Primary Rat Hepatocytes, Toxicol. Appl. Pharmacol., 172: 52-61.

Su, Y., Mcgrath, S., Zhao, F., (2010), Rice Is More Efficient In Arsenite Uptake And Translocation Than Wheat And Barley, Plant Soil, 328: 27–34.

Sweins A., (1983), Protective Effect Of Selenium Against Arsenic-Induced Chromosomal Damage In Cultured Human Lymphocytes, Hereditas, 98: 249-252.

Tinker S.W., John A., Jackson K.G., (2005), Texas Commission On Environmental Quality Austin, Texas August School of Geosciences, 78713-8924.

Uddin A.N., Burns F.J., Rossman T.G., (2005), Vitamin E And Organoselenium Prevent The Cocarcinogenic Activity Of Arsenite With Solar UVR In Mouse Skin. Carcinogenesis, 26: 2179-2186.

U.S. Department of Health and Human Services, (2005), Public Health Service Agency for Toxic Substances and Disease Registry, Division of Toxicology and Environmental Medicine.

Vaclavikova M., Gallios G.P., Hredzak S., Jakabsky S., (2008), Removal Of Arsenic From Water Streams: An Overview Of Available Techniques, Clean Technologies And Environmental Policy, 10: 89–95.

Vahter M., Marafante E., (1987), Effects Of Low Dietary Intake Of Methionine, Choline Or Proteins On The Biotransformation Of Arsenite In The Rabbit, Toxicol. Lett., 37: 41-46.

Walton F.S., Waters S.B., Jolley S.L., (2003), Selenium Compounds Modulate The Activity Of Recombinant Rat As111-Methyltransferase And The Methylation Of Arsenite By Rat And Human Hepatocytes, Chem. Res. Toxicol., 16: 261-265.

Welch, A.H., Westjohn, B.D., Helsel, D.R., Wanty, R.B., (2000), Arsenic Epidemiology And Drinking Water Standards, Groundwater, 38: 589–604.

WHO Regional Office for Europe, (2000), Air Quality Guidelines, chapter 6.1, Arsenic, Copenhagen, Denmark, 2nd Ed.

Woolson, E.A., Axley, J.H., Kearney, P.C., (1971), The Chemistry And Phytotoxicity Of Arsenic In Soils, Contaminated Field Soils, Soil Science Society Of America Proceedings, 35: 938–943.

Wuyi W., Linsheng Y., Shaofan H., (2001), Prevention Of Endemic Arsenism With Selenium, Curr. Sci., 81: 1215-1218.

Xu, X.Y., McGrath, S.P., Meharg, A.A., Zhao, F.J., (2008), Growing Rice Aerobically Markedly Decreases Arsenic Accumulation, Environmental Science And Technology, 42: 5574-5579.

Yamaji N., Ma J.F., (2009), A Transporter At The Node Responsible For Intervascular Transfer Of Silicon In Rice, The Plant Cell, 21: 2878-2883.

Yang L., Wang W., Hou S., (2002), Effects Of Selenium Supplementation On Arsenism: An Intervention Trial In Inner Mongolia, Environ. Geochem. Health 24: 359-374.

Yusof A.M., Malek N.A.N.N., (2009), Removal Of Cr(VI) And As(V) From Aqueous Solutions By HDTMA-Modified Zeolite Y, Journal Of Hazardous Materials, 162: 1019–1024.

Zhang J., Zhu Y.G., Zeng D.L., Cheng W.D., Qian Q., Duan G.L., (2008), Mapping Quantitative Trait Loci Associated With Arsenic Accumulation In Rice (*Oryza sativa*), New Phytol, 177: 350-5

Zhang X.H., Zhu Y.G., Chen B.D., Lin A.J., Smith S.E., Smith F.A., (2005), Arbuscular Mycorrhizal Fungi Contribute To Resistance Of Upland Rice To Combined Metal Contamination Of Soil, Journal Plant Nutrition, 28: 2065–2077.